Induction of apoptosis in cervical and breast cancer cells using quinoxaline derivatives

by

Teboho Yvette Satekge

A RESEARCH DISSERTATION

submitted in fulfilment of the requirements for the degree of

Master of Science in Biochemistry

in the

Department of Biochemistry Microbiology and Biotechnology

Faculty of Science and Agriculture

(School of Molecular and Life Sciences)

at the

UNIVERSITY OF LIMPOPO

Supervisor: Prof TM Matsebatlela
Co-supervisor: Prof VG Mbazima

April, 2024

DECLARATION

I declare that the dissertation hereby submitted to the University of Limpopo, for the degree of Master of Science in Biochemistry has not previously been submitted by me for a degree at this or any other university; that it is my work in design and in execution, and that all the materials contained herein has been duly acknowledged.

April 2024

Satekge Teboho Yvette **Date**

DEDICATION

This dissertation is dedicated to my amazing and loving family, whose encouragements have always sheltered me throughout the challenging journey. To my parents, (Sarah Satekge and Jack Satekge), all the sacrifices you have made and the belief you have in my potential have constantly propelled me in the right direction. To my heavenly grandparents, (Florah Ramabopa, France Ramabopa and MmaTlali Satekge), I will forever be grateful for your unwavering love and support.

ACKNOWLEDGEMENTS

- Through Gods words, there is always a reason to move forward with hope and faith, I am grateful for all the wisdom and protection I receive daily from the superior being above.
- My deepest gratitude goes towards my supervisor Prof TM Matsebatlela, I am constantly moved by his enthusiasm, vision, endless efforts, desire to see success in everyone, his forever availability to listen and help whenever possible and always seeking solutions to every problem ever encountered.
- To my co-supervisor Prof VG Mbazima, I will forever appreciate the commitment you have shown towards my study, your kindness, assistance and always propelling me in the right direction all that have been a gem throughout my study. Thanks for constantly reminding me to focus when I slack and thanks for your tireless efforts to explain and demonstrate concepts and always pouring out to me words that sharpened my views regarding certain research aspects.
- Mostly I would like to express my heartfelt special thanks towards my parents Mr SJ Satekge and Mrs MS Satekge for their never-ending support, love, and encouragement and again to my late grandmama Flora Ramabopa who is also my pillar of strength I cannot thank you enough for your love, your support and for believing in me.
- Special thanks to Miss Mangokoana. For constantly pushing for progress, your assistance can never go unnoticed.
- To Dr Laka, Dr Makola, Ms TE Mohale, Mr GW Ramasenya, my co-workers, and the entire departmental unit.
- I wouldn't have done it without my drive, enthusiasm, discipline, and tenacity I have shown throughout all the research seasons.

LIST OF CONFERENCE PRESENTATIONS

Oral presentations

1. Satekge TY., Nxumalo MW., Mbazima VG, and Matsebatlela TM. Induction of apoptosis in cervical and breast cancer cells using quinoxaline derivatives. Pan African Cancer Research Institute (PACRI) launch. University of Pretoria, Gauteng, 24-25 February 2022.
2. Satekge TY., Nxumalo MW., Mbazima VG, and Matsebatlela TM. Induction of apoptosis in cervical and breast cancer cells using quinoxaline derivatives. 3rd Ellisras and other Non-communicable Disease International Conference (ELSONCDIC). University of Limpopo and Kitty school, Kitty Village. Lephalale, Limpopo, 22-24 November 2022.
3. Satekge TY., Nxumalo Nxumalo., Mbazima VG, and Matsebatlela TM. Induction of apoptosis in cervical cancer cells using quinoxaline derivatives. Faculty of Science and Agriculture (FSA) 13th research day. Bolivia lodge, Polokwane, 20-22 September 2023.

Poster presentations

4. Satekge TY., Nxumalo MW., Mbazima VG, and Matsebatlela TM. Induction of apoptosis in cervical (CaSki) and breast (MCF-7) cancer cells using quinoxaline derivatives. Pan African Cancer Research Institute's Inaugural International Cancer meeting. Future Africa, University of Pretoria, South Africa. 26 February - 1 March 2023.
5. Satekge TY., Nxumalo Nxumalo., Mbazima VG, and Matsebatlela TM. Induction of apoptosis in cervical cancer cells using quinoxaline derivative LAM-21D. 13th annual Biomedical Research and Innovation Platform (BRIP). SAMRC, Cape Town, South Africa, 16-17 October 2023.
6. Satekge TY., Nxumalo Nxumalo., Mbazima VG, and Matsebatlela TM. Induction of apoptosis in cervical cancer cells using quinoxaline derivative LAM-21D. Arturo Falaschi conference, International Centre for Genetic engineering, and Biotechnology. Cape Town, South Africa, 31 October – 03 November 2023.

TABLE OF CONTENTS

LIST OF FIGURES

Chapter 1

Chapter 3

LIST OF TABLES

LIST OF ABBREVIATIONS

ADME	Absorption distribution metabolism and excretion
Apaf-1	Apoptotic protease activating factor.
ATCC	American Type Culture Collection
ATM	Ataxia-telangiectasia-mutated
ATP	Adenosine triphosphate
BBB	Blood brain barrier
Bcl-2	B-cell lymphoma-2
BRCA1and2	Breast cancer susceptibility gene 1and2
Ca^{2+}	Calcium ions
CAD	Caspase- activated DNase
CASKI	Cervical cancer cell
CIN	Cervical Intraepithelial neoplasia
CDK1	Cyclin-dependent kinase 1
CO_2	Carbon Dioxide
CQS	Chloroquinoxaline Sulphonamide
CYP1A2	Cytochrome P450 1A2 inhibitor
CYP2C19	Cytochrome P450 2C19 inhibitor
CYP2C9	Cytochrome P450 2C9 inhibitor
CYP2D6	Cytochrome P450 2D6 inhibitor
CYP34A	Cytochrome P450 3A4 inhibitor
DD	Death Domain
DISC	Death Inducing Signalling Complex
DMEM	Dulbecco's Modified Eagle Medium
DMSO	Dimethyl sulfoxide
DPPH	2,2-diphenyl-1-picrylhydrazyl
DNA	Deoxyribonucleic acid
DR4/DR5	Death receptor 4/5

EBRT	External beam radiation therapy
EndoG	Endonuclease G
ER	Oestrogen receptor.
FADD	Fas-associated Death Domain
FBS	Foetal Bovine Serum
FDA	Food and Drug Agency
Fe	Iron
FRAP	Ferric Reducing Antioxidant Power
g	Gram
GAE/g	Gallic Acid Equivalent per gram
GTP	Guanosine triphosphate
HEK-293	Human embryonic kidney cells
HER2	Epidermal growth receptor 2
HMW	High molecular weight
HPV	Human Papilloma Virus
HtrA2	High temperature requirement protein A2
IAPs	Inactivating apoptosis inhibitors
KI67	Proliferation marker
LAM-29A	3-(6-aminoquinoxalin-2-yl) pro-2-ynyl benzoate
LAM-21D	6-nitro-2-(oct-1-ynyl) quinoxaline
Log $P_{O/W}$	predicted octanol/water partition coefficient.
λmax	Lambda max
mAbs	Monoclonal antibodies
MCF-7	Breast cancer cells
MOMP	Mitochondrial outer membrane permeabilization
MDM2	Mouse Double Minute-2
MEK	Mitogen-activated protein kinase
Mg^{2+}	Magnesium ions
mg/ml	Milligram per Millilitre
mL	MilliLitre
mM	MilliMolar
MTT bromide	3-(4,5-dimethylthiazol-2-yl)-2,5-diphenyl-2H- tetrazolium
NADPH	Nicotinamide Adenine Dinucleotide Phosphate

nm	NanoMetre
NCI	National Cancer Institute
NcRNA	Non-coding RNAs
NO_2	Nitrogen dioxide
OD	Optical density
PBS	Phosphate buffered Saline.
PIDD	P53- Induced Death Domain
PRB	Retinoblastoma protein
PR	Progesterone receptor
PSN	Penicillin, Streptomycin and Neomycin
ROS/ RNS	Reactive Oxygen Species/Reactive Nitrogen species
RPMI	Roswell Park Memorial Institute-medium
RNA	Ribonucleic acid
SCC	Squamous Cell Carcinoma
SMAC	Second mitochondrial-derived activator of caspase
DIABLO	Direct inhibitor of apoptosis-binding protein with low pi
TDLUs	Terminal duct lobular units
TKIs	Tyrosine Kinase Inhibitors
TNBC	Triple negative breast cancer
TNF-1	Tumour necrosis factor-1
TNFR1	Tumour necrosis factor-α with its receptor
TPTZ	tripyridyl- s- triazine
TRADD	TNFR1 associated death domain.
TPC	Total Phenolic Content
µL	Microlitre
UV/Vis	UltraViolet/ Visible light
WHO	World Health Organization
XK469	2-(4-(7-chloroquinoxalin-2-yl) phenoxy] propionic acid

ABSTRACT

Background: Cervical and breast cancers remain a public health concern in South Africa with an increasing rate of incidences and mortalities globally. Current treatment options are not only costly but also present undesirable side effects, induce multidrug resistance, and result in high rates of cancer remissions. To limit cancer recurrences, the focus of anticancer drug development has been on increasing sensitivity of cancer cells to drug-induced apoptosis as a prospective cancer therapy. Apoptosis and its associated cancer hallmarks are the gold standard targets for the development of conventional cancer treatment strategies for management of cancers. In view of current challenges encountered in cancer treatment options, more target-specific, less costly, and highly effective inducers of apoptosis are urgently required. Quinoxaline derivatives are synthetic small molecules that hold a plethora of desirable biological activities with their structures being constantly modified to improve their therapeutic target specificity, response rate, and accessibility. **Aim of study:** Hence, this study primarily aimed at investigating the ability of selected novel quinoxaline derivatives to induce apoptotic cell death in cervical cancer (CaSki) and breast cancer (MCF-7) cells. **Methods:** To achieve this aim, characterisation of the quinoxaline derivatives, LAM21D and LAM29A, was performed to determine the UV-Vis absorption spectrum utilising the UV/Vis spectrophotometer. The antioxidant potential of the quinoxaline derivatives was evaluated using the ferric reducing antioxidant power (FRAP) assay and 2,2-diphenyl-1-picrylhydrazyl (DPPH) free radical scavenging assay while the total phenolic content was determined using the Folin Ciocalteu's total phenolic content assay. The ability of quinoxaline derivatives to inhibit the viability of CaSki cervical and MCF-7 breast cancer cells was assessed using the 3-(4,5-Dimethylthiazol-2-yl)-2,5-Diphenyltetrazolium Bromide (MTT) assay. The effect of the derivatives on morphological features of the described cancer cells was captured and analysed using the Ti-E inverted microscope and apoptosis induced by the derivatives was quantified using the Muse™ Annexin-V and dead cell assay. The effect of quinoxaline derivatives on ROS production in the cells was established using Muse™ oxidative stress assay. The Muse™ Ki67 proliferation assay was carried out to measure Ki67 expression levels which correlates with the proliferation percentages in CaSki cells. The Muse™ cell cycle assay was performed to evaluate the effect of

quinoxaline derivatives on cell cycle progression. The CB-Dock and SwissADME web-based softwares were used to evaluate the binding patterns of quinoxaline derivative LAM-21D and its drug-likeness propensity. **Results:** Preliminary screening showed that LAM-21D exerted high selectivity towards CaSki cells at 250 µM with minimal cytotoxicity on the noncancerous HEK-293 cells while LAM-29A exhibited high selectivity towards MCF-7 cells. However, although LAM-21D induced apoptosis in CaSki cells, LAM-29A did not induce apoptosis in MCF-7 cells. As a result, assays on downstream pathways were conducted to evaluate the activity of LAM-21D on CaSki cells. A reduction in Ki67 expression which correlated with a reduction in cell proliferation was observed when cells were treated with LAM-21D. There were insignificant changes observed in Ki67 expression when MCF-7 cells were treated with LAM-29A. Both derivatives, LAM-29A and LAM-21D, induced minimal cytotoxicity on the noncancerous cells and LAM-21D significantly reduced Ki67 expression, induced ROS production, S-phase cell cycle arrest, and apoptosis in Caski cervical cancer cells. The *In-silico* studies revealed an interaction of the compound with the anti- apoptotic BCL-2 protein and p65 NF-κB transcription factor. The compound also showed drug-likeness properties as per ADMET studies. Further studies are required to fully delineate the anticancer mechanisms of this compound. Nonetheless, this compound could be a potential candidate to explore in the therapeutic targets for cervical cancer. Structural modifications are recommended on both quinoxaline derivatives to improve their anticancer properties against cervical and breast cancer cells.

CHAPTER 1

INTRODUCTION

1.1 Background

Cancer is still a public health concern with increasing cases of death worldwide. It occurs when normal cells divide uncontrollably, undergoes transformation, metastasize, and invade nearby or remote organs (Ajani *et al.*, 2019). The complexity of this disease is due to mutations in genes, evasion of apoptosis and changes in the signal pathways (Prasad, 2022a). Cancer ranks among the world's leading causes of death (Ajani *et al*., 2019). An estimate of 19.3 million cancer cases was recorded in 2020 alongside the 10 million deaths that occurred. It is further expected that a 47% rise in cancer cases from 2020 to 2040 might occur which will account for almost 28.4 million new cases (Sung *et al*., 2021).

Breast and cervical cancers continue to be the most prevalent cancers in women worldwide, and they are also responsible for most cancer-related deaths and morbidities. (De Rose *et al*., 2022; Ryzhov *et al*., 2021. There were.3 million new cases due to breast cancer in 2020. (Costa *et al*., 2020; Harnden *et al*., 2022. Cervical cancer ranked on the fourth position with 604, 000 cases along with 342,000 deaths in 2020. South Africa is one of the regional places with most cervical cancer occurrence and mortality rates recorded (Sung *et al*., 2021.There has been a slight decline in cervical cancer rates due to an easy access to early detection, effective screening testing services as well as HPV vaccines however, illness and mortality rates remain high in the developing countries (Vijaya Rachel and Sivaraj, 2021).

Carcinogenesis is a multistage process and can be caused by various factors that can result into a high free radical production which can damage the DNA (Gaglia and Munger, 2018; Lagoa *et al*., 2020; Lewandowska *et al*., 2019; Vishlaghi and Lisse, 2020). ROS/RNS in moderate plays a crucial role in intracellular signalling. However, cancer cells constantly produce these species in high amounts to sustain their high metabolic activities and proliferation which can cause oxidative stress (Hayes *et al*., 2020) Increased oxidative stress is associated with DNA mutations that result in cell proliferation and genome

instability, that frequently promote the growth and survival of cancer cells as well as their invasion and metastasis. These elevated nitrogen and oxygen species in cancer can inactivates tumour suppressor proteins. Nonetheless, cancer cells have evolved mechanisms to alter the antioxidants levels and minimise ROS/RNS which creates resistance in chemotherapy (Ramalingam and Rajaram, 2021).

Cancer prevention is at the heart of apoptosis. The rate of cell proliferation and elimination is carefully regulated and balanced by apoptosis or programmed cell death. Apoptosis-related intermediates are primarily targeted in therapy because of an alteration of apoptosis mechanisms in cancer (Jan, 2019). The main goal of many anticancer therapies is to induce cell death in tumour cells (Pfeffer and Singh, 2018. However, the major challenge is therapeutic resistance (Cao and Tait, 2018). The process of apoptosis is tightly regulated by many crucial proteins such as the NF-kB, caspases, BCL- 2 proteins, and p53 to name a few. Dysregulation of this process is identified in majority of cancers. Effector caspases (caspase 3, 6 and 7) are downregulated in both breast and cervical cancers. Furthermore, there is overexpression of anti- apoptotic Bcl-2 family of proteins such that cancer cells cannot undergo apoptosis (Prasad, 2022b).

Loss of function of some of the components of the extrinsic pathway such as Fas/Fas ligand is the main driver of cervical cancer progression. Furthermore, dysregulation of the intrinsic pathway creates an advantage to the tumour cells since they can thrive in the presence of growth suppressors, able to avoid immune signals and render chemotherapeutic drugs unfeasible. Cancer is characterised by unregulated cell division, which promotes the growth and invasion of the tumour by mutating tumour suppressors (Nair and Yadav, 2022). Anticancer drugs are most likely to target proteins involved in the mentioned pathways. Hence, apoptosis is primarily targeted in cancer therapy since its dysregulation is often associated with the promotion of cancer and chemo-resistance (Prasad, 2022b).

Despite efforts to improve cancer treatment, the selection of medications is limited because cancer is often drug-resistant therefore innovative inducers of

apoptosis are urgently required (Human-Engelbrecht *et al*., 2017). There is a plethora of evidence which shows that heterocyclic compounds bearing nitrogen atoms holds important properties used in medicinal chemistry and pharmaceuticals. Majority of the drugs approved by the FDA, bears at least 59% of the N- heterocycle component. These have a wide spectrum of biological and pharmaceutical activities ranging from anti-(microbial, -cancer, -diabetic, -viral) to name a few (Elgemeie *et al* ., 2022). In many of the drug discovery projects these compounds are being exploited with which some are still under clinical trials (Suthar *et al* ., 2022). Quinoxaline derivatives are the nitrogen containing heterocyclic compounds formed from the fusion of a pyrazine ring to that of benzene ring (Sibiya *et al* ., 2019).

Their DNA binding abilities distinctively allows them an opportunity to be explored in the anticancer field as a potential chemotherapeutic agent. The scavenging of free radicals' ability of the quinoxalines owes to the aromatic group, which allows them to interact with several molecules. The pyrazine ring allows them to bind and creates an interference in DNA replication (Sibiya *et al*., 2019). This study focuses on inducing apoptotic cell death in cervical and breast cancer cells using quinoxaline derivatives. As a result, a novel group of quinoxaline derivatives have been synthesised to determine their capacity as anticancer agents. The structures of these compounds have different extinctive moieties added to the core benzopyrazine ring as demonstrated on figure (1.1 a- 1.1 b).

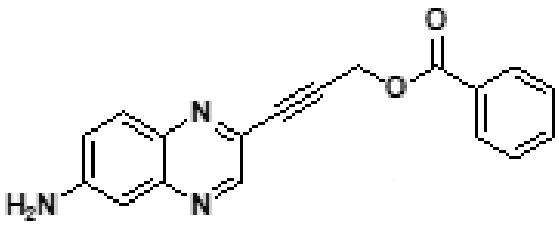

Figure 1.1 (a) The structure of quinoxaline LAM-29A. Quinoxaline LAM-29A is made of the quinoxaline core the pyrazine group with two nitrogen atoms and benzene ring attached to the amino group. In addition to the amino group the propanyl and

benzoate structures are added to modify the original core structure (Lekgau et al. (2022).

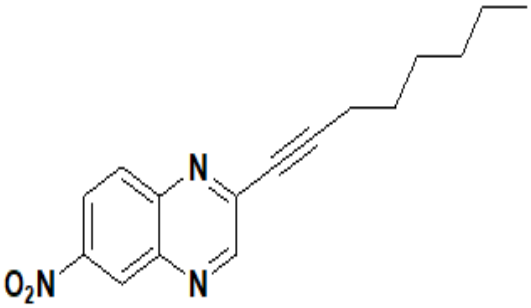

Figure 1.1. (b) The structure of quinoxaline LAM-21D. The structure of LAM-21D is composed of the dinitrogen oxide group attached to the benzene ring and the octane branch to the pyrazine ring (Lekgau et al. (2022).

1.2 Cancer

Human beings have been plagued by cancer for ages. This illness arises because of deviations from the normal set points in the cells' processes and functions. It is best described by (Hausman, 2019) that the human cells are cancer's agents of destruction that have somewhat been recruited into pathological organisms or tumour building blocks. The hallmark of cancer includes sustained and prolonged proliferative signalling, evasion of growth suppressors, avoidance of cell death signals, replication immortality, induction in angiogenesis and ability to become invasive and metastatic. Cancer formation starts with mutation on the DNA, these mutations can be due to errors that might occur during DNA replication or rather some chemicals that damages the DNA (Yamaguchi and Perkins, 2020). The main elements pertaining to the pathogenesis of this disease includes environmental (physical and chemical), biological and hereditary factors (Vaghari-Tabari *et al.,* 2020: (Lewandowska *et al*., 2019). Although these are labelled as the major contributors, cancer development in individuals can also be due to an interaction between various factors (Lewandowska *et al*., 2019.

1.2.1 Cancer and oxidative stress

Oxidative stress can be described as a disparity in the production of reactive oxygen species (ROS) such there are more oxidants and very few antioxidants which creates a disruption in the redox reactions resulting in a detrimental damage to the DNA and other essential macromolecules. To have a stable redox system, a balance should be maintained between reduction and oxidation reactions. If this balance is disrupted that can favour molecular changes which will eventually damage tissues and cells of the body. Free radicals/ROS are those molecules lacking paired electrons in their outermost energy levels which makes them highly reactive (Singh *et al*., 2022).

This includes peroxides, superoxide, and hydroxides radicals, as well as nitrogen and oxygen species. Free radicals are beneficial to the living systems only at lower concentrations where they play a crucial role in many signalling pathway processes. The only detrimental problem they pose occurs when they are overproduced. Their sources can be both internal and external. Their endogenous sources include the mitochondrial respiratory enzymes such as xanthine oxidase,

cytochrome oxidase, NADPH, and other metal compounds. Exogenous sources can be poor diet, smoking, radiation, and pollution (Singh *et al*., 2022).. In normal metabolic pathways hydroxyl radicals are produced as by- product of their metabolism, such radicals introduce DNA breaks that can be lessened by the presence of antioxidants (Eastman and Barry, 1992). Reactive oxygen species damages the DNA and may cause the intrinsic apoptotic cascade to begin which eventually activates p53. The activated p53 will in turn activate pro-apoptotic Bcl-2 proteins which will promote apoptosis (Liao, 2022). These species at high concentrations can damage mitochondrial DNA since it is located closer to the free radical production sites than the nuclear DNA. The DNA bases: purines and pyrimidines are attacked by the hydroxyl radicals which modifies the DNA by inducing single or double strand breaks that eventually alters the epigenetics, shorten the telomeres and cause mutations in the Y chromosomes (Singh *et al* ., 2022). Accumulation of the reactive oxygen species can give rise to mutated oncogenes or tumour suppressor genes (Dasgupta and Klein, 2014).Oncogenic proteins such as MEK and Raf ultimately will become overexpressed and tumour suppressors such as p53 and p21 will be silenced then causing cellular senescence (Kaushik *et al* ., 2022).

Majority of cancer treatments work by inducing ROS production in cancer cells. This causes oxidative stress which will results in irreversible apoptosis induction. They trigger what is commonly referred to as ROS-mediated apoptosis. This will re-activate the evaded apoptosis in cancer cells. However, this mechanism plays a double- edged sword role since it eliminates cancer cells but it also causes damage to the normal cells leading to neurotoxicity and cardiotoxicity. Antioxidants medications are often administered to manage the side effects of treatment (Conklin, 2004b).

1.2.2 Cancer and cell cycle

Once a cell gets acted on by a mitogenic or anti-mitogenic signal it can either proliferate or not. The progression of cell cycle in mammalian cells comprises of four distinctive phases, i.e., G0, G1, S and G2 which are tightly regulated by Cyclin-cyclin dependent kinase complexes (CDKs). There are also various checkpoints that ensures that cells can proceed into a different phase with no DNA damage. If there are damaged cells, then they tend to be arrested followed by expression of repair

proteins (Besser and Slingerland, 2016).. In the Gap 0 (G0) cells are not dividing and outside the cell cycle, (G1), cells get ready for DNA replication, synthesis (S) DNA gets synthesized, and (G2) where the size of the cells increase, and they grow further. Cell cycle regulators such as the tumour suppressor Retinoblastoma (pRb) plays a role of regulating the progression of cells at G1 phase. Once it is phosphorylated by CDK/cyclin complexes, it will liberate E2F so it can transcribe genes required for transiting G1 to S phase (Nair and Yadav, 2022).

Cancer cells are characterized by their adamant ability to continue dividing in phases were normal cells usually stop dividing (uncontrolled cell division) (Taylor and Grabovich, 2009). Once cell cycle regulators get mutated, the process will become deregulated and facilitate cancer formation and progression (Nair and Yadav, 2022). (Nair and Yadav, 2022). P53 has a role played in the cell cycle by arresting cells post DNA damage and downregulating cell cycle genes. This occurs when p53 gets phosphorylated by ATM (Ataxia-telangiectasia-mutated) which will decrease its binding affinity to MDM2 (Mouse Double Minute-2) ubiquitin ligase (Rivas and DeCaprio, 2022). Mutation of the cell checkpoint protein ATM (Ataxia-telangiectasia-mutated) results in loss of its function which then causes tumour progression (Nair and Yadav, 2022).

1.3 Breast cancer

Breast cancer increases mortality rates in women globally. It is linked to genetic susceptibility or family history in about 10% of cases, with differences depending on country and race. There are several genes which are linked to breast carcinogenesis, but BRCA1 and 2 are the most studied genes which are often used as markers for breast cancer testing. Mutations, deletions, and rearrangements in BRCA genes tends to yield the triple negative tumour phenotype (Shiovitz and Korde, 2015). Epigenetic factors such as Histone modifications, non-coding RNAs (ncRNA) and DNA methylation, and are also linked to breast cancer (Natesh *et al.*, 2022.

There are several attempts and literatures available that tried to cluster this disease into different respective groups according to shared characteristics. The two breasts contain ducts, fatty tissues, and glands (American Cancer Society, 2022). Majority of breast cancers develops in the epithelial cells of the terminal

duct lobular units (TDLUs) that serve as the breasts' functional units which are tiny channels that run from the lobules to the nipple, carrying milk Costa *et al*., 2020; American Cancer Society, 2022). The breast cancer subtypes are based on hormone receptivity, on whether the oestrogen receptor (ER) and/or progesterone receptor (PR) and the epidermal growth factor receptor 2 (HER2) are expressed or not Costa *et al*., 2020).

1.4 Breast cancer subtypes

1.4.1 Luminal A

Luminal name of this subtype owes to the similar immunophenotyping pattern of the luminal epithelial component of the mammalian milk duct (Horvath, 2021). When looking at the hormone receptivity of this subtype, it is characterized by the presence of both oestrogen and progesterone without HER2 receptors (Horvath, 2021). It also has low Ki-67 protein levels, which acts as a marker for proliferation. Luminal A cancers have a good prognosis and grows at a slower rate than other cancer types (Horvath, 2021). For this paper the specific breast cancer cell line is classified within this subtype, MCF-7.

1.4.2 Luminal B

Luminal B cancers are identified by positive oestrogen receptors, negative HER2 and progesterone and grows at a faster rate due to high Ki-67 protein levels. Because Ki-67 is higher than in Luminal A, they grow rapidly and have a worse prognosis (Horvath, 2021.

1.4.3 HER2 positive

In majority of the epithelial tumours the HER2 proto-oncogene located on chromosome 17 is over-expressed and it encodes for a tyrosine kinase protein found in the membrane of malignant cells. Tumour cells in this subtype are characterised by an additional copy of the HER2 gene that has been linked with the action of altering some other genes inclusive of angiogenesis genes. This cancer subtype has high levels of the Ki-67 protein and is also associated with inducing mutations in protein responsible for executing DNA repair mechanisms and fostering cell death in case the cell, p53. With a mutated/altered p53, cancer cells will divide and avoid cell death signals. Due to all these alterations, this breast cancer subtype is aggressive. The other two groups within this subtype are HER2 luminal and enriched HER2 (Horvath, 2021).

1.4.4 Triple negative (TNBC)

This is named after a phenotypic pattern of tumours that are negative for all the three; oestrogen, progesterone and HER2 (Horvath, 2021). About 15–20 percent of all TNBC cases are linked to BRCA1 or BRCA2 hereditary mutations (Loibl *et al* ., 2021). TNBC tumours do not express the HER2 and lacks ER and PR receptors (Borri and Granaglia, 2021; Harbeck *et al* ., 2019). This is the most invasive subtype owing to high mutation rates of the p53 with poor prognosis and more likely to recur after therapy (Horvath, 2021; American cancer Society, 2022).

1.5 (a) Treatment options available for breast cancer

1.5.1 Chemotherapy

This is applicable to tumours that are highly proliferative or expresses more of Ki-67 antigen, such as Luminal B, Triple negative cancers and HER2 positive (Horvath, 2021). Chemotherapy uses medications to prevent cancer cells from growing, dividing, or surviving. Chemotherapeutic drugs can be used as a single treatment for cancer, or in concert with other cancer treatments to shrink tumours and make them easier to remove by surgery or radiation therapy (Anisman and Kusnecov, 2022). There are different chemotherapeutic drugs that exhibit different mode of actions this includes alkylating agents, antibiotics, antimetabolites, corticosteroids, and inhibitors (signalling, mitotic and topoisomerase inhibitors) which interferes with the synthesis of DNA and its replication (Mathan *et al*., 2022).

These drugs primarily target actively dividing cells, but they also harm normal cells, resulting in harmful adverse effects. Chemotherapy causes harm to the gastrointestinal tract and lead to cardiac toxicity, nausea, vomiting, weight loss, anaemia, and diarrhoea (Mathan *et al*., 2022). Chemoresistance is one of the issues with this treatment option. This poses a threat in cancer therapy. There is a need to develop/explore new cancer therapy strategies to avoid the issues of drug toxicity and resistance.

1.5.2 Radiation therapy

The use of high-energy radiation works in such as electrons, protons, gamma, and x-rays to treat early, or localized, and metastatic tumours (Mathan *et al*., 2022). Radiation therapy works by inducing enormous DNA damage in cancer cell genomes, which causes cell death through apoptosis (Makhoul, 2018). This can either be a direct

or indirect DNA damaging mechanism. In the direct act, the target DNA within the cell is directly affected by a particular radiation particle while with indirect there is interaction between the molecules within the cell together with the radiation particles mainly the electrons and protons to produce free radicals that will eventually damage the DNA (Rodrigues, 2021). 2021). Radiation therapy when used to treat breast cancer its often associated with long term side effects such as dermatitis, breast edema, shrinkage, pain, and fibrosis (Yazbeck *et al*., 2022).

1.5.3 Targeted therapy

This relies on the use of specific molecules to administer/exhibit a specific action towards a certain cell type as the name suggests. Targeted therapies are drugs or chemicals that limit the growth and spread of cancer through the interference of specific molecules that are involved in the growth of tumour and its progression as defined in accordance with National Cancer Institute (NCI) (Desai *et al* ., 2019). Targeted therapies are a diverse range of drugs used to treat cancer, including monoclonal antibodies, tyrosine kinase inhibitors, and other small molecule inhibitors. The most studied therapeutic agents include tyrosine kinase inhibitors (TKIs) which work on cancer cells by blocking upregulated signal pathways in the cell, resulting in reduced cellular growth and proliferation (Reeves, 2016). Some of the side effects associated with the usage of TKIs include fatigue, diarrhoea, nausea, and hypertension (Reeves, 2016).

1.5.4 Endocrine therapy

Endocrine/hormonal therapy is for all patients whose breast cancers expresses oestrogen and progesterone receptors at all stages, excluding those with hormone receptor negativity. Endocrine therapy is effective in 75 to 80 percent of patients with malignancies that are positive for both ER and PR (Harichand-Herdt *et al*., 2009). Endocrine treatment works primarily by inhibiting ER binding using an agonist or deprives the tumour of oestrogen (Rasha *et al*., 2021).Cell division is aided by oestrogen and progesterone hormones and these hormones have receptors in some breast cancers as already outlined on the previous sections of this literature. The presence of these hormones in tumour cells is a clear indication that these are highly required to fuel the formation and proliferation of tumour cells (Horvath, 2021).

Breast cancers with low levels of progesterone and oestrogen receptors (PR and ER), and high KI67 and HER2 expression are less sensitive to hormonal treatment while those with high PR and ER, low KI67 and HER2 expression are more sensitive to endocrine treatment. Tamoxifen is a common modulator of oestrogen used in hormonal therapy has been shown to suppress breast cancer cell proliferation by competing with estrogen at the oestrogen receptor (ER). Even though tamoxifen is an effective treatment for all phases of hormone receptor–positive disease, it is linked to several negative side effects, including thromboembolic events, menopausal-like, and endometrial cancer (Harichand-Herdt *et al*., 2009). Other shortcomings about hormonal therapy are the issue of acquired resistance to ER-targeted medications which is due to ER mutations that occur on conserved regions of the ER which are essential for the activity of ER (Rasha *et al*., 2021).

1.5.5 Immunotherapy

The main target here is not tumour cells per se but the goal of immunotherapy is to reactivate the numerous antitumor immunological processes in the host (Horvath, 2021) Immunotherapies primarily targets immunological checkpoints, which are biological mechanisms that tumour cells exploit in suppressing the immune responses (Skala *et al*., 2022). This makes use of monoclonal antibodies (mAbs) which are developed for this treatment and employ a number of mechanisms, including (a) eliminating tumour cells directly which can trigger apoptosis or by delivering cytotoxic molecules such as drugs, enzymes, radioisotopes and toxins, (b) stimulation of immune cells so they can execute tumour cell eradication mediated by the immune system, and (c) disruption of the vascular and stromal systems (Barzaman *et al*., 2021).

Commercially available recombinant humanized mAbs for breast therapy include Pertuzumab, and Trastuzumab (Jain *et al*., 2021).The problem with using mAbs is that mutations in tumour cells may frequently occur, resulting in monoclonal antibody resistance through alternate mechanisms (Barzaman *et al*., 2021). There are diverse approaches that can be exploited for this treatment others includes, cancer vaccines, radio immunotherapy, adoptive cell, and oncolytic viral therapies (Barzaman *et al*., 2021; Jain *et al*., 2021; Shahidian *et al*., 2020; Skala *et al*., 2022).

1.6 Cervical cancer

Cervical cancer is ranks on the fourth position among the most common malignancy in women worldwide. It primarily affects women in countries with limited access to health-care services such as vaccination, screening, and treatment options (Jalil *et al*., 2021). Several cross-sectional analyses in South Africa have indicated that between 60 and 80% of women test positive for Human papilloma infection, with a cervical cancer diagnosis incidence of 30.2 cases per 100 000 women (Burmeister *et al*., 2022). Almost all cervical malignancies are caused by persistent infection with forms of human papillomavirus (HPV) (Jalil *et al*., 2021). These viruses inhibit the apoptotic signals and cell cycle checkpoints so they can replicate resulting in chromosome instability and genome instabilities generating mutations that can ultimately lead to cancer (Krump and You, 2018; Teruel *et al*., 2019).. In this study CaSki cells which are HPV-16 positive cell line are used.

1.7 Classification of cervical cancer

The cervix is the region where cervical cancer starts, which is a thin entrance into the uterus that is connected to the vaginal canal via the endocervical canal. The cervix is separated by two sections: the ectocervix and the endocervix. Stratified squamous epithelial cells makes up the ectocervix, whereas the endocervix is coated with simple columnar epithelial cells. The "transformation zone," which is made up of metaplastic epithelial cells, it is where the two regions meet and at that area it is where cervical cancer is most likely to grow and spread. Histologically cervical cancer is divided into two major sub-types which are squamous cell carcinoma (SCC) and adenocarcinoma (Burmeister *et al*., 2022).

1.7.1 Squamous cell carcinoma (SCC)

SCC arises from squamous cells of the ectocervix and contributes 75% of cervical cancer cases and it is the most common subtype of cervical cancer (Burmeister *et al*., 2022). In the cervical epithelium, squamous cells go through alterations as cervical cancer progresses, which results in lesions known as cervical intraepithelial neoplasia (CIN) (Burmeister *et al*., 2022). This subtype is highly linked with infections by the Human Papilloma viruses (Jhingran and Meyer, 2021. SCC of the cervix are characterized by high mutation rates of p53 and pathologically (Knottenbelt *et al*., 2015).

1.7.2 Adenocarcinoma of the cervix (AC)

Adenocarcinoma arises from glandular cells in the endocervix that produces mucus (Burmeister *et al.*, 2022). This carcinoma is identified by abnormal levels of mediators involved in the cell cycle that includes p53, cyclin E, p21, p16 and p27 (Hopkins and Smith, 2004). This subtype can spread locally around the pelvic regions (Jhingran and Meyer, 2021).

1.8 (b)Treatment options for cervical cancer

1.8.1 Surgery

This is used to remove cancers in their early detected stages through the removal of a cancerous and metastasized tissue physically. There are several types of surgery involved in the treatment of cervical cancer and they rely on the stage of the disease and how it has spread (Burmeister *et al*., 2022).

1.8.2 Chemotherapy

This is often administered following surgery treatment when tumour highlights recurrence risks. In the treatment of cervical cancer. Chemotherapy makes use of a platinum-based cisplatin. To treat tumour that has advanced or spread to the local cells, chemotherapy can be combined with radiation therapy which can also help mitigating the recurrence of the disease. Chemotherapy lacks specificity in terms of which cells to eliminate since it targets both normal and cancerous cells which can weaken the body by causing alopecia and anaemia (Burmeister *et al*., 2022).

1.8.3 Radiation therapy

To treat cervical cancer, the commonly used form of radiation therapy is the external beam radiation therapy (EBRT) which directs high energy radiant beams to the tumour which emanates from outside of the body. Radiotherapy like any other cervical cancer treatment options is also associated with several side effects ranging from diarrhoea, sexual dysfunction to pelvic pain and abdominal cramps (Burmeister *et al*., 2022).

1.8.4 Immunotherapy (HPV vaccines)

This primarily targets the expression of oncoproteins pertaining to the Human Papilloma Virus. HPV vaccines have been created to prevent cervical cancer. To provoke or induce an immune/antibody response, HPV vaccines make use of virus-like particles. This has been shown to offer defence against the high-risk HPV-16 and

18 strains that account for nearly 70% of instances of cervical cancer. However, the cost of producing these vaccines is high (Fatemi *et al*., 2022).

1.8.5 Targeted therapy

This primarily focuses on eliminating or targeting molecules that are expressed and required by the cancer cells to thrive, grow, proliferate, and spread. In terms of cervical cancer, the developed therapeutic targets' potential aims at targeting pathways used by oncogenes and drug resistance mechanisms in the cervical cancers. Cell cycle components become activated in cancer cells, and they become recognised as the targets for therapy. Whenever there is DNA damage, cells are constraint to enter the mitosis phase by the Wee1 through the inhibition of cyclin B/CDK1 phosphorylation. In cervical cancer, Wee1 is upregulated, and its action is inhibited by MK-1775 which is an identified therapeutic target (Burmeister *et al*., 2022).

1.9 Apoptosis

Death is also an important aspect in the life cycle of cells together with development and differentiation. To maintain homeostasis in the living environment, a balance needs to be maintained between cell proliferation and cell death (Walia *et al*., 2021). Apoptosis is in fact one of the most important processes for cell survival. Apoptosis is defined as a programmed cell death, which is a widespread occurrence that is essential to many pathological and bodily processes (Walia *et al*., 2021). It maintains homeostasis by eliminating cells that have a potential to pose danger in the cellular environment, this includes surplus lymphocytes, damaged as well as infected cells. Apoptosis not only maintains homeostasis it also plays a role during embryonic development where it removes unnecessary tissues during morphogenesis and tissue organization (Liao, 2022). This form of cell death depends on ATP, and it is characterized by condensation of the chromatin, cytoplasmic shrinkage, fragmentation of nuclear DNA, blebbing of the plasma membrane, development of apoptotic bodies, and eventually dead cells elimination by the phagocytes (Kim-Campbell *et al*., 2019).

Apoptosis is considered a non-inflammatory process since cells undergoing apoptosis releases metabolites which serves as a signal to be engulfed by phagocytes within the neighbouring cells therefore no immunogenic signals are released (Liao, 2022 2022).This is a tightly regulated process such that it does not cause neurodegenerative illnesses if it occurs excessively and also not neoplastic diseases

if its inefficient (Matsuura *et al*., 2016). There are two pathways apoptosis follows based on the origin of the initiating stimuli/signal (Kim-Campbell *et al*., 2019) of the two pathways one interacts with the death receptors together with their corresponding ligands including the Fas and TNF-1 (tumour necrosis factor-1) receptor. The other pathway involves the mitochondria and is regulated by the members of the BCL-2 includes the proapoptotic and antiapoptotic proteins. Although these two pathways may involve different components, but they ultimately lead to activation of the caspases resulting in cleavage of diverse proteins causing metabolic/biochemical and morphological changes (Walia *et al*., 20212021).

1.10 Biochemical features of apoptosis

Apoptotic cells may experience protein cross-linking as part of the apoptosis process. The DNA can break in fragments of 180-200 base pairs catalysed by Mg^{2+} -and Ca^{2+}-dependent endonucleases. DNA fragmentation can be detected by analysing DNA degradation using gel electrophoresis were by the degraded fragments usually appear having high molecular weight (HMW) (Khodavirdipour *et al*., 2021). Additionally, there is a production of cell surface markers, which ultimately results in the early phagocytic identification of apoptotic cells by nearby cells, enabling quick phagocytosis of the nearby tissue. This is accomplished by shifting the cell's normally inward-facing lipid bilayer to show itself on the plasma membrane's outer layers. Exposure of the phosphatidylserine on the external environment attracts phagocytes on the surface of apoptotic cells. Another prominent feature is the recruitment and activation of caspases which are a group of intracellular, aspartate-specific, cysteine-dependent proteases which plays a role of initiating and executing apoptosis (Kim-Campbell *et al*., 2019; Walia *et al*., 2021).

A homodimer is the functional unit of caspases consisting of a bigger and a smaller subunit within each monomer. They exist in their procaspase, inactive form that upon activation they can stimulate other caspases and accelerate the apoptotic signalling which will ultimately lead to cell death due to their proteolytic action. Caspases are grouped into three functional classes. Caspase- 2, - 8, - 9, - and -10 are initiators, caspase- 3, -6, and 7 are effectors/executioners while caspase- 1-, 4-, -5, -11, and 12 are inflammatory ones. Initiator caspases can activate effector caspases while activation of the initiator caspases can be due to apoptosome for caspase -2, P53-Induced Death Domain (PIDD) for caspase -2 and Death Inducing Signalling Complex

(DISC) for caspase -8 (Walia *et al*., 2021).Upon this cascade of proteolysis, apoptotic cells then undergo diverse morphologic changes which can cause the cytoskeleton to break down and the lipid composition of the cell membrane changes (Elkon and Oberst, 2018).

1.11 Apoptosis signalling pathways.

1.11.1 Intrinsic pathway

In this route, signal from the stimuli originate from inside the cell and then mediated by the mitochondria as shown on figure 1.2 (a). The series of events that occurs are better explained by (MOMP) which is the mitochondrial outer membrane permeabilization. In this process, proteins that are originally attached to the intermembrane of the mitochondria gets released whenever there is an interruption to the outer mitochondrial membrane (Elkon and Oberst, 2018. There are several cellular stresses such as endoplasmic reticulum stress due to unfolded proteins, oxidative stress, overloaded calcium in the cytosol, and damaged DNA which can activate the intrinsic pathway (Madkour, 2020b).

Upon DNA damage or any other triggers of this pathway, the levels of Bax increases and/or Bcl-2 decreases which result in permeabilization of the mitochondrial membrane to release proapoptotic proteins such as cytochrome-c which will subsequently activate procaspase-9. The released cytochrome- c then binds to Apaf-1 which is the (apoptotic protease activating factor) in an ATP- dependent manner to form an apoptosome which is a 7-subunit complex apoptosome (Walia *et al*., 2021). Recruitment and dimerization of caspase- 9 occurs through the action of the activated apoptosome which will eventually trigger apoptosis by cleaving and activating executioner caspases. Smac/Diablo and HtrA2/Omi are a couple of proapoptotic proteins that are also released during MOMP. They play a major role of attaching to and inactivating apoptosis inhibitors known as (IAPs) (Elkon and Oberst, 2018).

Other proapoptotic proteins includes Bax, Bak, Puma and Noxa. Both Puma and Noxa causes a p53- mediated apoptosis, Puma facilitates cytochrome-c release from the mitochondria by increasing the level of Bax while Noxa activates caspase-9 through binding to the antiapoptotic proteins. During the later stages of apoptosis other proteins such as Endonuclease G (EndoG), Apoptosis- inducing factor (AIF), and caspase- activated DNase (CAD) gets to be released (Madkour, 2020),

DNA gets to be fragmented into approximately 50 000 kilo base parts by the AIF whereas EndoG creates oligo-nucleosomal fragments of DNA from cleaving nuclear chromatin. Eventually CAD will enter the nucleus and cause DNA condensation. This pathway is strictly regulated by Bcl-2 antiapoptotic proteins by inhibition of the cytochrome-c which is the main component for the activation of caspase-9. The Bcl-2 proteins are also regulated by the tumour suppressor protein, p53 which arrests cells in the G1 phase of the cell cycle in case of DNA damage due to cellular stress. It then mediates apoptosis if the DNA is beyond repair by downregulating Bcl-2 or upregulating Bax (Madkour, 2020).

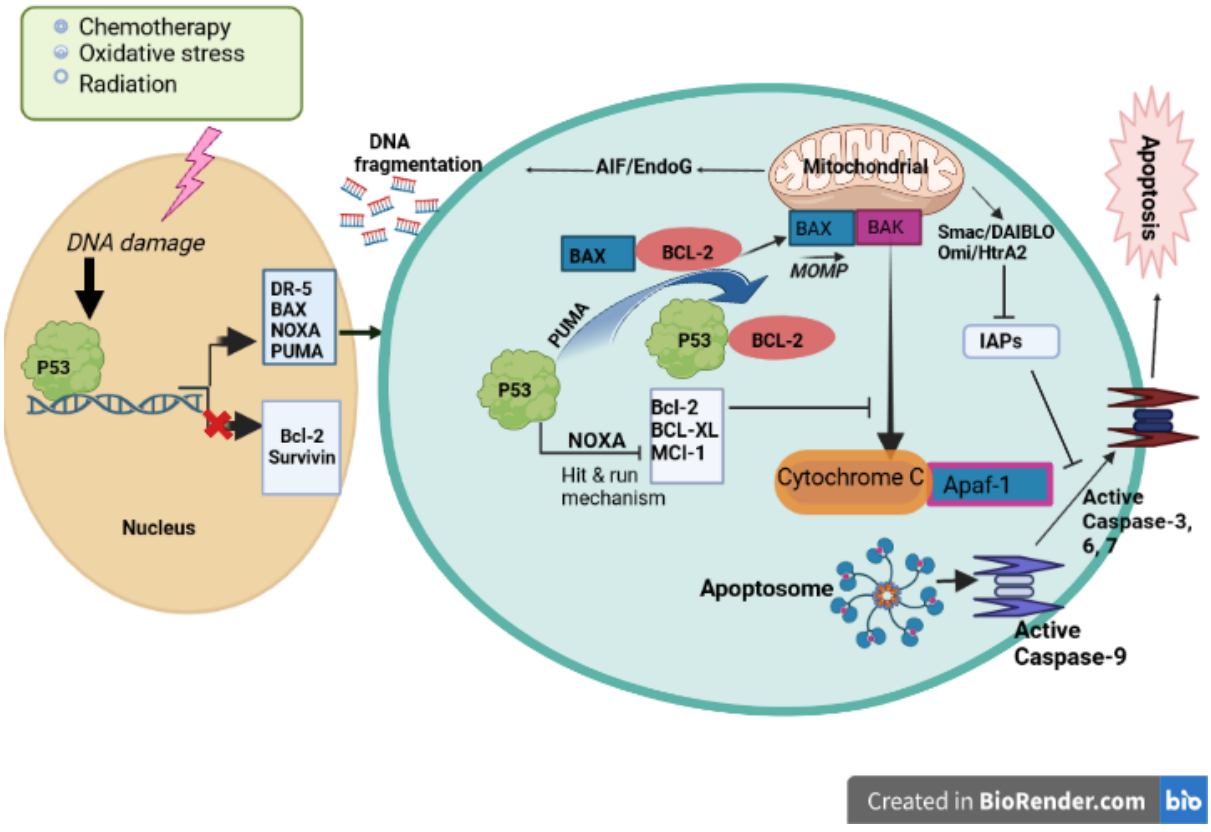

Figure 1.2 (a): A detailed summary of all the events taking place in intrinsic pathway of apoptosis. That starts with a signal from either oxidative stress or DNA damage due to cancer treatment strategies. This triggers p53 which then upregulated the pro-apoptotic proteins in which Bax and Bak forms a complex and binds on the mitochondria to trigger MOMP. This membrane permeabilization then releases other pro-apoptotic proteins such as Sma/Omi and cytochrome-c that forms a complex with Apaf-1. This results in an apoptosome formation of which activates caspase 9. Then

Caspase-9 activates executioner caspase-3,6 and 7 which will cause apoptosis. AIF/EndoG are also released by the mitochondria to cause DNA fragmentation on the cells undergoing apoptosis. The Bcl-2 proteins and IAPs tightly regulate this pathway (Nieuwenhuijs-Moeke *et al*., 2020).

1.11.2 Extrinsic pathway

The signal from the stimuli originates from outside the cell. This is based on transmembrane receptor- mediated interaction which can be seen on figure 1.2 (b). This pathway is inclusive of the death receptors which form part of the superfamily of the tumour necrosis factor receptor genes. Death signal from the cell surface is transmitted to the intracellular signal pathway through the extrinsic route. For this pathway there are several death receptors corresponding to their ligands, these includes TNF-α /TNFR1, FasL/FasR, Apo2L with DR4/DR5, and Apo3L/DR3 which are the major pairs. However, the extrinsic pathway events are prevalently characterised using (Tumour necrosis factor-α with its receptor) TNF-/TNFR1 and (Fas ligand with its receptor) FasL/FasR. Once ligand bind to its respective death receptor, adapter proteins get recruited from the cytoplasm (Walia *et al*., 2021).

When the TNF ligand bind to its receptor, TRADD (TNFR1 associated death domain) adaptor protein gets recruited and the binding of Fas ligand to its receptor allows FADD (Fas-associated Death Domain) adapter protein. These adapter proteins help in bridging death receptors to the procaspases so that a cascade of signalling events can begin (Walia *et al*., 2021). This will allow FADD to interact with the procaspase-8, then Procaspase-8 will be auto catalytically activated at this point because of the death-inducing signalling complex formation. Ultimately apoptosis gets triggered from the activation of caspase 8 (Walia *et al*., 2021).

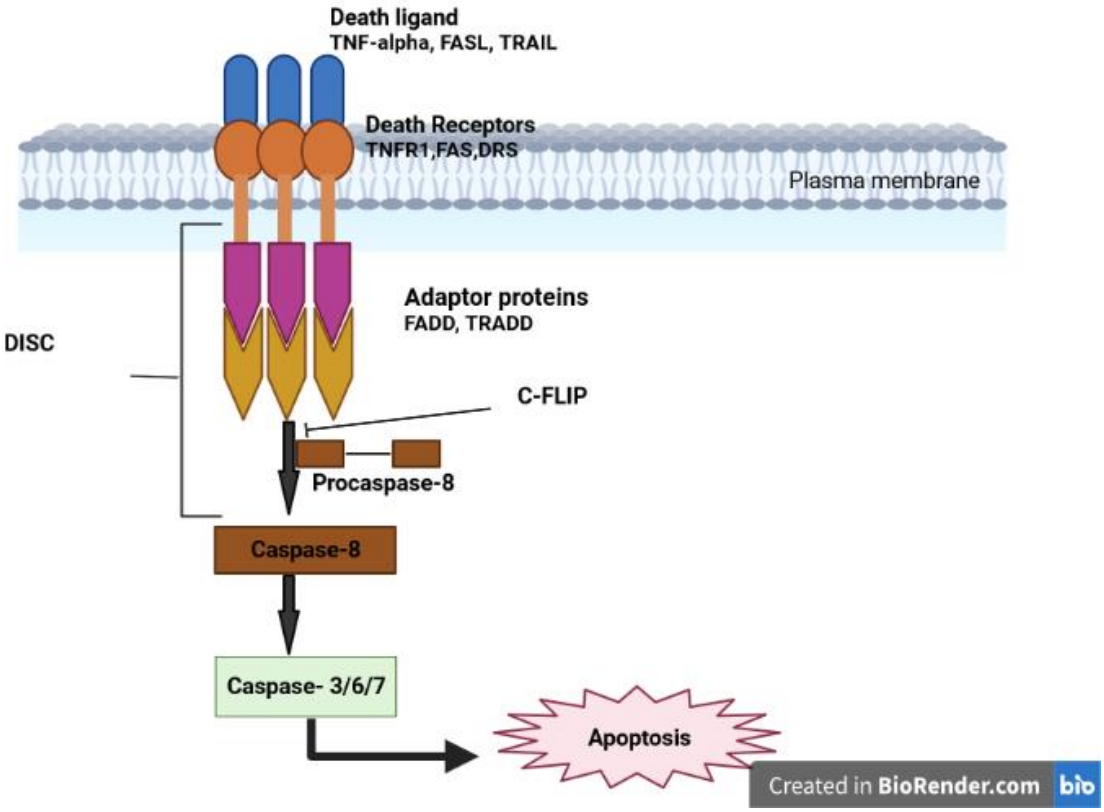

Figure 1.2 (b): A schematic representation depicting a summary of crucial aspects of extrinsic apoptosis. For extrinsic pathway death ligands binds to their corresponding receptors. The common models include the ones of TNF-alpha/TNFR1, FAS/FASL and DRs/TRAIL. Once an interaction forms among the pairs, adapter proteins FADD and TRADD gets recruited to the cytoplasm. This interaction allows procase-8/10 to bind, and this will eventually form Death inducing signalling complex (DISC) which will allow activation of pro caspases to caspases, then activation of caspase-3,6 and 7. This will eventually execute apoptosis (Nieuwenhuijs-Moeke *et al*., 2020; Thind and Arora, 2012).

1.13 Apoptosis as a therapeutic target for cancer

Just after the initiation of cancer, apoptosis is the first line of defence to respond to the rapid tumour proliferation. Resistance to apoptotic signals presents one of the hallmarks of cancerous cells (Kashyap *et al*., 2021). Defects in apoptosis mechanisms protect cancerous cells from hypoxia and oxidative stress, allow time for cancerous cells to accumulate genetic changes that suppress cell proliferation, obstruct differentiation, supports angiogenesis, and increase cell motility and invasiveness.

These genetic changes play important roles in the pathogenesis of tumors by allowing cancerous cells to live longer than they would otherwise be expected to (Reed, 2002). Moreover, there is high expression of antiapoptotic proteins in cancer which can drive apoptosis resistance (Fulda, 2015). Since tumour cells are constantly dividing, they become more susceptible to treatment strategies that evokes DNA damage and cause an interference in the cell cycle phases (Taylor and Grabovich, 2009). As a result, over the last decades the sole focus of drug development was on increasing sensitivity of cancer cells to apoptosis. Due to defined molecular activities and structures of major regulators of apoptosis large-scale efforts have been made to create small molecule compounds to trigger this programmed cell death in cancer cells as prospective cancer therapies. (Liao, 2022).

Therapeutic strategies employed to eliminate cancerous cells via apoptosis can work by directly acting on pro-apoptotic proteins, modulate anti-apoptotic proteins, act on death receptors, or rather restore the functions of tumour suppressor gene (p53) (Fleischer *et al*., 2006; Fulda, 2015). Apoptosis process can be triggered by enormous stimuli in cells this can include cancer treatment strategies such as chemotherapy and radiation which damages the DNA and induce the p53- mediated apoptosis in cells (Kashyap *et al* ., 2021). Anticancer agents that are platinum- based such as cisplatin can induce DNA adducts which forms DNA interstrands that would eventually result in kinking and unwinding of the DNA (Siddik, 2013). In case of a mutated p53 mediated pathway, therapeutic drugs such as 5-fluorouracil and cisplatin are used to induce apoptosis in breast and colorectal cancers. The Bcl-2 proteins engage in the intrinsic pathway of apoptosis and when they get mutated, therapeutic drugs such as Doxorubicin, Tamoxifen and G3139 assist in inducing apoptosis in cancers where Bax is mutated (Prasad, 2022c).

Again, death receptors are suitable structures for apoptosis target by therapeutic drugs since they have an extracellular domain to facilitate binding by antagonistic antibodies or recombinant ligands. In a way the surface of cancer cells has death receptors that can directly be targeted by these strategies (Fulda, 2015). These antagonist antibodies are still in human clinical trials which are designed in case of mutated death receptors which are required to transmit signals in extrinsic apoptosis (Prasad, 2022c). Beside the side effects of targeting apoptosis in convention cancer therapies, targeting apoptosis as a means of killing cancer cells has some critical drawbacks since some

apoptotic proteins may develop mutations that cause their production to be downregulated or fail to activate in their own wild-type form. For instance, mutations in the p53 proapoptotic gene are identified in roughly 50% of human malignancies, which reduces the responsiveness to anticancer drugs (Siddik, 2013).

1.14 Quinoxaline derivatives

Quinoxaline derivatives are a crucial class of heterocyclic compounds which are formed from the fusion between a benzene ring to that of a pyrazine. A couple of carbon atoms of the naphthalene ring are replaced by nitrogen atoms. These containing compounds can donate and accept electrons hence forming a network of interactions with other molecules. Most importantly, the N- containing heterocycles forms a crucial part of the pyrimidines and purine bases of the DNA They have a chemical formular of $C_8H_6N_2$ with a molecular weight of 130.15 g/mol. Quinoxalines are characterized by their ability to dissolve in water, and they have a low melting point of roughly (29-30) º C with a boiling point of (108-111/12) º C (Elgemeie *et al*., 2022). They are weak bases and tend to form salts when reacting with acids (el Newahie *et al*., 2019). Quinoxalines are synthetic with only few of the compounds occurring in nature such as echinomycin. There are various methods of deriving quinoxalines and lately the focus has been on those in green technology (Khatoon and Abdulmalek, 2021a)..

These group of compounds possess a wide array of biological activities, they are effective against neurological disorders, leishmania, depression, cancer, bacterial and viral diseases. These outstanding activities are made possible by their core structure derivatives' spectrum of activities depends on the different substitutions of groups on the core nucleus. The potential towards cancer relies on substitutions that occur on the carbonyl group which has an increasing activity in this order: ethyl < isopropyl < tertbutyl < phenyl groups (el Newahie *et al*., 2016). The structures of quinoxalines can be modified to create vast moieties with outstanding pharmacological effect having the capacity to fight various diseases with minimal or no side effects (Khatoon and Abdulmalek, 2021a). The world is evolving, and chemotherapy would require novel anticancer drugs to surpass the associated side effects. There are various known quinoxalines that inhibit the growth of neoplastic cells. These includes chloroquinoxalinesulfonamide (CQS), and 2-(4-(7-chloroquinoxalin-2-yl) phenoxy] propionic acid (XK469) (Fayed *et al*., 2021).

1.15 Mechanism of action as anticancer agents

There is still a need to develop anticancer treatments that will be specific to the cancerous cells which will create very minimal or no side effects as well. The discovery of quinoxaline derivatives has attracted so much research interest such that they are explored in medicine and in pharmaceuticals. The ability of quinoxalines to bind DNA and hinder the replication process is made possible by the pyrazine ring structure of the quinoxalines. Then the benzene ring structure allows the quinoxalines to scavenge free radicals and additionally grant it the ability to chemically interact with various molecules/substances of biological systems (Sibiya *et al.*, 2019).

Quinoxaline structures are aromatic also known as chromophores; they can intercalate in between the base pairs of the DNA forming non- covalent bond with the bases. The formation of this complex between the DNA and the compounds affects the structure of the DNA by uncoiling it and distorting the shape. The changes in the structure of the DNA due to the intercalation have an effect in the DNA recognition as well as its interaction with linked proteins, and relative enzymes which plays a crucial role during DNA synthesis, transcription and repair processes hence prohibiting the normal functions of these systems. Furthermore, the intercalation by the aromatic compounds has an impact on the reduction of DNA length as well as its helical twists. A well-studied quinoxaline analogue which acts as a DNA intercalator is echinomycin and it has demonstrated to be having anticancer potential and currently placed under phase I and II of clinical trials (El-Adl *et al*., 2020).

Majority of the chemotherapeutic agents are known to create breaks in the DNA that is sufficient to induce apoptosis in the cells (Eastman and Barry, 1992). Quinoxaline derivatives have the capacity to induce apoptosis in cancer cells as one of their modes of action (el Newahie *et al*., 2019). Recently synthesized quinoxalines such as 8-chloro-4-(4-chlorophenyl)pyrrolo[1,2-a]quinoxaline was found to selectively inhibit the proliferation of breast cancer cell lines and had a regulation of the cell cycle proteins such as p21 and p21 (Sibiya *et al*., 2019). Other novel synthesized quinoxalines such as Grazoprevir have been approved to treat several resistant strains of Hepatitis- C virus (Elgemeie *et al*., 2022). Brimodine has been approved to treat glaucoma, and Erdafitinib to treat bladder cancer. Those that are still under clinical trials includes Chloroquinoxaline Sulphonamide (CQS) which has been assessed to

treat small cell lung cancer and stage IV colorectal cancer (Montero *et al*., 2022). There are enormous structures of quinoxalines that are synthesized to explore their potential in inducing cell death in various cancer cell lines. The research on quinoxalines has drawn attention in exploring the potential of these remarkable group of compounds that might create breakthroughs in medicinal and pharmaceutical research.

1.16 Aim, objectives, and hypothesis of the study

AIM

To investigate the ability of quinoxaline derivatives to induce apoptotic cell death in cervical and breast cancer cell lines.

OBJECTIVES

The objectives of the study are to:

i. determine the maximum spectral wavelengths and the antioxidant potential of the quinoxaline derivatives using absorbance spectra, DPPH, ferric reducing power, and total phenolic content assays.
ii. determine the effect of quinoxaline derivatives on cell viability of MCF-7 breast cancer, CaSki cervical cancer and Hek 293 kidney cells using MTT assay.
iii. assess the morphological changes of CaSki and MCF-7 cells after treatment with quinoxaline derivatives.
iv. analyse the apoptotic inducing effects of quinoxaline derivatives on CaSki and MCF-7 cells using Muse^{TM} Annexin-V and dead cell assay.
v. evaluate the effect of the quinoxaline derivative on production of reactive oxygen species in CaSki cells.
vi. determine the effect of quinoxaline derivatives on the proliferation of cancer cells using Muse^{TM} KI67 proliferation assay.
vii. assess the effect of quinoxaline derivatives on the cell division cycle in CaSki cells.

HYPOTHESIS

The novel synthesized quinoxaline derivatives have anticancer, free radical scavenging and reducing power properties that can induce cell death through apoptosis against cancer cells of the breast (MCF-7) and cervix (CaSki).

CHAPTER 2

METHODS AND MATERIALS

2.1 Materials, equipment, and cell lines

Quinoxaline derivatives (LAM-29A and LAM-21D) were synthesized from department of Chemistry at University of Limpopo, DU® 730 Life Sciences UV/Vis spectrophotometer (Beckman Coulter, South San Francisco, California, USA), Multiskansky plate reader (Thermofisher Scientific, USA), DMEM (Dulbecco's Modified Eagle Medium) (Hyclone, USA), RPMI (Roswell Park Memorial Institute) medium) (Hyclone, USA), L-glutamine (Sigma-Aldrich, Germany), PSN (Penicillin, Streptomycin and Neomycin) (Sigma-Aldrich, Germany), FBS (Foetal Bovine Serum) (Sigma-Aldrich, Germany), Life Technologies countess II FL automated cell counter (Thermofisher Scientific, USA), Trypan blue dye (Thermofisher Scientific, USA), MTT (3-(4,5-dimethylthiazol-2-yl)-2,5-diphenyl-2H-tetrazolium bromide) solution (Thermofisher Scientific, RSA), DMSO (Dimethyl sulfoxide) (Saarchem, South Africa), Muse™ assay kits (Ki67 proliferation kit, Annexin V and dead cell kit, oxidative stress kit and cell cycle kit) (Luminex corporation in Austin, U.S.A), Trypsin (Lonza, USA), Curcumin (Sigma-Aldrich, Germany), PBS (Phosphate buffered Saline) (Sigma-Aldrich, Germany), MCF-7 cells (ATCC HTB-22), CASKI cells (ATCC CRM-CRL-1550), HEK-293 cells (ATCC CRL-1573), Guava® Muse™ Cell analyser, CO_2 incubator (NAPCO model, Instrulab cc, Johannesburg, RSA), and Fluorescence microscope and inverted microscopes (Nikon, Japan).

2.2 Drug preparation

Synthesis of 6-nitro-2-(oct-1-ynyl) quinoxaline (LAM-21D) Lekgau et al, (2022).

Compound LAM-21D (300 mg, 0.9 mmol) was treated with 1-octyne (0.15 mL, 1 mmol, 1.2 eq.). Purification on flash silica, eluting with 1:9 EtOAc: n-hexane afforded 6-nitro-2-(oct-1-ynyl) quinoxaline as a brown solid (172 mg, 67 %). M.p 200.5-202.5 °C; 1H NMR (400 MHz, CDCl3, ppm) 0.88 (t, 3H, J = 6.8 Hz), 1.31 (m, 4H), 1.47 (quin, 2H, J = 7.2 Hz), 1.68 (quin, 2H, J = 7.2 Hz), 2.55 (t, 2H, J = 7.2 Hz), 8.15 (d, 1H, J = 9.2 Hz), 8.50 (dd, 1H, J = 9.2 Hz and 2.4 Hz), 8.91 (s, 1H), 8.93 (d, 1H, J =2.4 Hz); 13C NMR (100 MHz, CDCl3, ppm) 14.0, 19.7, 22.5, 28.0, 28.6, 31.2, 78.8,99.9, 123.9, 125.5,

130.6, 139.4, 142.9, 144.5, 147.6, 149.4; Vmax (FTIR) 538, 742, 741, 1072, 1182, 1337, 1516, 2214, 2923, 3037 cm-1; HRMS (ESI) [M + H+]: m/z 284.1404.

Synthesis of 3-(6-aminoquinoxalin-2-yl)prop-2-ynyl benzoate (LAM-29A) Lekgau et al, (2022).

To a suspension of compound LAM-29A (60 mg, 0.18 mmol) in EtOAc (10 mL) was added SnCl2 (171 mg, 0.9 mmol, 5 eq.) according to procedure of reduction reaction. Purification on prep TLC with EtOAc: n-hexane (1:1) afforded 3-(6- aminoquinoxalin-2-yl)prop-2-ynyl benzoate as yellow solid (41 mg, 75 %). M.p 199.3- 201.5 °C. 1H NMR (400 MHz, CDCl3, ppm) 4.35 (brs, 2H), 5.22 (s, 2H), 7 .08 (d, 1H, J = 2.5 Hz), 7.18 (dd, 1H, J = 9.0 and 2.6 Hz), 7.43-7.47 (m, 2H), 7.55-7.60 (m, 1H), 7.82 (d, 1H, J = 9.0 Hz), 8.08-8.10 (m, 2H), 8.73 (s, 1H); 13C NMR (100 MHz, CDCl3, ppm) 52.9, 84.3, 85.7, 107.6, 122.7, 128.4, 129.3, 129.9, 130.4, 133.4, 133.9, 137.1, 143.3, 147.3, 148.9, 165.8; Vmax (FTIR) 546, 705, 1096, 1260, 1476,1614, 1708, 2087, 2919, 3221, 3335 cm-1; HRMS (ESI) [M + H]+ :m/z 304.1094.

Quinoxaline LAM-21D with a mass of 240 mg, and molecular weight = 283 g/mol was dissolved in 20 mL (100%) DMSO to make final concentration of 42.5 mM. The stock solution of 42.5 mM was diluted with DMEM/RPMI-free FBS to 2 mM to be used in cell culture assays. LAM-29A with a mass of 22.3 mg, and molecular weight of 303 g/ml was suspended in 5 mL DMSO to a final concentration of 14.8 mM. This stock solution of LAM-29A was further re-suspended in DMEM/RPMI-free FBS to a final working concentration of 2 mM. For the non-cell-based assays the compounds were re-suspended in distilled water.

2.3 non-cell-based assays.

2.3.1 Wavelength determination

To measure the spectral wavelength of LAM 29A and LAM 21D, 10 µL of the compounds were diluted with 990 µL of distilled water in micro centrifuge tubes and the solution was transferred to cuvettes. Distilled water was used as a blank. Optical properties of LAM-29A and LAM-21D were measured using the DU® 730 Life Sciences UV/Vis spectrophotometer at broad wavelength (200 nm-700 nm).

2.3.2 Reducing power assay.

Ferric reducing antioxidant power (FRAP) assay.

The ferric reduction potential of quinoxaline LAM 29A and LAM 21D was determined using FRAP assay. This is based on the conversion of the colourless Fe3+/ tripyridyltriazine complex into a vivid blue Fe2+/ tripyridyltriazine complex once there is presence of antioxidants in the quinoxalines (Spiegel *et al*., 2020). An increase in absorbance measurement correlates with the antioxidants present in the quinoxaline derivatives. Quinoxalines and (1%) ascorbic acid in varying concentrations ranging from (0.0125, 0.025, 0.2 and 1 mM) were suspended in 100 µL of distilled water together with 250 µL of both phosphate buffer (0.2 M, pH 6.6) of and (1%) of potassium ferricyanide then incubated at 50 ºC for 20 minutes. To add to the mixture, (250 µL) of (10%) trichloroacetic acid was transferred. The upper layer of the solution (250 µL) was mixed with distilled water (250 µL) and (0.1%) ferric chloride solution of 50 µL. Blank was prepared with the same reagents except the addition of quinoxalines. Absorbance was measured at 700 nm.

2.3.3 Free radical scavenging activity

2.2-diphenyl-1-(2,4,6-trinitrophenyl) hydrazyl (DPPH) assay

To further analyse the antioxidant activity, 2.2-diphenyl-1-(2,4,6-trinitrophenyl) hydrazyl (DPPH) radical scavenging activity assay was used. The DPPH radical is reduced in the presence of an antioxidants-containing compound through the transfer of hydrogens that will ultimately lead to a colour transformation of the purple DPPH to a yellow DPPH molecule (Kitima *et al*., 2018). This can be quantified by measuring the absorbance at 517 nm wavelength.

a) Qualitative DPPH

The 0.4 mM DPPH solution, Mw= 394,32 g/mol was prepared by weighing 7.88 mg of the powdered form of DPPH and dissolved in 50 mL methanol. Both the drugs and the standard solution were prepared with similar concentrations of 1 mM. The volumes of 10 µL per drug were dot blotted on the Merc Silica gel F284 plates. Similar volumes (10 µL) of ascorbic acid and water were dot blotted and the plates were allowed to dry at room temperature. The plates were sprayed with the 0.4 mM DPPH solution after they were completely dry to observe the colour transformation on the purple background.

b) Quantitative DPPH

To determine the percentages of the free radicals scavenged by the quinoxalines, the drugs were prepared in 1 mL with a concentration range of 0,125; 0.2; 0.4; and 1 mM. These were dissolved in dH2O. Similar concentrations of ascorbic acid were prepared (standard). DPPH solution of 0.1 mM in 10 mL was prepared from the 0.4 mM stock solution and dissolved in ethanol. The control was prepared by mixing methanol with DPPH whereas blank contained methanol with distilled H2O. Then 1mL of the DPPH was added in the Eppendorf tubes containing the samples and were incubated in a dark place for 30 minutes. Post the incubation period, 200 µL of the samples were transferred in 48 well plates (triplicates) and absorbance were recorded at 517 nm using the spectrophotometer. The free radical scavenging activity was calculated using the equation below.

% scavenging activity= (Abs Control-Abs test)/ (Abs control) x 100.

2.3.4. Determination of the total phenolic content

The total phenolic content of LAM-29A and LAM-21D were evaluated using the Folin-Ciocalteu's reagent. Compounds with phenolics reacts with the folin reagent which has a mix of heteropolyphosphotungstate-molybdate that forms a coloured blue complex when sodium carbonate is added (Kupina *et al*., 2018). The phenolic content of the quinoxalines was evaluated by comparing their absorbance at 750 nm to a calibration curve using gallic acid as a standard. Briefly concentrations of 1 mg/ml of LAM-21D, LAM-29A and quercetin were prepared which served as a standard. Gallic acid concentrations ranging from (0- 0.5 mg/ml) were prepared. Weighed 3.75 g of sodium carbonate and dissolved in 50 mL distilled water. The Folin reagent was prepared by diluting it tenfold of the original concentration, 2.5 mL of this reagent was transferred in each test tube. Then 2 mL of the sodium carbonate was added to the mixture after five minutes. The samples were incubated and left in the dark for a duration of 30 minutes. Post the incubation period, absorbances of the mixtures were measured at 750 nm. A standard curve was then constructed using gallic acid. The experiment was performed in sextuplicate. The total phenolic content was expressed as mg of GAE/g of the compounds and calculated using the formula below.

TPC=CV/M

On the equation, ´C´ is the concentration of gallic acid mg/ml, ´V´ is the volume of compound in ml and the weight of the compound in grams is denoted as ´M´.

2.4 Cell culture

Cervical CaSki, breast MCF-7, and Hek-293 kidney cells were obtained from ATCC, (ATCC CRM-CRL-1550, ATCC HTB-22 and ATCC CRL-1573). The cells were incubated at 37°C, with a humidified 95% air and 5% CO_2 in cell culture flasks. The cells were propagated in RPMI (Roswell Park Memorial Institute) medium for CaSki and DMEM (Dulbecco's Modified Eagle Medium) for MCF-7 and HEK-293 cells, which were supplemented with 2 mM L-glutamine, 1× (penicillin, streptomycin, and neomycin, PSN) and 10% Foetal Bovine Serum (FBS). Cell densities were calculated using a Life Technologies countess II FL automated cell counter after diluting and staining cells with 10× trypan blue dye.

2.5 Cell viability analysis

MTT (3-(4,5-dimethylthiazol-2-yl)-2,5-diphenyl-2H-tetrazolium bromide) assay

The cytotoxicity of the compounds was measured by using the MTT (3-(4,5-dimethylthiazol-2-yl)-2,5-diphenyl-2H-tetrazolium bromide) assay. This is based on the ability of the mitochondria in viable cells to actively secrete the NADPH-dependent oxidoreductase that can convert the tetrazolium salt to yield an insoluble purple formazan product. The outcomes are quantified by reading the absorbance at 570 nm (Ghasemi *et al*., 2021). Briefly (MCF-7 and CaSki cells) were seeded with a density of 5000/well, (HEK-293 cells, 4000/well) using a 96 well plate overnight. These were treated with the compounds (LAM-29A and LAM-21D), DMSO-media, and Curcumin followed by an incubation period of 24 hours. MTT reagent (5 mg/ml) was then added to the wells making a final concentration of 0.5 mg/ml. This was incubated for 3 hours. Upon the incubated period, the formazan salts were solubilised by adding 100 µL of DMSO which led to a further 30 minutes' incubation in a photosensitive area. Quantification of the outcomes was successfully done by recording the OD values at 570 nm

using the MultiskanSky plate reader. The viability percentage were expressed by the formula:

$$\%\ \text{Viability} = \frac{\text{Absorbance of treated cells}}{\text{The absorbance of untreated cells}} \times 100$$

2.6 Morphological analysis

The effect of the treatment on the morphology of cancer cells was conducted using the Ti-E inverted microscope. Cells were seeded in 48 well plates overnight. Then treated with the controls and compounds for 24 hours. Post treatment, images of the cells were captured on Ti-E inverted microscope connected to a computer.

2.7 Proliferation analysis

Muse™ Ki67 proliferation assay

The tumour Ki67 antigen was used as a marker to assess the percentages of proliferating and non-proliferating cells. Its expression assessment was done using Muse™Muse™Ki67 proliferation kit (Luminex corporation in Austin, U.S.A). Protocol was conducted according to the manufacturer's instructions. MCF-7 and CaSki cells were seeded in 46 well plate with a density of 2×10^4/well overnight. Various concentrations of quinoxaline LAM-29A (62.5 and 125 µM) and LAM-21D (125 and 250 µM) DMSO was used as a negative control, whilst the positive control was curcumin. Briefly, cells were washed with PBS and harvested post 24-hour treatment with 1× trypsin. Then centrifuged, fixed and permeabilised. The Muse™ Hu Ki67-PE was added, and samples were incubated in a dark place at room temperature for 30 minutes. Post incubation 1× assay buffer was added then samples were run on Guava® Muse™ Cell analyser.

2.8 Apoptosis analysis

Muse™ Annexin V and Dead Cell assay

To analyse the apoptotic inducing effects of LAM-29A and LAM-21D on CaSki and MCF-7 cells, Muse™ Annexin V and dead cell assay was used. Annexin V reagent binds strongly to the phospholipid layer of a plasma membrane. For cells that are undergoing apoptosis, the plasma membrane becomes compromised, and the phospholipid layer becomes externalized and susceptible to the annexin which will bind with high affinity. This was be detected using

flow cytometry. To quantify that, cells were seeded with a density of 2×10^4/well overnight. The following concentrations of LAM-21D were used to treat CaSki cells; 0, 125 µM, 250µM, 0.6% DMSO and 250 µM Curcumin. MCF-7 cells were treated with LAM-29A with 62.5 µM, 125 µM, DMSO and 125 µM Curcumin. Post 24-hour treatment cells were harvested by washing with 1× PBS and trypsinised then followed by centrifugation at 300 rpm for 5 minutes. Cells were resuspended with 50 µL. Within the resuspended cells, 50 µL of Annexin V reagent was added. The samples were then incubated in the dark for 20 minutes then analysed using Muse™.

2.9 Oxidative stress analysis

Muse™ oxidative stress assay was employed to determine the percentages of ROS positive, and ROS negative cells post treatment with quinoxaline LAM-21D. CasKi cells were seeded at a density of 20000 cells/well overnight. The cells were pre-treated with LAM-21D; 125 µM and 250 µM, DMSO and curcumin for 20 hours, then exposed to Hydrogen peroxide for 4 hours before harvesting. Post treatment cells were washed and trypsinised. Then centrifuged at 300 rpm for 5 minutes. The cells were washed again, then 10 µL of the cells and 190 µL of Muse™ oxidative stress working solution then mixed. This was followed by incubation at 37°C for 30 minutes and samples were analysed on the Muse™ cell analyser.

2.10 Cell cycle analysis

To determine the effect of the compounds on cell cycle, Muse™ cell cycle assay was conducted were by percentages of DNA in various cell cycle phases was determined. CaSki cells were seeded at a density of 2 x 10^5 cells/flask overnight. The cells were then synchronized by adding media without FBS overnight. Following synchronization, the cells were treated with curcumin, 0.6% DMSO, and LAM-21D (125 µM and 250 µM). After 24 hours the cells were washed with PBS, trypsinised, and centrifuged at 300 x g for 5 minutes. The cells were then washed with PBS and centrifuged at 300 x g for 5 minutes. The supernatant was discarded, and the cells were re-suspended in 50 µL PBS. Within the tubes containing the cells, 200 µL drops of 70% ethanol was added while gently vortexing the cell suspension. The cells were then placed

in -20°C for 3 hours. The ethanol fixed cells were then centrifuged at 300 x g for 5 minutes. The supernatant was discarded, and cells were re-suspended in 250 µL of PBS and centrifuged again for 5 minutes. The pellet was then re-suspended in 200 µL of Muse™ cell cycle reagent and incubated at room temperature for 30 minutes in a light-sensitive area samples were analysed on Muse™ cell cycle analyser.

2.11 *In silico* analysis of the compounds

2.11.1 Molecular docking

The molecular mechanisms linked to the antiproliferative activity of the compounds were predicted. Molecular docking was performed on quinoxaline derivative LAM-21D and curcumin structures drawn from ChemSpider against the BCL-2 and p65 NF-KB structures which were obtained from Protein Data Bank. To perform the molecular docking, the binding affinities of the compounds on the target proteins NF-kB and BCL-2 was performed using CB dock. The entire protein was docked to determine the probable binding sites. This performed blind docking at only predicted sites. The yielded bound poses were ranked in a docking score. The highest negative vina score gave the best binding pose. The optimal binding site was ranked first. Then the pharmacokinetics ADME (Absorption, Distribution, Metabolism and Excretion) properties of the compounds were studied on SwissADME web-based software. In SwissADME, the 2D structures of the compounds were imported and converted into SMILES (Simplified Molecular Input Line Entry Systems). This gave pharmacokinetic properties of ligands and BOILED egg simulations to show absorption destination of the ligands within the human body.

2.12 Statistical analysis

The determination of the samples' statistical differences was conducted by statistical analysis. The results were expressed as mean ± SEM from three independent experiments performed in triplicates. Differences were considered significant at, * $p \leq 0.05$; ** $p \leq 0.01$; *** $p \leq 0.001$ and **** $p \leq 0.0001$. The analysis of two way (ANOVA) or mixed models were used to make comparisons using Graphpad prism version 8.4.2.

CHAPTER 3
RESULTS

3.1 Spectral analysis of quinoxaline LAM-21D and LAM-29A

Characterisation of Quinoxaline derivatives was conducted using the UV-Vis spectroscopy. Looking at the results in Figure 3.1 LAM-29A has two broad peaks that shifted to the right side. The first band is at 285 nm, with absorption of 0,312while the second one is found at 410 nm and 0.241 absorption. LAM-21D has the first peak at 280 nm at 0.513 followed by a peak at 380 nm at 0,523. The combined spectra clearly show that LAM- 21D has higher absorbance due to high energy available for molecules to create a transition hence the presence of shorter wavelength. On LAM-29A, the electronic energy levels are closer together due to the presence of the above-mentioned groups as a result less energy is required to make a transition from the ground to the excited state which explains the longer wavelength and less absorption intensity.

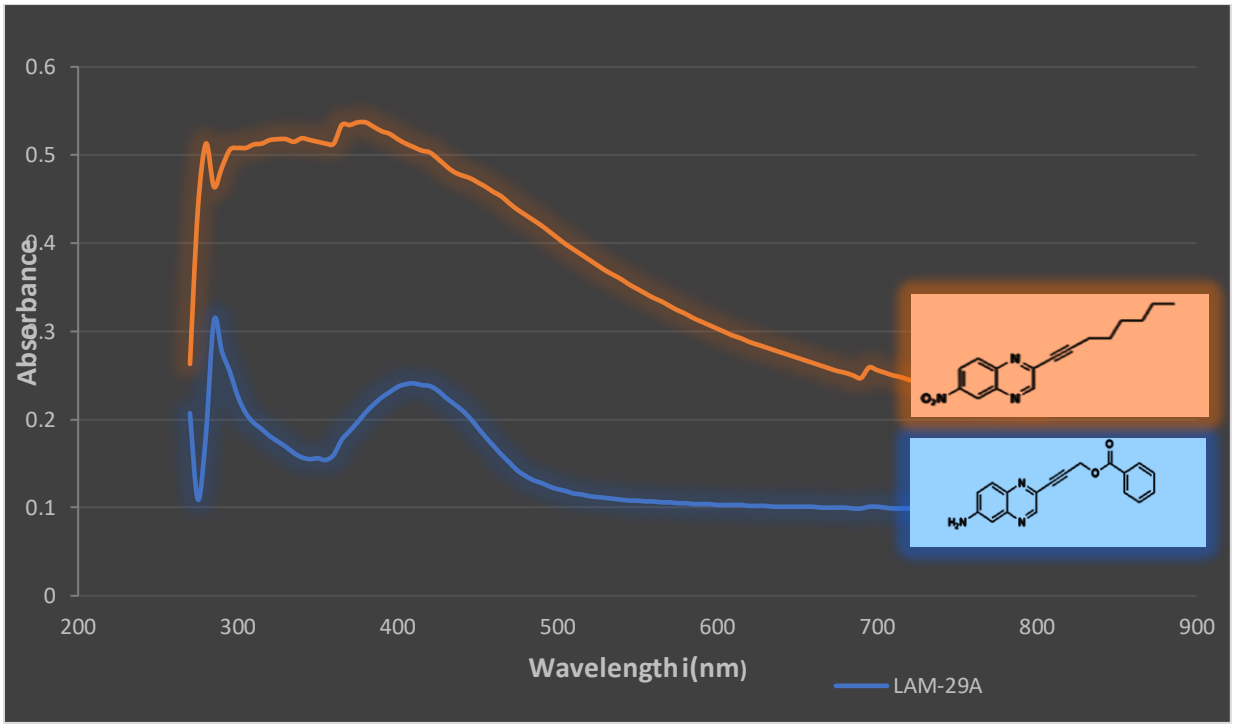

Figure 3.1: Ultraviolet-visible absorption spectra of quinoxaline LAM-29A and LAM-21D. LAM-29A and LAM-21D were diluted in distilled water and the absorbance was measured using the DU® 730 Life Sciences UV/Vis spectrophotometer. Wavelength detection was conducted from 200- 900 nm.

3.2 Antioxidants assays

3.2.1. Ferric Reducing Antioxidant Power (FRAP) Assay

In the FRAP assay an increase in absorbance signifies an increasing antioxidants activity. The antioxidant power was quantified by measuring an increase in absorbance at 593 nm using a spectrophotometer. The three lower concentrations (0,125- 0.5) mM for both compounds exhibited lower absorbance values ranging from 0,10 – 0.18 (Figure 3.2.1). It can be observed that the absorbance gradually increased to 0.5 and 0.8 at higher concentrations of 1 mM and 2 mM. This is an indicative of an increased reducing powers and more antioxidant activity in these concentrations respectively.

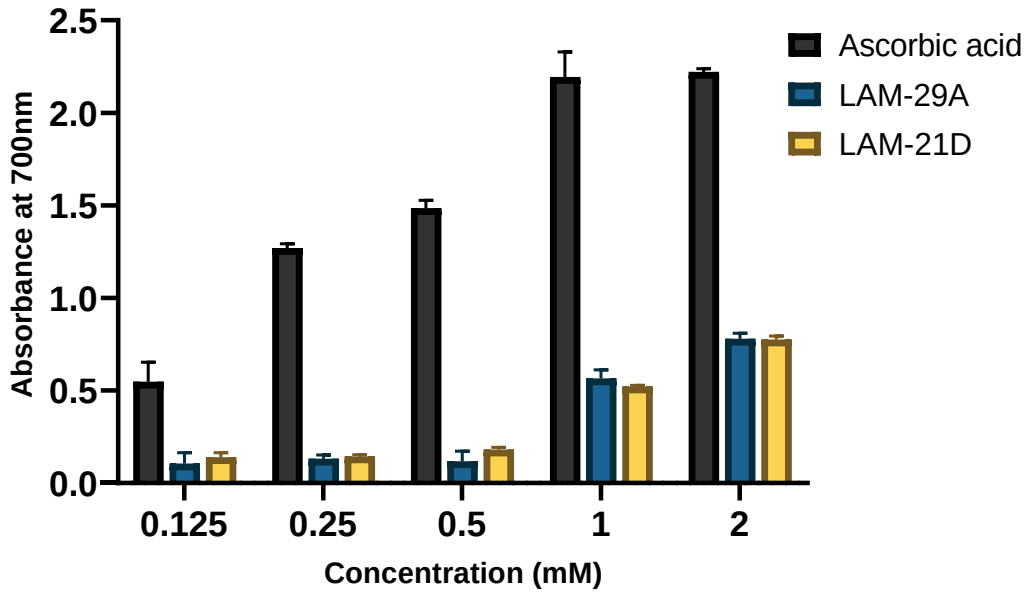

Figure 3.2.1: Ferric reducing potential of LAM-29A and LAM-21D. LAM-29A and LAM-21D at different concentrations ranging from (0.125-2 mM) were prepared with ascorbic acid as a standard. Following incubation of the samples with (0.1%) ferric chloride solution, the absorbance was measured at 700 nm using spectrophotometer. An increase in absorbance at 700 nm from (0.125- 2 mM) correlate with the antioxidants present.

3.2.2 Free radical scavenging activity assay

For compounds to effectively scavenge the DPPH free radical, they should have a certain level of antioxidants potential. This assay aided in testing the antioxidant capacity of the compounds. A qualitative observation was obtained on Figure 3.2.2.1 where, the compounds, water and ascorbic acid were dot blotted against the DPPH solution. The blotted spots of both compounds against the ascorbic acid appears to be having even colour intensities. The degree of the paleness of the spots implies that both compounds might be having somehow similar free radical scavenging activities. From the quantitative outcomes (Figure 3.2.2.2) it can be observed that across all concentrations ranging from (0.125 – 2 mM), LAM-29A and LAM-21D were able to scavenge 80% of the DPPH free radical. Whereas the positive control had percentages below 80% in the two lowest concentrations. Highest scavenging activity of 91% is observed with LAM-21D at 2 mM concentration. The outcome of the latter analysis correlates with those of the qualitative DPPH radical evaluation.

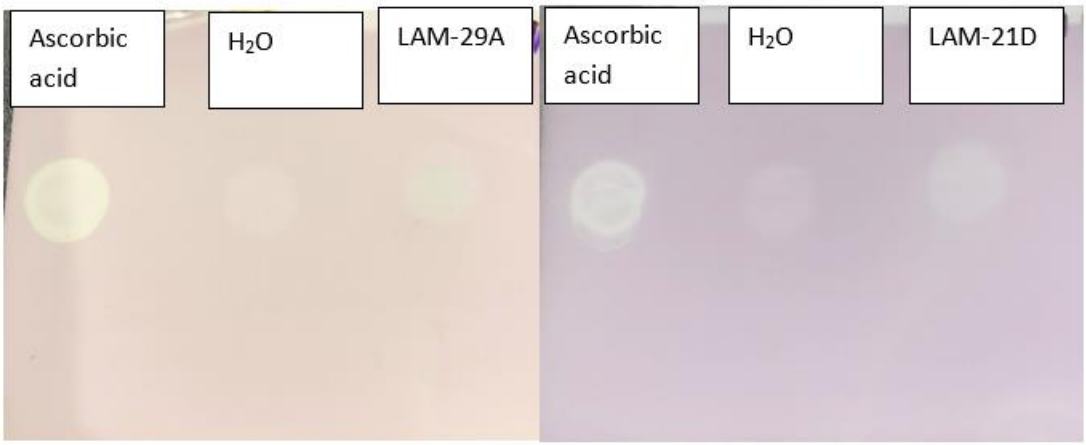

Figure 3.2.2.1: Qualitative antioxidants scavenging activity of Ascorbic acid, LAM-29A and LAM-21D. Similar concentrations of 0.5 mM for LAM-29A, LAM-21D and ascorbic acid were dissolved in water then were dot blotted against the 0.4 mM DPPH solution on the Merc Silica gel F284 plates.

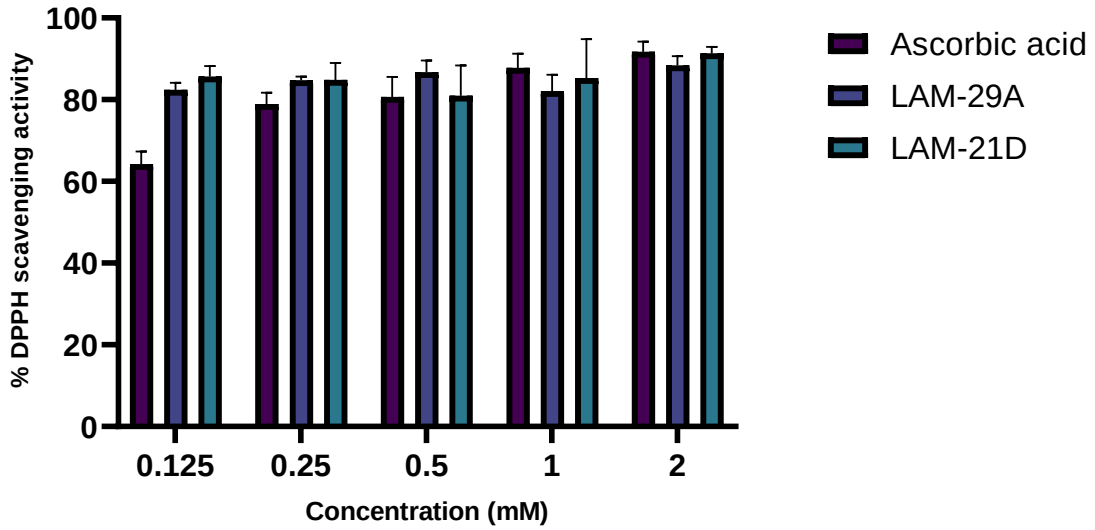

Figure 3.2.2.2: DPPH free radical scavenging activity of both LAM-29A and LAM-21D at varying concentrations. Ascorbic acid served as a standard. DPPH solution of 0.1 mM was added into the samples, incubated for thirty minutes. Then absorbance was measured absorbance at 700 nm using a spectrophotometer. The % DPPH scavenging activity was then calculated.

3.2.3 Total phenolic content

The quantification of the phenolic content using Folin Ciocalteu relies on the reaction of phenols with a mixture of sodium molybdate, sodium tungstate within the Folin Ciocalteu's reagent which then produces a blue coloured complex which absorbs at 765 nm. When comparing the phenolic content of the compounds using Quercetin as reference, LAM-29A had more phenolic content of 51.70 mg/g of GAE compared to LAM-21D which only had 10.31 mg/g of GAE (Figure 3.2.3). This results from the presence of phenolic group on the main quinoxaline core. These results suggest that both compounds exhibit a certain level of antioxidants due to the presence of the phenols. However, LAM-29A exhibited more phenolic content compared to LAM-21D in relation to the positive control (quercitin).

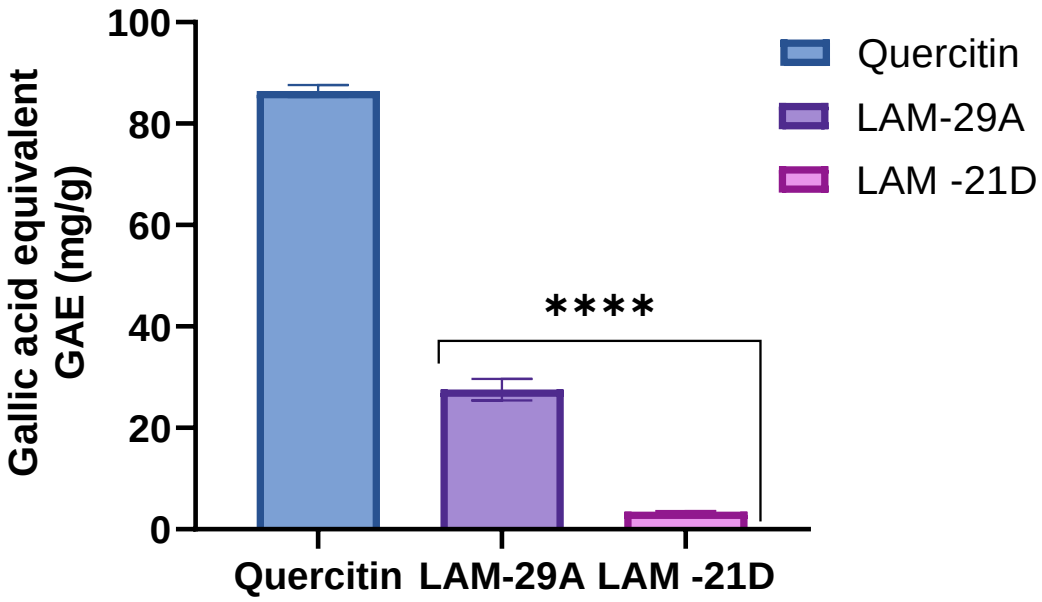

Figure 3.2.3: The phenolic content analysis of quinoxaline LAM-21D and LAM-29A. After the addition of the Folic Ciocalteu's reagent in samples, they were incubated in a light-sensitive room for thirty minutes. Quercetin was used as a positive control. The phenols in each sample were quantified by measuring the absorbance values at 750 nm. The results were obtained from three independent repeats which were performed in sextuplicate, with **** $p \leq 0.0001$ between the compounds showing a significant difference.

3.3 The effects of LAM-29A and LAM-21D on viability of MCF-7 and CaSki

For preliminary screening of quinoxaline derivatives (LAM-21D and LAM-29A). MTT assay was carried out using CaSki and MCF-7 cells. CaSki cells were treated with concentrations ranging from 31.25- 500 µM, DMSO and Curcumin. On Figure 3.3.1 (A), there was an observed dose-dependent decrease in cell viability when CaSki cells were treated with LAM-21D. At concentration of 250 µM, 53% of cells were viable. CaSki cells treated with LAM-29A (Figure 3.3.1 (B)) has not shown any significant variation in cell viability except at 500 µM where only 78% of the cells were viable. The DMSO content of LAM-29A had a significant contribution in the reduction of the viability of CaSki cells, where only 62% of the cells where viable, hence LAM-29A could not be used to treat CaSki cells. With regards to MCF-7 cells, LAM-21D (Figure 3.3.2 (A)) was very cytotoxic at 500 µM whereas LAM-29A Figure 3.3.2 B showed a high selectivity towards MCF-7 cells at the lowest concentration of 125 µM. The effective concentrations of LAM-21D (125 and 250 µM) were used to investigate apoptosis in CaSki cells for the downstream assays, while 62.5 µM and 125 µM LAM-29A were investigated in MCF-7 cells.

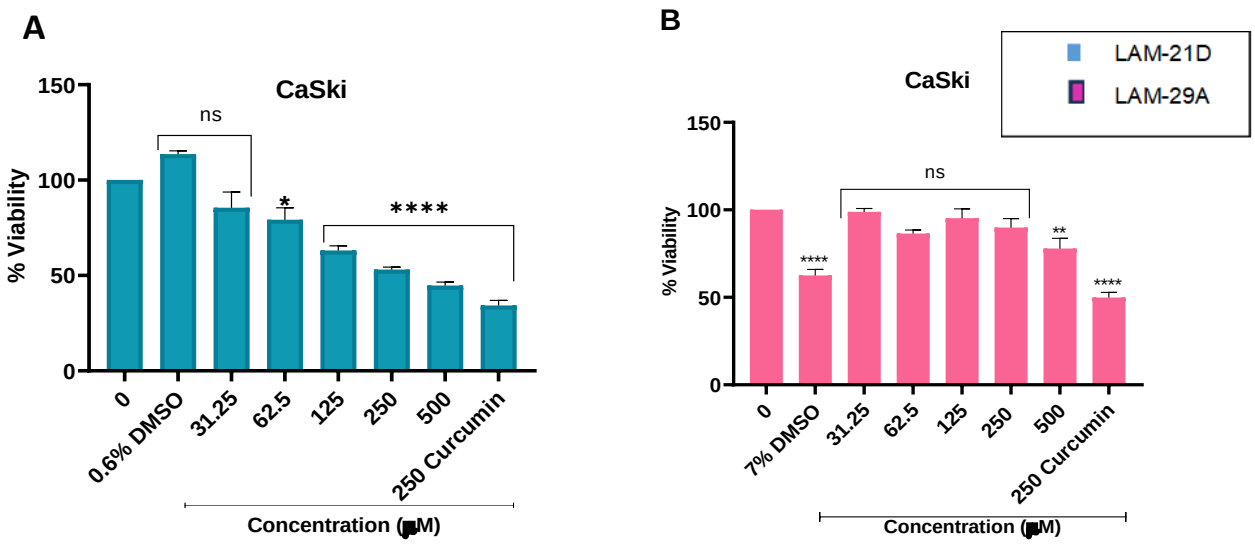

Figure 3.3.1: The effect of LAM-21D and LAM-29A on the viability of cervical CaSki cells. CaSki cells were seeded overnight and treated with different concentrations of LAM-21D (31.25-500 µM) and LAM-29A ((31.25-500 µM)) for 24 hours. MTT was added and cells were quantified by measuring absorbance at 570 nm using MultiskyScan, after which MTT was carried out. The data is a representation of three independent experiments, (percentages mean ± SEM). Statistical differences were established with p values of (*p≤ 0.05, **p≤ 0.01 and ****p≤ 0.0001).

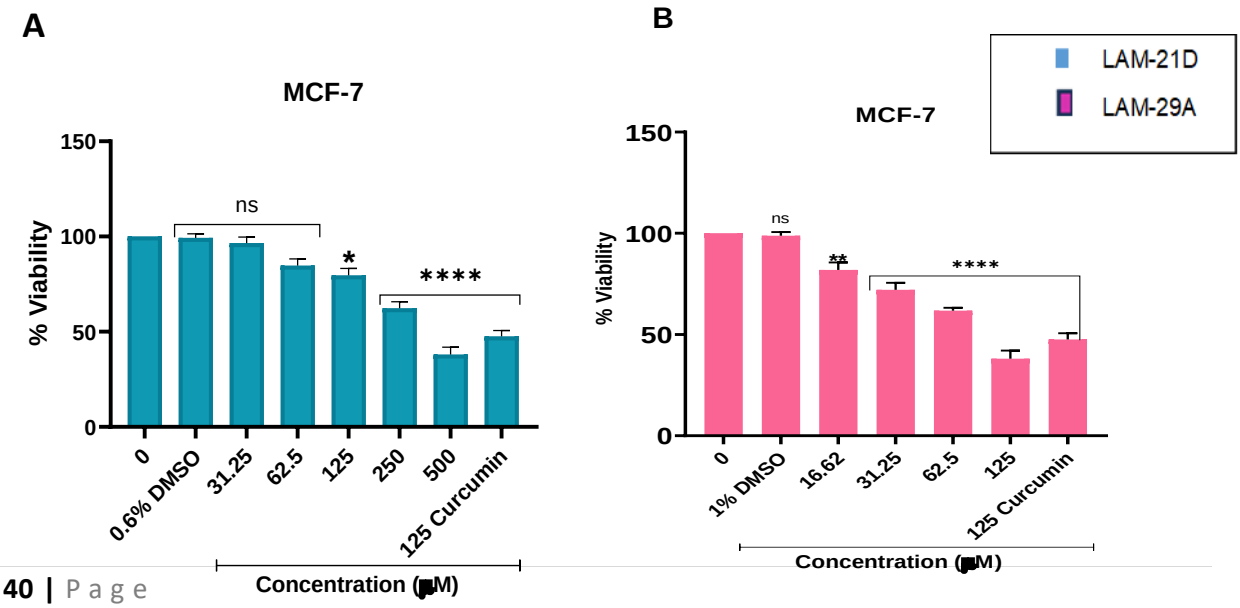

Figure 3.3.2: The effect of LAM-21D and LAM-29A on MCF-7 breast cells cancer cells over 24-hour treatment. MCF-7 cells were also seeded overnight and treated with different concentrations of LAM-21D (31.25-500 µM) and LAM-29A (16.62-125 µM) for 24 hours. Following MTT addition, cells were quantified by measuring absorbance at 570 nm using. The data represents three independent experiments with percentage mean ± SEM. The differences were statistically significant with p values of (*p≤ 0.05, **p≤0.01, ***p≤ 0.0005, and ****p≤ 0.0001).

3.4 Effect of LAM-21D and LAM-29A on viability of HEK-293 cells

A promising anticancer agent must effectively inhibit the growth of cancerous cells without harming the normal cells. To show the effect of the derivatives on the viability of the non-cancerous cells, MTT assay was carried out on Hek 293 cells. LAM-29A (Figure 3.4 B) had negligible toxicity towards HEK293 cells at IC50=125 µM where viability percentages were maintained at 84%. LAM-21D (figure 3.4 A) also had minimal toxicity towards the kidney cells at IC50=250 µM, where 72% of the cells where viable. Concentrations above 250 µM for both drugs were found to be highly toxic towards the kidney cells. The toxicity of these compounds on HEK-293 cells increases with an increase in the concentration.

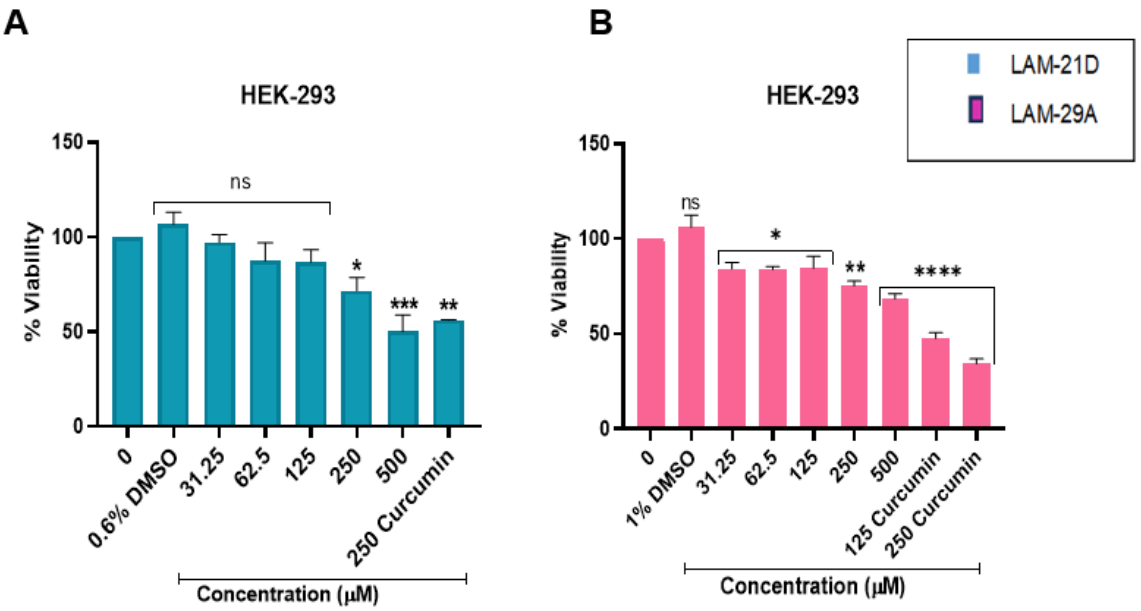

Figure 3.4: The effect of LAM-21D and LAM-29A on HEK-293 embryonic kidney cells over 24-hour treatment. HEK-293 cells were seeded overnight and treated with similar concentrations of the compounds as used in cancer cells. MTT was added and cells were quantified by measuring absorbance at 570 nm using MultiskyScan.Hek-293 embryonic kidney cells were utilized as the toxicity model to assess how these compounds will affect a human body. Similar doses to those used on the cancerous cells were also used.

3.5 Morphological analysis of CaSki and MCF-7 cells

3.5.1 The effect of LAM-21D on morphology of CaSki cells

The effect of LAM-21D on the morphology of CaSki cells was assessed post 24-hour treatment with the compound. Looking at Figure 3.5.1 it can be observed that the morphology of the cells in 0.6% DMSO and untreated groups remained intact, cells were still attached to their binding surfaces and maintained contact with one another. When cells were treated with both concentrations of LAM-21D and curcumin; cell shrinkage was observed, confluency decreased, and cells were round. There was condensation of the cytoplasm, cells detached from the cell surface, and they lost contact from their neighbouring parts.

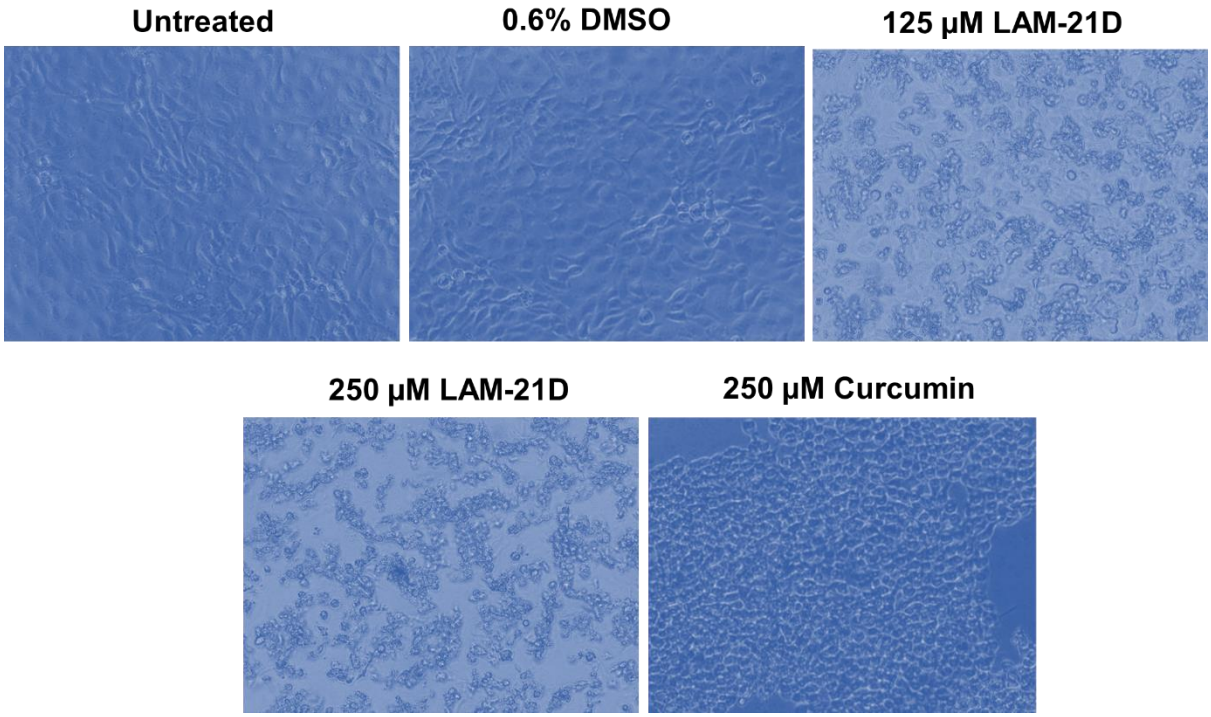

Figure 3.5.1: Morphological analysis of CaSki cells. Post treatment of CaSki cells with LAM-21D and Curcumin in 48 well plates. The images of the cells were captured on Ti-E inverted microscope connected to an LC-microscope software on the computer. This allowed visualization of the changes in the morphology of the cells after treatment.

3.5.2 The effect of LAM-29A on the morphology of MCF-7 cells

The effect of LAM-29A on the morphology of MCF-7 cells was assessed post 24-hour treatment with the compound. Looking at figure 3.4.2 it can be observed that the morphology of the cells in 0.6% DMSO and untreated groups remained intact. Under normal circumstances MCF-7 cells possesses an epithelial-like structures. When cells were treated with both concentrations of LAM-29A and curcumin the morphology changed such that there was; cell shrinkage, cells became round, loss of cellular contact, cells detached from their binding surfaces and their confluency decreased. There was condensation of the cytoplasm, cells detached from the cell surface, and they lost contact from their neighbouring parts.

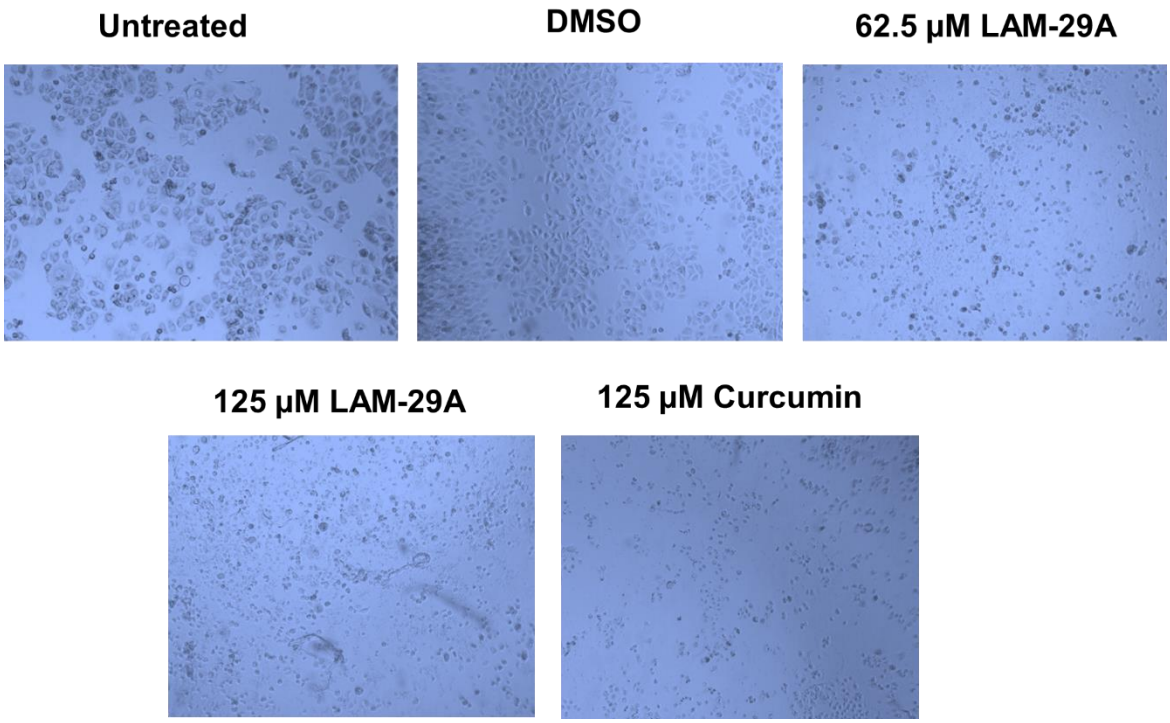

Figure 3.5.2: Morphological analysis of MCF-7 cells. Following treatment of MCF-7 cells with LAM-29A and Curcumin in 48 well plates. The images of the cells were captured on Ti-E inverted microscope connected to an LC-microscope software on the computer. This allowed visualization of the changes in the morphology of the MCF-7 cells after treatment.

3.6 Effect of the quinoxaline derivatives on the proliferation of cancer cells

3.6.1 Assessment of the effect of LAM-21D on the proliferation of CaSki cells

The effect of LAM-21D on the proliferation of actively dividing CaSki cells was investigated on Muse™ KI67 proliferation marker. This allows differentiation of proliferating cells from the non-proliferating cells based on the KI67 expression. On figure 3.6.1 A, the histograms show how the two populations of KI67 positive and KI67 negative cells are distributed across different concentrations of LAM-21D and the controls. A decline in the expression of KI67 is observed as concentrations increases. A lower concentration of the compound did not evoke any change in the reducing the KI67 expression. Nonetheless, a significant decrease in cell proliferation due to a decrease in the expression of KI67 from 76% in the negative control to 54% in 250 µM of LAM-21D was observed.

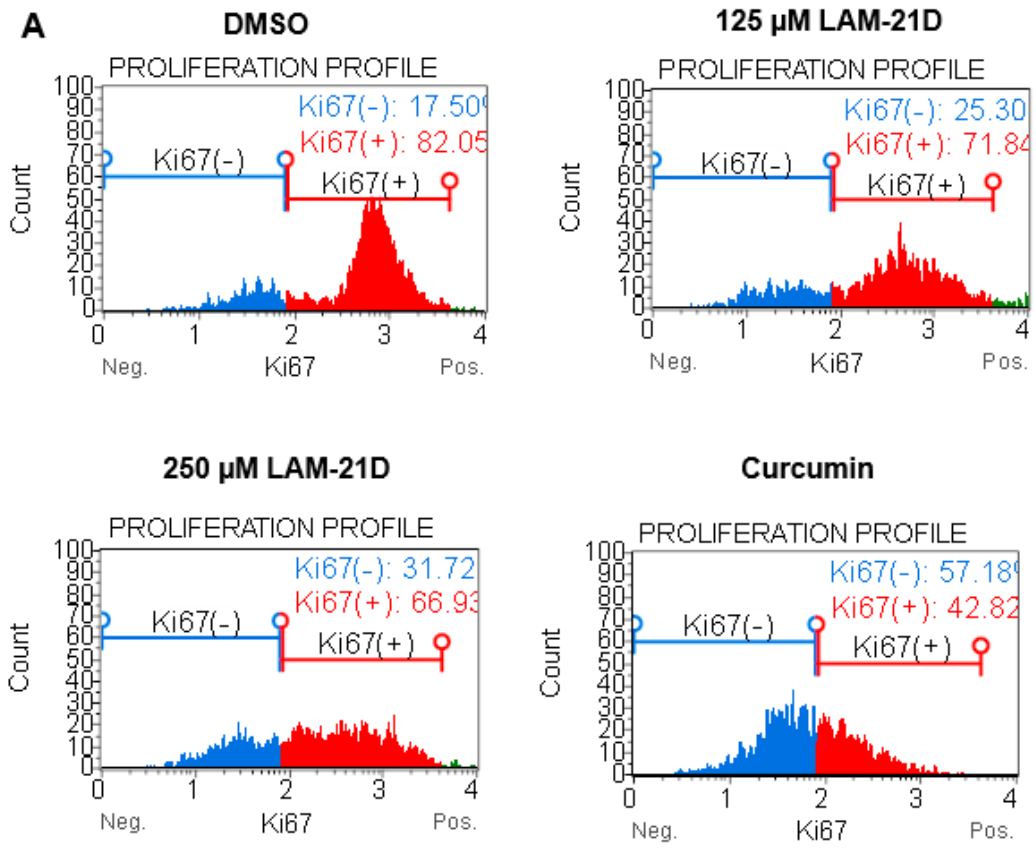
A
DMSO
PROLIFERATION PROFILE
Ki67(-): 17.50
Ki67(+): 82.05
Ki67(-)
Ki67(+)
Count
Neg.
Ki67
Pos.
125 µM LAM-21D
PROLIFERATION PROFILE
Ki67(-): 25.30
Ki67(+): 71.84
Ki67(-)
Ki67(+)
Count
Neg.
Ki67
Pos.
250 µM LAM-21D
PROLIFERATION PROFILE
Ki67(-): 31.72
Ki67(+): 66.93
Ki67(-)
Ki67(+)
Count
Neg.
Ki67
Pos.
Curcumin
PROLIFERATION PROFILE
Ki67(-): 57.18
Ki67(+): 42.82
Ki67(-)
Ki67(+)
Count
Neg.
Ki67
Pos.

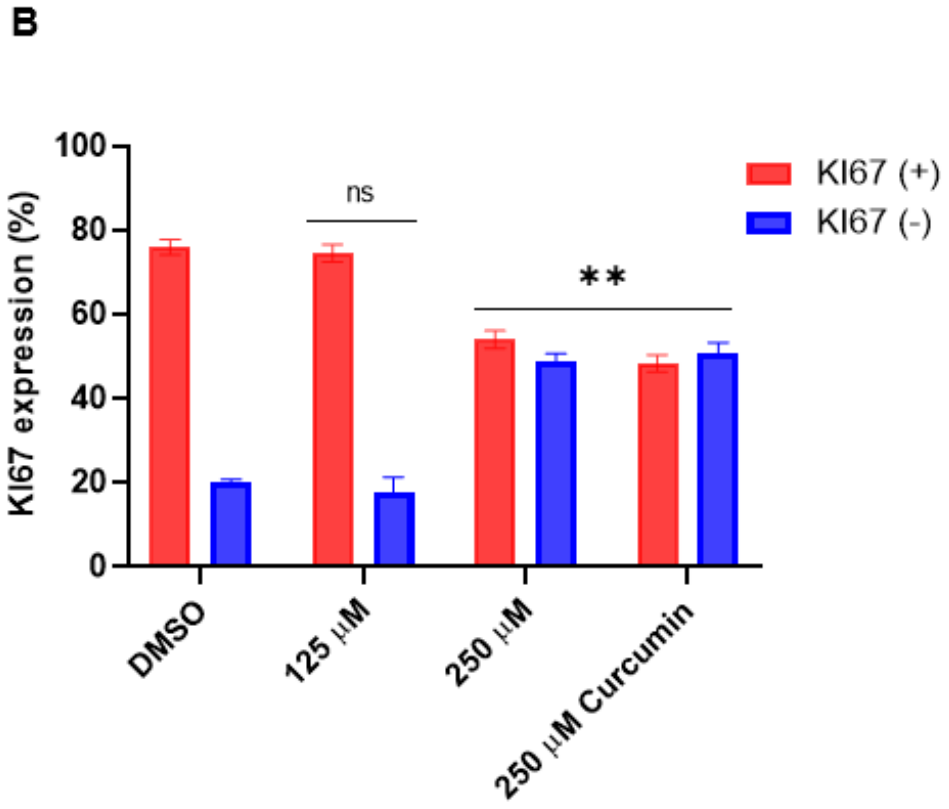

Figure 3.6.1: Analysis of the KI67 proliferation of the CaSki cells. KI67 expression in CaSki cells post treatment with LAM-21D. The results were obtained from the muse cell analyser after incubation of the samples with the KI67 reagents. The histogram in A clearly depicts the differences in the KI67 populations across the various concentrations. (B) CaSki cells treated with 125 µM of the compound did not show any significant effect on proliferation. At 250 µM the KI67 expression of the CaSki cells decreased (KI67 + population). The graphical data is a representation of three independent experiments performed in triplicates with percentage mean ± SEM. The differences were statistically significant with p values of (****p≤ 0.05).

3.6.2 Effect of LAM-29A on the proliferation of MCF-7 cells

The effect of LAM-29A on the proliferation pf MCF-7 cells was also investigated using Muse™™ KI67 proliferation marker. This compound did not exert any anti-proliferative activity towards the MCF-7 cells as can be seen across all the concentrations (figure 3.5.2). The effect of LAM-29A on the proliferation of MCF-7 cells was investigated on Muse™ KI67 proliferation marker. This allows differentiation of proliferating cells from the non-proliferating cells based on the KI67 expression. The distribution of KI67 positive and KI67 negative cells are shown by histograms on figure 3.6.2 A and B, it can be noted that the concentrations of LAM-29A did not evoke any change in reducing the KI67 expression.

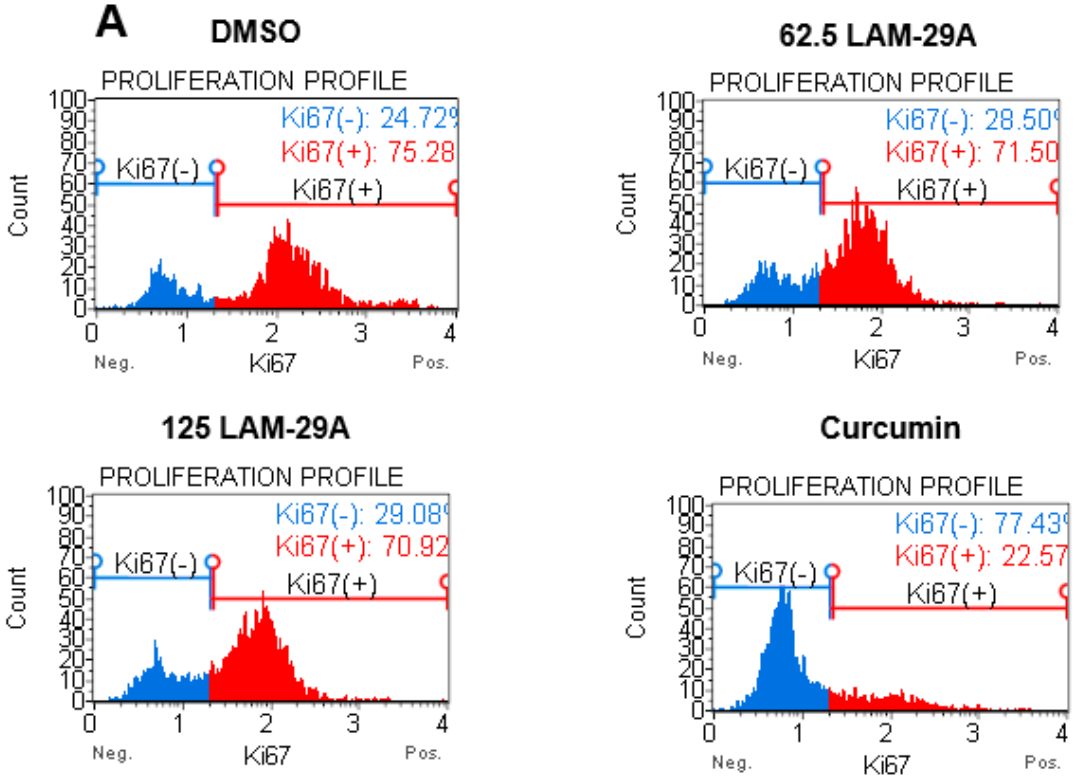
A
DMSO
PROLIFERATION PROFILE
Ki67(-): 24.72%
Ki67(+): 75.28%
Ki67(-)
Ki67(+)
Count
Neg.
Ki67
Pos.
62.5 LAM-29A
PROLIFERATION PROFILE
Ki67(-): 28.50%
Ki67(+): 71.50%
Ki67(-)
Ki67(+)
Count
Neg.
Ki67
Pos.
125 LAM-29A
PROLIFERATION PROFILE
Ki67(-): 29.08%
Ki67(+): 70.92%
Ki67(-)
Ki67(+)
Count
Neg.
Ki67
Pos.
Curcumin
PROLIFERATION PROFILE
Ki67(-): 77.43%
Ki67(+): 22.57%
Ki67(-)
Ki67(+)
Count
Neg.
Ki67
Pos.

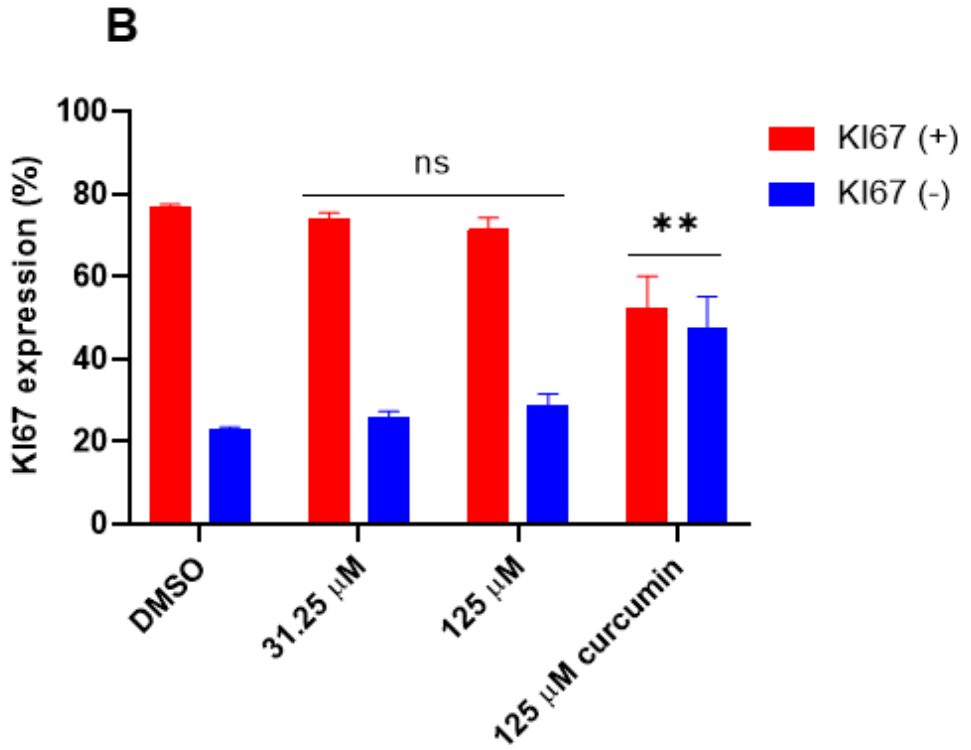

Figure 3.6.2: Assessment of the KI67 proliferation of the MCF-7 cells. KI67 expression in MCF-7 cells post treatment with LAM-29A. The histogram above the graphical data (A) shows the populations of gated cells that fall on either KI67(+) or KI67 (-). (B) When comparing the results with the vehicle control, LAM 29A may have only evoked a non-significant change on the expression of KI67 in MCF-7 cells however there is a significant reduction in the KI67 expression within the positive control (**p≤ 0.05). The graphical data is a representation of three independent experiments performed in duplicates with percentage mean ± SEM.

3.7 Analysis of the apoptotic inducing effects of quinoxaline derivatives on CaSki and MCF-7 cells

Cellular apoptosis detection and quantification was performed using flow cytometry. Apoptosis plays a major role in various physiological processes. It's one of the pathways targeted for drug discoveries. Muse™ Annexin V and PI was used to stain cells undergoing apoptosis and to distinguish between different populations of live cells and those undergoing programmed cell death/necrosis. For the detection of apoptosis, a conjugated Annexin preferably binds to the negatively charged phosphotidylserine residues. Another defined feature of plasma membrane of live cells is that they can repel charged cationic molecules such as propidium iodide (PI) and 7-aminomycin-D (7-AAD) so cells with disintegrated and ruptured membranes will take up PI in the late stages of apoptosis (Nunes-Santos *et al.*, 2022). Post twenty-four-hour treatment of CaSki (Figure: 3.6.1) and MCF-7 (Figure 3.6.2) cells with the quinoxaline derivative LAM-21D and 29A, Curcumin and the vehicle control; it was observed with untreated and vehicle control groups that over 95% of cells were localized within the live quadrant where they still have their phospholipids distributed within the inner and outer membrane of the plasma membrane while phosphotidylserine (PS) on the inner side. In 125 µM of LAM-21D almost similar proportion of the cells where evenly distributed within the early stages of apoptosis where cells expose the PS on the outside, there was a total percentage of 43%. When the concentration increased to 250 µM the total percentage reached 59%. The percentages of apoptosis induced by LAM-29A in MCF-7 cells were relatively insignificant.

Quantitative apoptosis analysis in CaSki cells using Muse™ Annexin-V

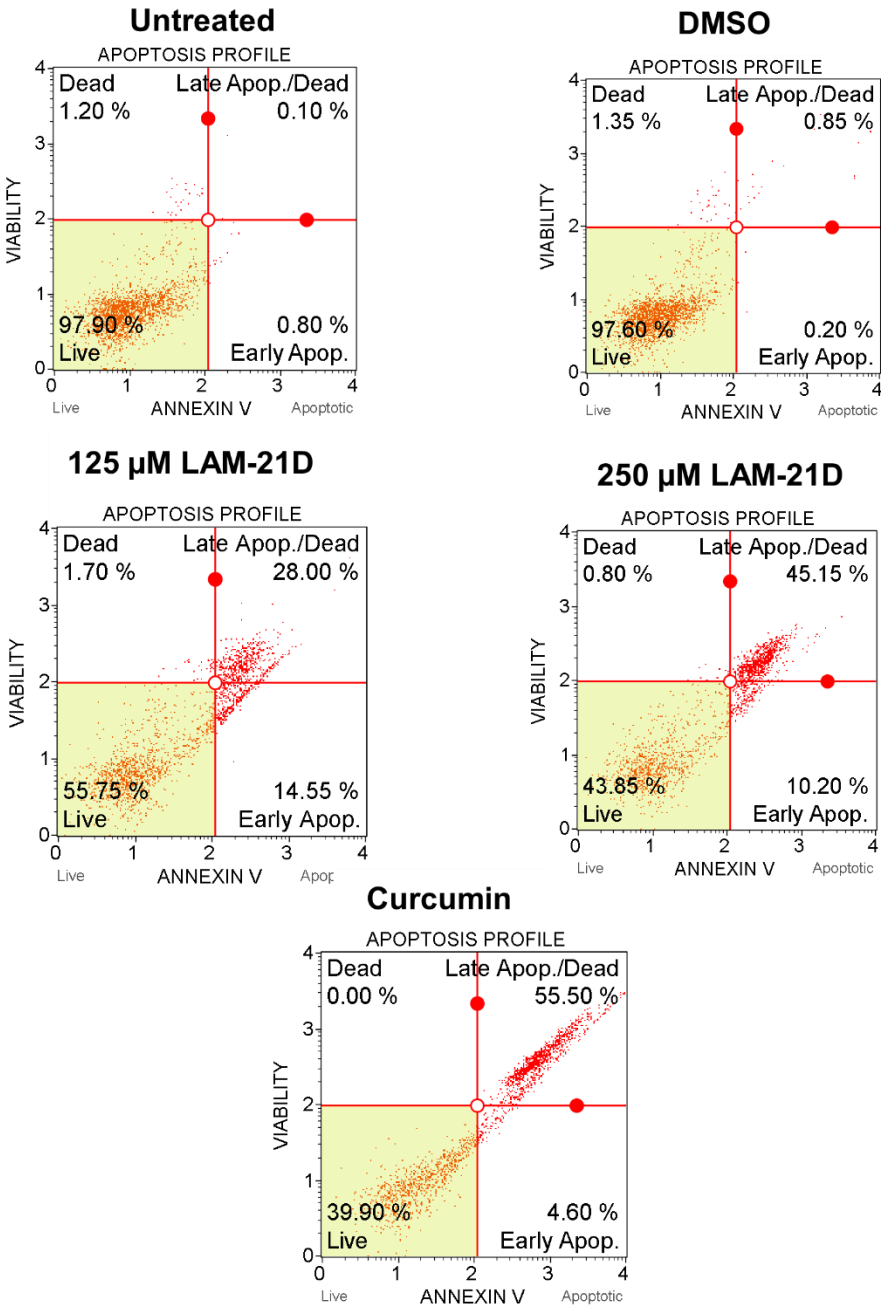

assay

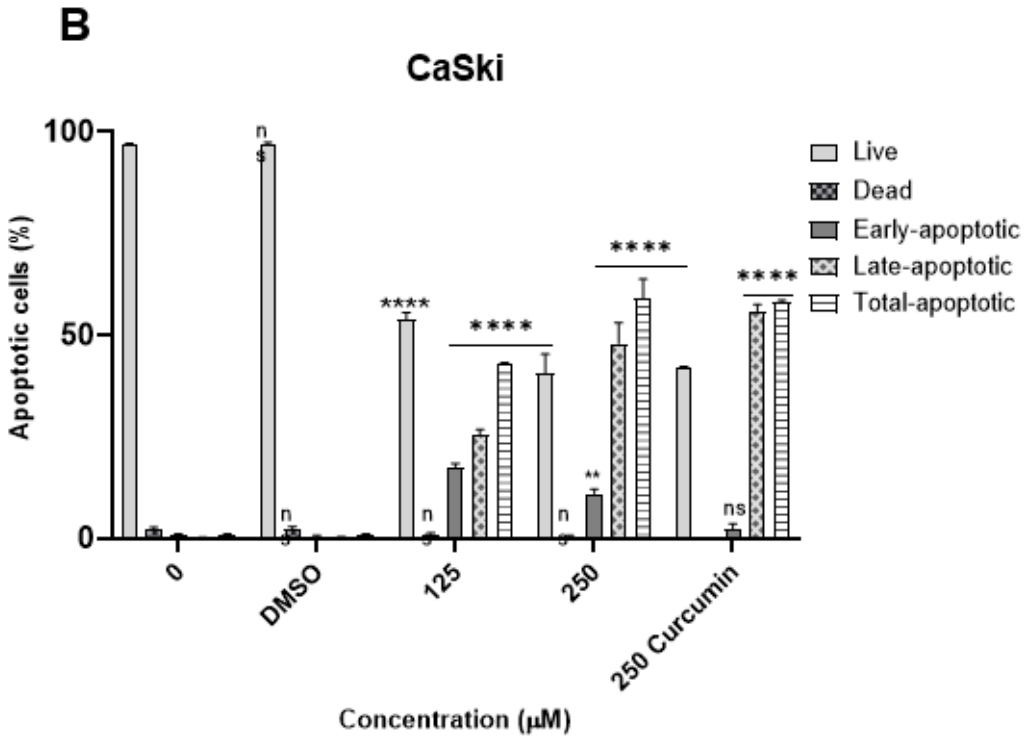

Figure 3.7.1: Apoptosis analysis of CaSki cells post treatment. CaSki cells were treated with LAM-21D (125 µM and 250 µM), 250 µM Curcumin and DMSO-media. Post 30 minutes incubation of the samples with annexin V reagent. Apoptosis percentages were quantified. (figure 3.7.1 A) shows the Apoptosis profiles, highlighting the distribution of cells across different quadrants; live, early, and late apoptosis and necrosis. The graphical data is a representation of three independent experiments performed in duplicates with percentage mean ± SEM. The differences were statistically significant with p values of (*p≤ 0.05, **p≤0.01, ***p≤ 0.0005, and ****p≤ 0.0001).

Quantitative apoptosis analysis in MCF-7 cells using Muse™ Annexin V assay.

A

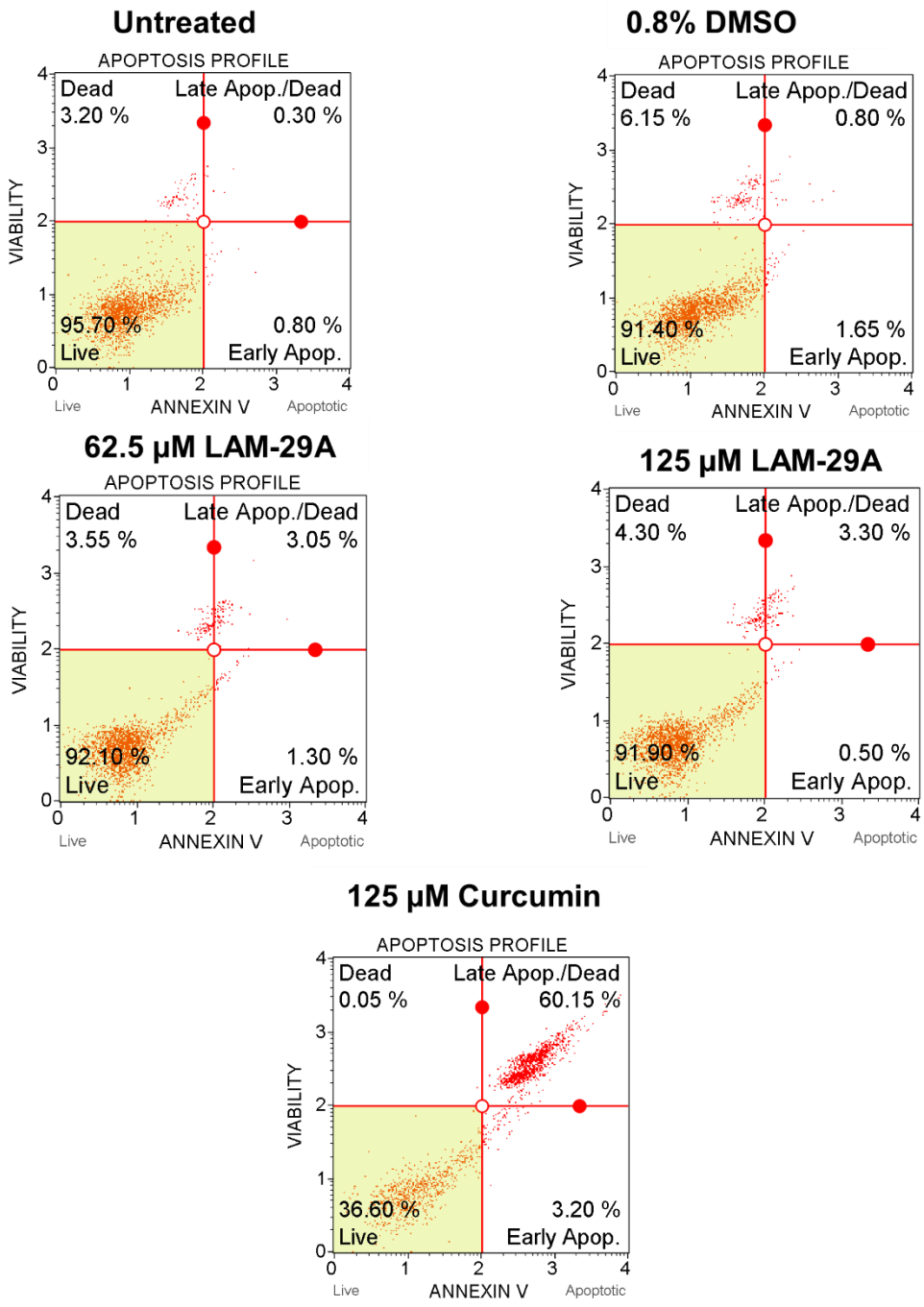

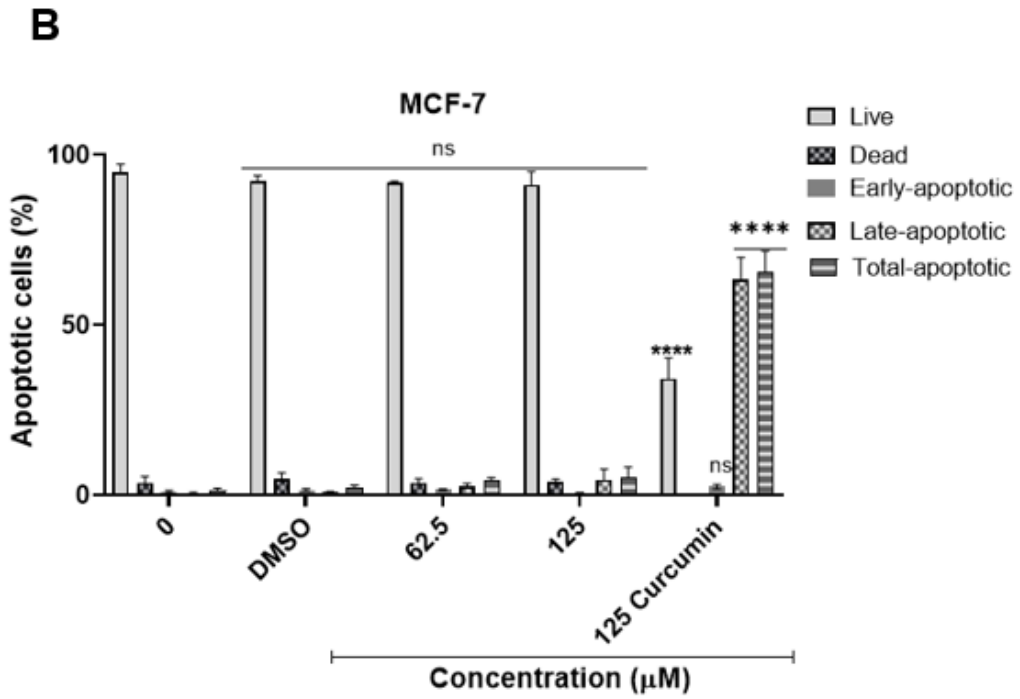

Figure 3.7.2: Apoptosis inducing potential of LAM-29A in MCF-7 cells. Post treatment of the cells with the compound for 24-hourscells were trypsinised, washed and the Muse™ reagent was added. The population of the cells were quantified on Muse™ analyser. LAM-29A did not exhibit any apoptotic effect on the cells, as can be seen by both the histograms (A) and graphical data (B). The data represents three independent experiments with percentage mean ± SD. The differences were statistically significant with p values of (****p≤ 0.0001).

3.8 Reactive oxygen species production analysis

The capacity of LAM-21D to induce ROS production in CaSki cells was analysed using the Muse™ oxidative stress analysis following a 24-hour treatment. The detection of ROS levels was made possible by using the ROS reagent, dihydroethidium (DHE). Upon an encounter/reaction of this reagent with superoxide anions, oxidation reactions take place and DNA-binding fluorophore (ethidium bromide) will intercalate with the DNA and fluoresce. This will then allow differentiation of the two populations of cells, ROS (-) which are live cells, and ROS (+) which are those exhibiting ROS. CaSki cells were treated with the vehicle control, two concentrations of the LAM-21D (125 µM and 250 µM) and curcumin (figure 3.8 B). From the averages of the three independent experiments. There were 28% of ROS positive cells in the lower concentration of the drug and the percentage increased significantly to 46% in higher concentration. The ROS profiles are also depicted in (figure 3.8 A) which clearly shows the two populations of the cells.

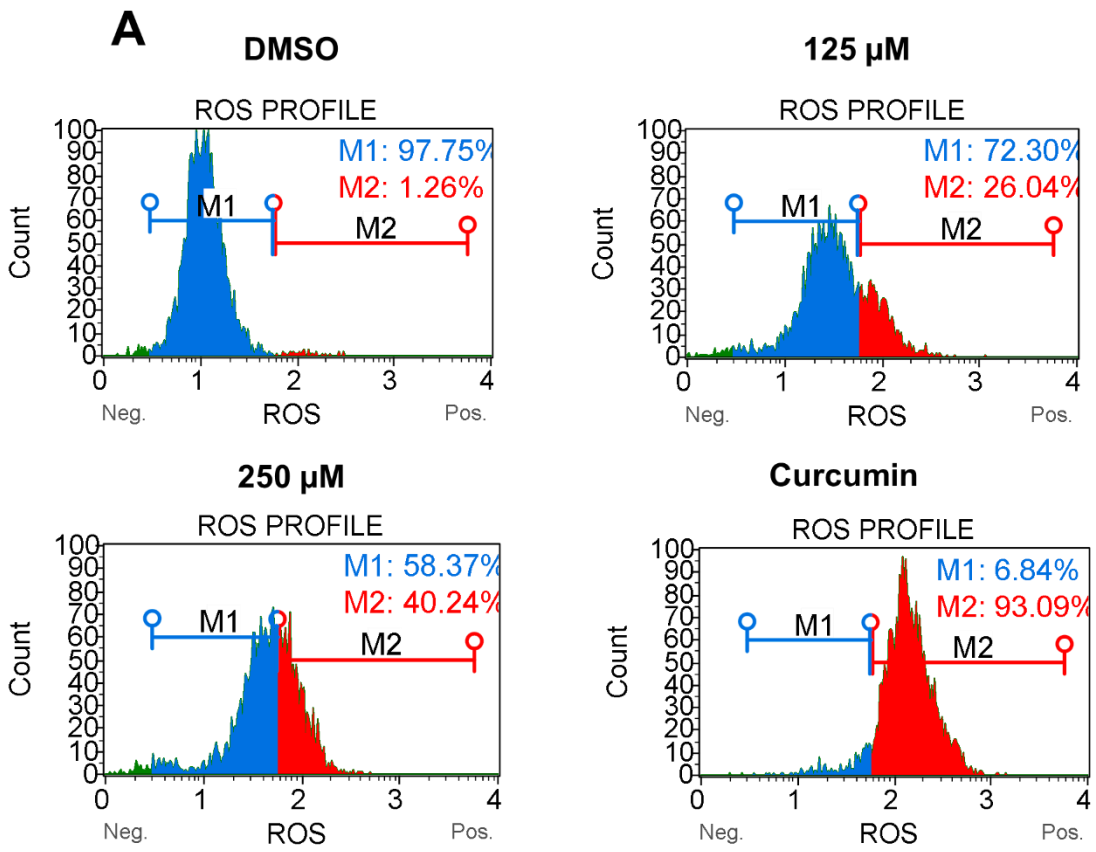
A
DMSO
ROS PROFILE
M1: 97.75%
M2: 1.26%
M1
M2
Count
Neg.
ROS
Pos.
125 µM
ROS PROFILE
M1: 72.30%
M2: 26.04%
250 µM
ROS PROFILE
M1: 58.37%
M2: 40.24%
Curcumin
ROS PROFILE
M1: 6.84%
M2: 93.09%

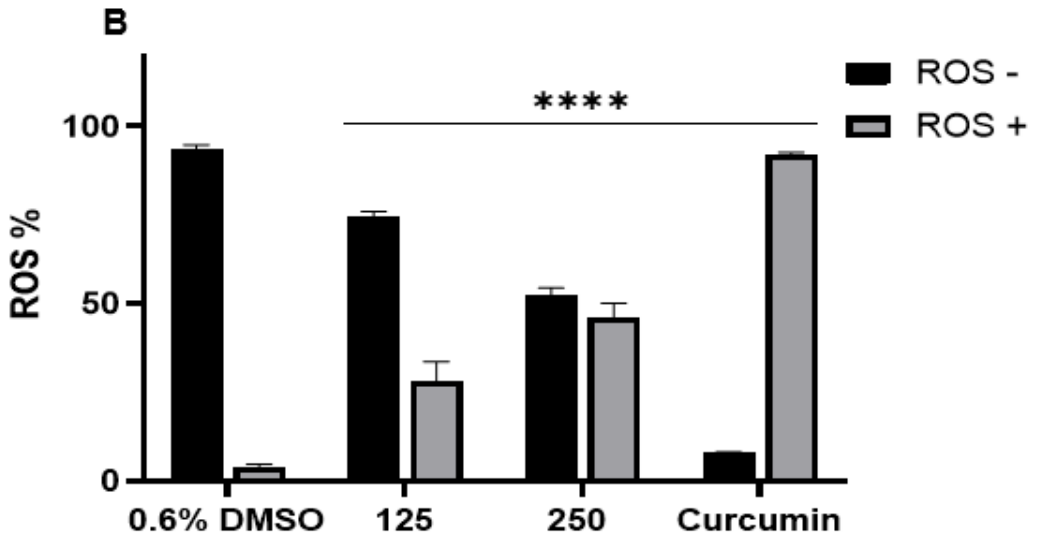

Figure 3.8: Oxidative stress analysis of CaSki. Post treatment of CaSki cells. The muse working reagent was added followed by a *30-minute* incubation. The different ROS populations were then detected and analysed on Muse™ cell analyser. The data is accumulated from three independent experiments which were performed in duplicates, with percentage mean ± SEM. The differences were statistically significant with p values of (****p≤ 0.0001).

3.9 Analysis of CaSki cell cycle progression

The effect of LAM-21D on the progression of CaSki cells throughout the cell cycle phases was assessed using Muse™ cell cycle analysis. Measurement of the percentages of the DNA content in all the three phases (G0/G1, S and G2/M) is made possible using DNA-based Propidium iodide and RNAse A to increase the DNA staining specificity. From the quinoxaline- treated cells (Figure 3.9) in 125 µM there was insignificant changes made to the percentages of the DNA content of the cells across the different phases of the cell cycle when comparing to the negative control. When the concentration increased to 250 µM significant changes were observed in the G0/G1 cells as they decreased from 48.15% in the negative control to 12.2%. Majority of the cells convocated within the S-phase, from 12.55% in the negative control to 28.1%. Curcumin treated cells demonstrated the highest percentage of cells in the G2/M with 89% of cells.

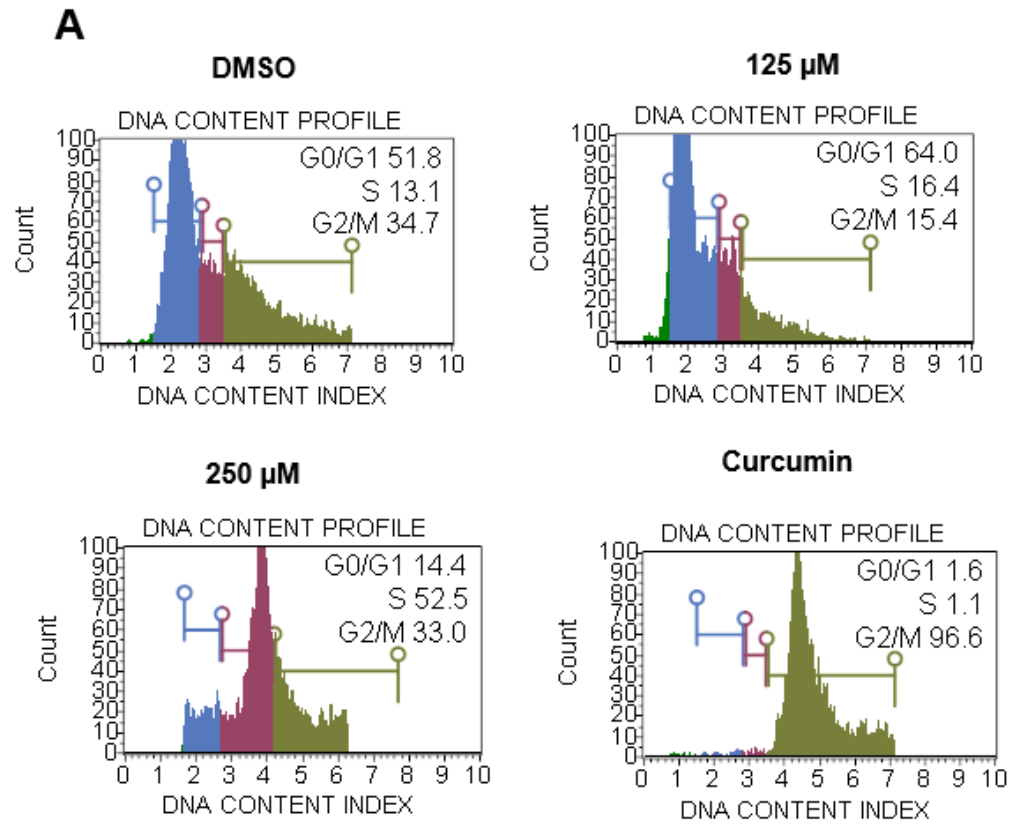
A
DMSO
DNA CONTENT PROFILE
G0/G1 51.8
S 13.1
G2/M 34.7
Count
DNA CONTENT INDEX
125 µM
DNA CONTENT PROFILE
G0/G1 64.0
S 16.4
G2/M 15.4
Count
DNA CONTENT INDEX
250 µM
DNA CONTENT PROFILE
G0/G1 14.4
S 52.5
G2/M 33.0
Count
DNA CONTENT INDEX
Curcumin
DNA CONTENT PROFILE
G0/G1 1.6
S 1.1
G2/M 96.6
Count
DNA CONTENT INDEX

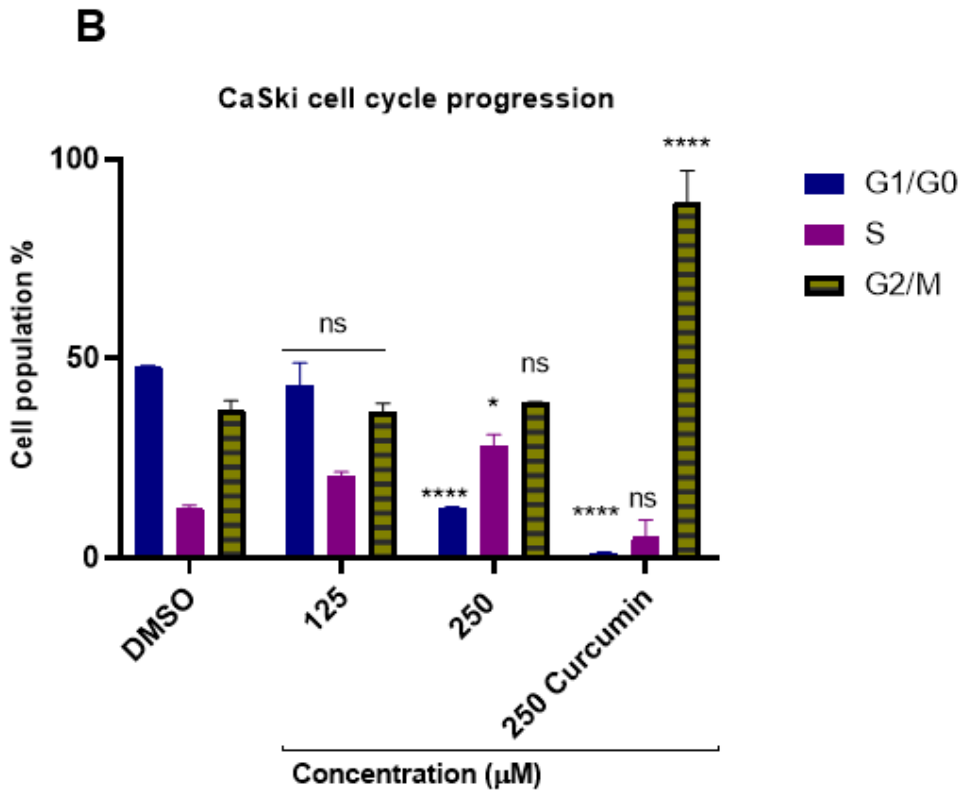
B
CaSki cell cycle progression
Cell population %
100
50
0
G1/G0
S
G2/M
ns
ns
ns
*
****
****
****
DMSO
125
250
250 Curcumin
Concentration (µM)

Figure 3.9: Cell cycle assessment of the CaSki cells across G0/G1, S, and G2/M phases obtained by treating the cells. The cells were fixed in ethanol and incubated with the cell cycle reagent. Analysis was carried out utilizing the Muse™ cell analyser. Notably, high dose of LAM-21D has significantly influenced the cell cycle at synthesis phase. The was also a significant decrease of cells in the G0/G1.Lowerr doses did not have any significant effect. The histograms in (A) also shows the distribution of the DNA content of the cells across G0/G1, S, and G2/M. The statistical data correlates with the percentages mean ± SEM. The differences were statistically significant with p values of (*p≤ 0.05 and ****p≤ 0.0001).

3.10 *In silico* evaluations of quinoxalines LAM-21D

To comprehend the molecular mechanisms that are involved in the antiproliferative and anti-cancer activities of compound LAM-21D, CB- Dock web-based binding predictor was utilized. The 3D structures of the ligand and protein were used to anticipate the binding affinities. The ligands styles were set as licorice and the protein receptors were set as cartoon (figure 3.10). The ligands interact with the receptor proteins at depicted amino acids residues within the core structures and the binding scores are also shown on table 1. The knowledge on the pharmacokinetics fate of the compounds in the organisms are also conducted using the SwissADME software were by physicochemical, pharmacokinetic, and lipophilicity properties are studied table 2 and 3). The Human intestinal absorption (HIA) and BBB (blood brain barrier permeation was visualized on BOILED egg simulation model (figure 3.11).

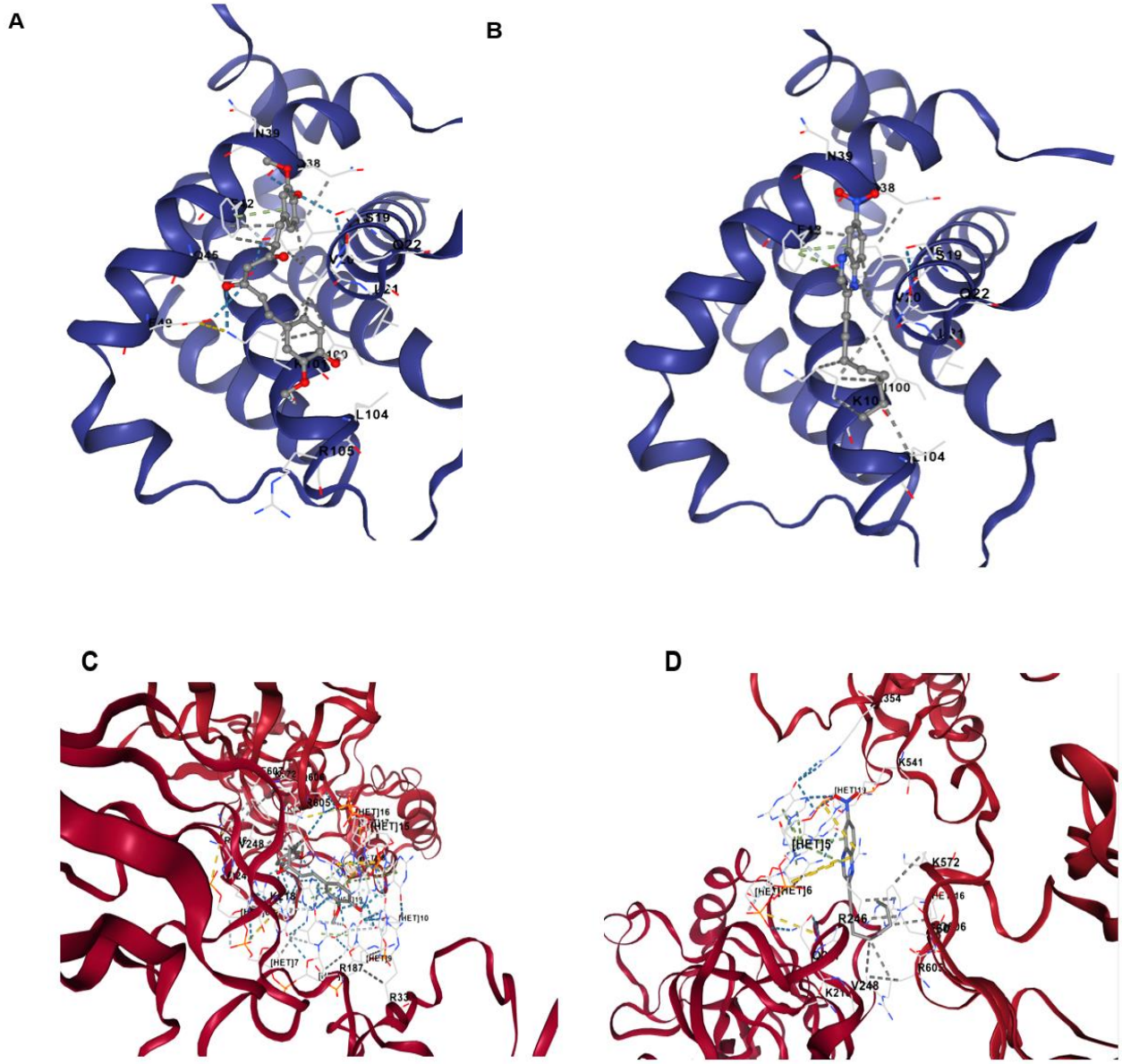

Figure 3.10: The molecular binding predictions between ligand A (Curcumin and BCL-2 receptor), B (LAM-21D and p53 receptor) C (Curcumin and NF-kB), and D (LAM-21D and NF-kB). The figures represent the best binding modes between curcumin and LAM-21D ligands with the BCL-2 and NF-kB active cavity sites which were predicted by the CB dock software. The ligands are shown within the interior of the receptor conformational structure in licorice style whereas the receptors are depicted as cartoon structures. The amino acids involved in the interactions are also shown.

Table 1: Predicted molecular binding poses for ligands and the protein targets.

Ligands	Protein targets	Vina Score	Cavity volume	Types of bonds
Curcumin	BCL-2	-7.0	124	Hydrogen bonds
	p65 NF-kB	-9.3	11647	Hydrogen bonds
LAM-21D	BCL-2	-6.0	124	Hydrogen bonds
	p65 NF-kB	-7.3	1389	Hydrogen bonds

Table 2: Physicochemical properties of LAM-21D and Curcumin

Property	Curcumin	LAM-21D
Formula	C21H20O6	C16H17N3O2
Molecular weight	368.38 g/mol	283.33 g/mol
Num. rotatable bonds	8	5
Num H-bond acceptors	6	4
Num. H-bond donors	2	0
Num. heavy atoms	27	21

Table 3: Pharmacokinetics, and lipophilicity properties of LAM-21D and Curcumin

Property	Curcumin	LAM-21D
GI absorption	High	High
BBB permeant	No	Yes
Log Kp (skin permeation)	-6.28 cm/s	-4.88 cm/s
CYP1A2 inhibitor	No	Yes
CYP2C19 inhibitor	No	Yes
CYP2C9 inhibitor	Yes	Yes
CYP2D6 inhibitor	No	Yes
CYP3A4 inhibitor	Yes	No
Log $P_{O/W}$	3.03	3.18
Lipinski rule of 5	Yes, 0 Violation	Yes, 0 Violation

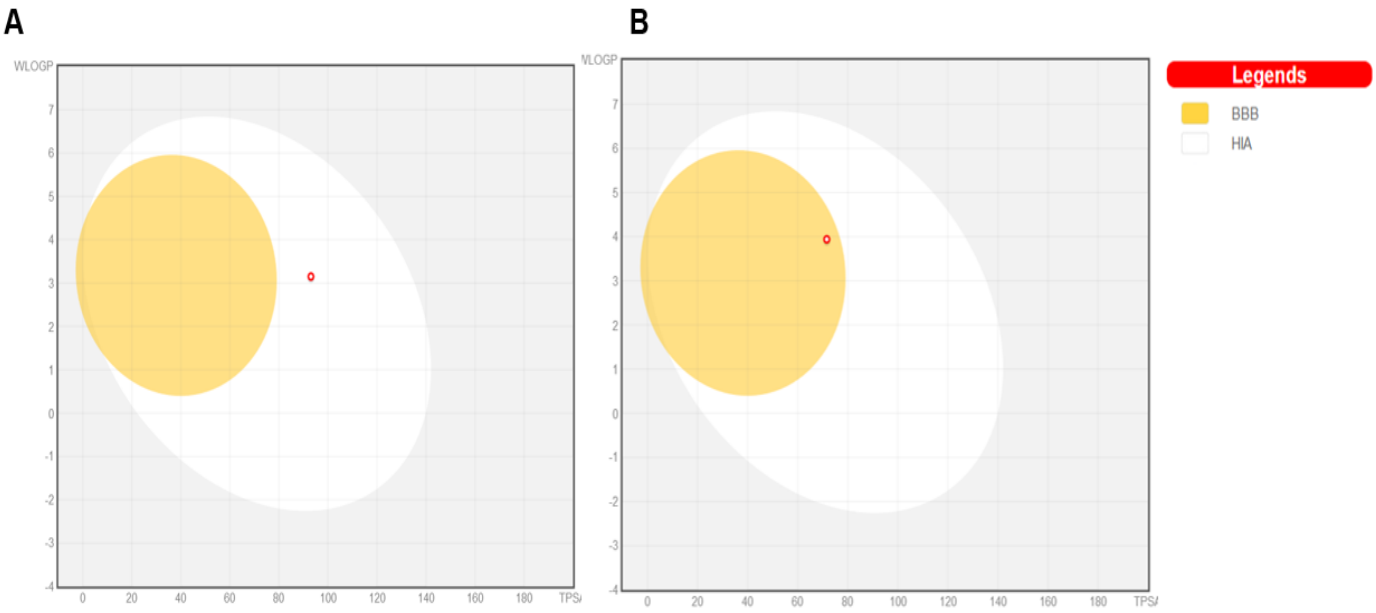

Figure 3.11: Predicted BOILED- egg model of A (Curcumin) and B (LAM-21D) from SwissADME web tool. This shows the dotted areas where the compounds are most likely to be absorbed. The yellow part (yolk) is for penetration of the compound within the BBB while the white part is passive absorption within the GI tract. Curcumin is predicted to be absorbed within the human intestinal tract and LAM-21D in the Blood Brain Barrier.

CHAPTER 4
DISCUSSION

Programmed cell death or apoptosis plays a crucial role in maintaining multicellular homeostasis by balancing the rate of cell proliferation with that of elimination. This process occurs in a carefully orchestrated manner to avoid it occurring in excess and triggering onset of degenerative diseases or it being insufficient and resulting in cancer or autoimmune diseases. Understanding apoptosis mechanisms has prompted the development of novel therapeutic approaches for the treatment of cancer, the majority of which trigger apoptosis to impede the growth and spread of the disease. There are several ways to trigger this process, and one of them is by producing ROS, which is how most FDA-approved anticancer drugs such as doxorubicin and paclitaxel, and cisplatin inhibit cancer growth (Choi *et al*., 2015; Mohiuddin and Kasahara, 2021; Ren *et al*., 2018) . The current study uses the Caski cervical cancer and MCF-7 breast cancer models to primarily evaluate the *in vitro* apoptosis-inducing ability of selected novel synthetic compounds in the form of newly synthesised quinoxaline derivatives, LAM-21D and LAM-29A.

Numerous experiments were carried out in this work to investigate the anticancer properties of these novel quinoxalines. Firstly, to characterise the compounds, Ultraviolet-Visible (UV-Vis) light spectroscopy was used. This assay is widely used to demonstrate and highlight the interactions that occurs between electromagnetic radiations with the matter (Picollo *et al*., 2019). Since many compounds are largely labile, sensitive, and responsive to energy changes at their maximum wavelengths it is important to characterise them using this UV-Vis method. When compounds receive a suitable amount of ultraviolet or visible light radiation, with sufficient energy, triggering electronic transitions that ultimately lead to promotion of electrons from the ground to the excited state (Picollo *et al*., 2019). Electrons found in the π – orbitals are the ones responsible for the absorption of light in the visible and ultraviolet spectrum (Huillet, 1953). Quinoxaline cores exhibit high absorption at two broad bands (Fagour *et al*., 2017). The first one is at 270 nm and the other bigger peak is found at 370 nm (Hirt *et al*., 1956; Linstrom and Mallard, 2023). These findings are in

alignment with those of this current study although there is variation that is brought by functional groups/substituents added to the core structures. Results from the current study show that both quinoxaline derivatives experienced a bathochromic shift wherein the λ_{max} increased towards the longer red wavelength region. As depicted in figure 3.1, LAM-29A displayed two broad peaks that shifted to the right side. The first band was observed at 285 nm while the second one was located at 410 nm. LAM-21D displayed the first peak at 280 nm followed by a subsequent peak at 380 nm. There were several factors that could be responsible for the observed shifts in wavelengths. These include but not limited to the presence of chromophores which are group of atoms that have more localised electronic transitions responsible for absorbing intense light in the UV-Vis spectrum. Quinoxaline structures having double symmetrical substitutions on the second and third carbons experienced an increase in the Bathochromic shift in this order; H< CH_3 < C_6H_5< $C_6H_4OCH_3$ < $C_6H_3O_2$< $C_6H_3O_2CH_2$ < CH = CH— C_6H_5 < $(CH = CH)_2C_6H_5$ < $(CH = CH)_3C_6H_5$. Electron donor groups that can be substituted at position 2, 3, 4, 5, 6, and 7 would ultimately propel the compounds to absorb light at longer wavelengths (Sawicki *et al*., 1957).

This longer wavelength absorption effect was observed with quinoxaline LAM-29A which has an amino group (auxochrome) substituted at carbon 6 and 2-propynyl benzoate group at position 2. Both the propynyl group, with a triple bond, and benzoic acid strongly contributed to the shift of wavelengths to longer wavelengths. On the other hand, LAM-21D contains electron accepting NO_2 group at position 6 and a branched chain 6 carbon aliphatic group at position 2 which give rise to the observed shorter wavelengths. In addition, the absence of suitable substituent groups in LAM-21D could be attributed the shorter wavelengths that were recorded. With regards to the spectral absorption, LAM-21D recorded higher absorbance values due to high energy available for molecules to create a transition state, hence the presence of shorter wavelengths. In LAM-29A, the electronic energy levels were in closer proximity due to the presence of the above-mentioned groups as a result less energy was required to make a transition from the ground state to the excited state

which explains the longer wavelength and less absorption intensity (Huillet, 1953).

Heterocyclic rings rich in nitrogen atoms are important organic compounds with abilities to interact with DNA-binding transcription factors and DNA-associated proteins. Not only do they exist in synthesised molecules and natural products, but these rings are also present in RNA, DNA as well as GTP and ATP energy molecules (Samir *et al*., 2020). Structural modifications on the quinoxaline core structure are constantly performed to introduce or attenuate various structural moieties with a potential to improve therapeutic efficacy in managing various disease conditions while inducing minimal or no side effects (Khatoon and Abdulmalek, 2021; Pereira *et al*., 2015).

Antioxidant-producing substances are essential for regulating the production of highly reactive oxygen and nitrogen species. The Ferric Reducing Antioxidant Power (FRAP) assay measures the reduction of the ferric ions complex, 2,4,6-tripyridyl- s- triazine complex $[Fe^{3+}\ (TPTZ)_2]^{3+}$ to a blue coloured ferrous ions complex $[Fe^{2+}\ (TPTZ)_2]^{2+}$. Reduction power of a reaction mixture would then positively correlate with an increase in absorbance at 593 nm to signify an increase in antioxidants activity (Gulcin, 2020). This demonstration is observed on figure 3.2. The three lower concentrations (0.125; 0.25; and 0.5) for both compounds exhibited lower absorbance values ranging from 0.10 – 0.18. However, only a few antioxidants are required to neutralise many free radicals (Zeb, 2020). Absorbance values then gradually increased to 0.5 and 0.8 at higher concentrations of 1 mM and 2 mM, this is indicative of an increased reducing power and more antioxidant activity in these concentrations, respectively (Lim and Lim, 2013; Takatsuka *et al*., 2022). Additionally, the 2,2-diphenylpicrylhydrazyl (DPPH) assay was used to measure an antioxidant's capacity to scavenge free radicals by using a free radical DPPH solution which absorbs maximally at 517 nm. (Gulcin, 2020). Both the qualitative and quantitative studies were obtained on figures 3.2.1 and 3.2.2. The evenness of the dot blotted spots for both compounds may imply that these compounds scavenge the DPPH radical at similar proportions. Across all the concentrations, LAM-29A and LAM-21D were able to scavenge 80% of the DPPH free radical.

The results for both studies showed a positive correlation between quinoxaline concentration and free radical scavenging activity.

Since most antioxidants are phenolic in nature, a total phenol quantification assay was carried out on the quinoxaline derivatives with the purpose of characterising its phenolic status. Phenols are an important component of antioxidants with one or more hydroxyl groups that are mostly present in plants and are easily regenerable. In the Folin Ciocalteu assay, phenolic compounds can reduce the Folin reagent composed of a mixture of phosphotungstic acid complexes to produce a blue coloured complex that absorbs maximally at 745 - 750 nm. This is due to the electrons transferred from phenolic compounds to the phosphotungstic acid complexes under alkaline solution or medium (Gulcin, 2020). The majority of phenolics are measured in various plant species and since quinoxaline derivatives have comparable structures, their phenolic constituents can also be assessed using the same assay. The antioxidant properties of phenolic compounds are granted by the presence of the benzene ring and several hydroxyl groups on the benzene ring. The benzene ring serves to stabilise antioxidants whenever they interact with free radicals. LAM-21D recorded a higher phenolic content of 27.5 mg/g of GAE compared to that of LAM-29A at 3.4 mg/g of GAE. This has marked a significant structural difference between these two compounds with regards to phenolic composition.

Furthermore, the viability inhibitory effect of quinoxaline LAM-29A on MCF-7 cells and LAM-21D on CaSki cells was determined by using MTT (3-(4,5-dimethylthiazol-2-yl)-2,5-diphenyl tetrazolium bromide) assay. The results showed a concentration-dependent decrease in cell viability in response to an increase in the concentration of the compounds over 24-hour period, with curcumin used as a positive control (figure 3.3.1 and 2). The IC_{50} value, which is the concentration required to inhibit 50% of the cell viability, for CaSki cells was at 250 µM and in MCF-7 it was 125 µM, suggesting that MCF-7 breast cancer cells are more sensitive to LAM-29A compared to Caski cervical cancer cells. These findings on LAM-29A correlate with those of a study by (Lekgau *et al.*, 2022) conducted on the inhibitory role of 6-amino-quinoxaline- alkynyl groups in inhibiting aromatase activity on MCF-7 cells using LAM-29A. The decrease in MCF-7 cell viability in response to LAM-29A was in line with those of the previous studies

albeit at slightly high doses. However, no previous data from other studies was available on the activity of LAM-21D in any of the current cancer cell lines due to its novelty. It is worth noting that the cytotoxic activity of these compounds was specific to the cell lines used in this study. It was observed that when LAM-29A was used to treat CaSki cells little to no activity was found and so is LAM-21D on MCF-7 cells (figure 3.3.1 and 2). Hence, Caski cells were observed to be more sensitive to LAM-21D compared to LAM-29A. These variations might be explained by the specific origin of the tumour, various receptors, and signalling mechanisms (Mirabelli *et al*., 2019). The activity might also vary in other cell lines. There was minimal cytotoxic activity observed at IC_{50} values in non- cancerous HEK-293 cells. Nonetheless, concentrations above 250 µM were found to be lethal (figure 3.4).

Since LAM-29A and LAM-21D affected viability of Caski and MCF-7 cells, a morphology evaluation was carried using a Ti-inverted microscope to track the changes that might have occurred on the morphology of the cancer cells after treatment with the two quinoxaline compounds. As depicted in figure 3.4.1, the untreated and vehicle control cells appear elongated in their usual characteristic spindle-like conformation. The CasKi cells were spherical and lost their characteristic spindle shape. A similar pattern was observed in figure 3.4.2 with MCF-7 cells. They assumed their epithelial-like structures in their normal untreated conformation. The treated cells were less confluent, spherical and had lost contact with the neighbouring cells. Modifications in biological structures may lead to termination of regular activities, particularly those involving the synthesis of proteins, whose binding conformations are extremely sensitive to even the slightest modifications in structures (Guo *et al*., 2021). Hence, the observed changes in the morphology correlate with the reduction in the viability of both Caski and MCF-7 cancer cells upon treatment with LAM-29A and LAM-21D.

Fluorescence dyes can be utilised to assess nuclear and chromatin integrity. Since there was a reduction in cell viability and notable morphological changes after treatment of the cells with LAM-29A and LAM-21D, the effect of these quinoxaline derivatives on the proliferation of cancer cells was evaluated by the

nucleus-specific Ki67 proliferation assay. The Ki67 nuclear protein serves as a gold standard marker for cell proliferation. This protein is highly expressed in tumour cells and is associated with growth and proliferation. There is a lower level of expression of Ki67 nuclear protein in normal cells (Li *et al*., 2015; Urruticoechea *et al*., 2005). The MTT results have revealed a reduction in the cell viability of the cancer cells following treatment with the compounds in respective cells. A previous study has reported a decrease in expression of Ki67 after treatment of oral squamous cell carcinomas with a novel quinoxaline molecule (Wang *et al*., 2019).

Since CaSki cervical cancer cells and MCF-7 breast cancer cells displayed sensitivity towards LAM-21D and LAM-29A, respectively, the effect of LAM-21D on growth and proliferation of CaSki cells, and LAM-29A on MCF-7 cells was studied using the Muse™ Ki67 proliferation assay. As represented in figure 3.5.1, there was a significant reduction in the expression levels of Ki67 when CaSki cells were treated with 250 µM of LAM-21D and curcumin, implying that LAM-21D modulated proliferation of CaSki cells. It is worth noting that Ki67-depleted cells experience challenges during mitotic division, mitotic delays are experienced, and apoptosis occur (Juríková *et al*., 2016). MCF-7 treated cells did not show any significant reduction in Ki67 expression, suggesting that LAM-29A may have minimal effect on the proliferation and cell cycle progression of the MCF-7 cells. Elevated levels of Ki67 are associated with high grade lesions, hence it is used in the prognosis and diagnosis of breast cancer (Yerushalmi *et al*., 2010).

In addition to the Ki67 expression-based assay, Muse™ Annexin V and dead cell marker assay was used to confirm apoptosis as the cell death mode induced by the quinoxaline derivatives. One of the prominent biochemical features of apoptosis includes the externalisation of phosphotidylserine residues during early stages and compromised membrane integrity that is observed in later stages of apoptosis (Liao, 2022). This current study investigated the apoptosis-inducing ability of LAM-21D in CaSki cells and LAM-29A in MCF-7 cells. Using this flow cytometry-based assay, it was demonstrated that the percentage of CaSki cells undergoing apoptosis significantly increased with an

increase in the concentration of LAM-21D quinoxaline derivative (figure 3.6.1). There was insignificant apoptosis induced by LAM-29A in MCF-7 cells (figure 3.6.2). The results are in alignment with those of the previous studies where quinoxaline derivative molecule selectively induced apoptosis in cervical cancer cells inclusive of CaSki cells and colon cancer cells (Sheaffer *et al*., 2016).

Several quinoxaline derivatives were found to be possessing anticancer activity against MCF-7 cells through apoptosis induction (Ezz Eldin *et al*., 2022; Ghattass *et al*., 2014). The selective activity of quinoxaline derivatives across different cancer cell lines highlights their potency to be considered as anticancer drug candidates (Khatoon and Abdulmalek, 2021). Previous studies conducted on the activity of quinoxaline derivatives such as 2-benzoyl-3-phenyl-6,7 dichloroquinoxaline 1,4-dioxide (DCQ) in MCF-7 cells by (Choi *et al*., 2015; Mohiuddin and Kasahara, 2021; Ren *et al*., 2018) has shown a significant amount of apoptosis induced by this compound. This can be due to several side chains substituted on the quinoxaline core increasing its apoptotic activity. LAM-29A exhibited cytotoxicity towards the MCF-7 cells although the mode of cell death might not be apoptosis since Ki67 and Annexin V assays were not affirmative. The different mode of cell death induced by LAM-29A in MCF-7 cells can still be investigated. The potency of LAM-21D was also evidenced by the elevated number of cells in the late apoptosis wherein membrane integrity of the CaSki cells was severely compromised, allowing larger dyes to filter through the cells. This suggest that these quinoxaline derivatives can disrupt the cellular and nuclear membrane integrity of the cancer cells. Apoptosis alterations in cancer cells has created a foundation for drug discoveries targeting this cellular process (Kim-Campbell *et al*., 2019; Walia *et al*., 2021). A majority of the known chemotherapeutic agents used in the treatment of breast and cervical cancers such as cisplatin, carboplatin, doxorubicin and paclitaxel exerts their anticancer activities through apoptosis induction (Choi *et al*., 2015; Mohiuddin and Kasahara, 2021; Ren *et al*., 2018). The structures of quinoxalines are constantly modified to enhance their pharmacological activities and provide alternative means of treatment with less severe side effects as opposed to the conventional methods (Khatoon and Abdulmalek, 2021). Therefore, novel

quinoxaline structures such as LAM-21D have been synthesized so their capacity to eliminate cancer cells can be assessed and improved based on the outcomes.

Following an observed effectiveness of LAM-21D in reducing the viability, inhibiting proliferation and inducing apoptosis in CaSki cells, the effect of this derivative on ROS production was evaluated. ROS are highly reactive molecules engaged in a variety of metabolic processes in both normal physiology and implicated in numerous diseases. In gene regulation and signal transduction pathways, ROS products act as second messengers *albeit* at lower concentrations. The ability of a treatment to induce ROS production in cancer cells has long been utilised as a hallmark in cancer therapy (Conklin, 2004a). In figure 3.7, a population of ROS positive cells increased two-fold when concentrations of LAM-21D were doubled. Increase in ROS production was significantly noticeable across all these concentrations. Commonly used chemotherapeutic drugs exerts their anticancer activities through ROS generation in cancer cells (Mohiuddin and Kasahara, 2021b). In another study, suppression of cervical cancer growth by quinoxaline derivatives was linked to oxidative stress as a result elevated ROS levels. Although beneficial in acute inflammation, ROS production plays a double-edged sword role in cancer treatment; its ability to induce cancer cell cycle arrest and apoptosis are advantageous in eliminating cancer cells but they can cause damage to the normal cells hence causing severe side effects such as neurotoxicity and cardiotoxicity associated with the conventional cancer treatment. Even though there are certain antioxidant-based medications administered to prevent the development of the side effects induced by cancer treatments, cancer treatments need to be improved to minimise the occurrence of severe side effects (Conklin, 2004b).

Although LAM-21D does not counteract ROS production to inhibit the cancer cell growth, it has shown to have antioxidant properties which can assist in counteracting some of the negative side effects of treatment. This dual property of LAM-21D can be of a great importance in cancer therapeutics. Therefore, cancer therapies that rely on ROS production can still be improved to increase specificity in an attempt to minimise side effects (Conklin, 2004b).

Since induction of apoptosis is a tightly regulated process linked to cell cycle progression, a flow cytometry-based cell cycle analysis of cancer cells treated with LAM-21D quinoxaline derivative was conducted to investigate the stage in cell cycle contributing to the observed reduction in cell proliferation. All eukaryotic cell division is accompanied by a series of phases known as cell cycle that includes G_1, S, G_2 and M phases. There are four cell cycle checkpoints which regulates the cell cycle to ensure that the genomic integrity is maintained throughout the cell progression cycle. Progression to the next phase can only occur if the previous phase was executed appropriately in healthy cells (Yılmaz Sarıaltın *et al*., 2022).

Among others, cell cycle will be arrested if DNA damage is detected at the G_1 and G_2 checkpoints, if errors with DNA replication are encountered, if the S phase checkpoint is activated, and the M phase checkpoint or irregularities in the assembly of the mitotic spindles. An arrest at any of the checkpoints implies that the detected defect needs repair, or the cell would undergo apoptosis if the damage is beyond the repair capacity (Conklin, 2004a; Ismail *et al*., 2023). In a recent study conducted to analyse the cell cycle in three cancer cell lines which included MCF-7 cells it was found that cell cycle was arrested at the S phase with DNA content percentages of 48.16% compared with untreated control at 29.79%, after treating the cells with dithiolo[4,5-b]quinoxaline derivative (Ismail *et al* ., 2023). In another study using the CaSki cell model, quinoxaline QW1–24 induced cell cycle arrest in the S phase (Fan *et al*., 2022). The outcomes of these studies are comparable with those of this current study. Quinoxaline LAM-21D exerted minimal effects on the cell cycle at a lower concentration of 125 µM but when the concentration increased to 250 µM the cell cycle was arrested at S phase where the cell population increased significantly (figure 3.8). Simultaneously the population of cells in the G_0/G_1 significantly decreased with ****$p \leq 0.0001$, signifying progression of the cell cycle through the G_0/G_1 checkpoint. It can be noted that the reduction in Ki67 expression and production of ROS by LAM-21D could account for the slow progression through the S phase (Conklin, 2004).

In silico techniques, have gained prominence recently, and are being used in the field of small molecule drug development to study molecular interactions ad

pharmacokinetic profiles of candidate therapeutics. The expression of the antiapoptotic genes such as BCL-2 is induced by NF-kB p65 transcriptional factor. Anti-apoptotic BCL-2 overexpression encourages cancer survival, which results in the development, growth, and maintenance of tumours as well as further chemoresistance (Dey *et al*., 2023). Upon activation of NF-kB p65, ROS accumulation is inhibited which then suppresses the programmed cell death. Hence inhibition of this protein promotes apoptosis induction (Luo *et al*., 2005). As a result, LAM-21D was docked against NF-kB p65 and BCL-2 and CB dock revealed interactions of the ligand, with NF-kB and BCL-2 protein on several contact residues which are depicted on figure 3.10 and table 1. In addition to avoid the pharmacokinetics failure of the drugs during clinical trials their ADME properties should be studied. For compounds to be considered as drugs they need to satisfy Lipinski's rules. These includes MW < 500, HBA (Hydrogen bond acceptors) ≤5, HBD (hydrogen bond donors) ≤10 and Log $P_{O/W}$ (predicted octanol/water partition coefficient) = (−2.0 to 6.50) (Bakchi *et al*., 2022; Flores-Holguín *et al*., 2021). Therefore, LAM-21D did not violate the rules (tables 2 and 3). How molecules/compounds interact with the cytochrome P450 superfamily of proteins is crucial since these play central roles in drug metabolism and clearance, so inhibition of these isoenzymes can result in adverse side effects of drugs. LAM-21D does affect any of the different isoforms of the proteins unlike the control which only showed selectivity towards few isoforms (table 2). The results show that the quinoxaline derivatives can interact with intermediates of apoptosis and inflammation to regulate cell proliferation and cell survival.

CHAPTER 5

CONCLUSION

In conclusion, the outcomes of this study have clearly demonstrated the anticancer potentials of LAM-21D and LAM-29A against CaSki cervical cancer cells and MCF-7 breast cancer cells, respectively. Some of the features of an anticancer agent is its ability to generate antioxidants which are important in stabilising the highly reactive free radicals. Both compounds were able to reduce the ferric reagents and scavenged the DPPH free radical, demonstrating their antioxidant potential. LAM-29A selectively inhibited the viability of MCF-7 cells *albeit* with minimal effect on induction of apoptosis. However, the structure of LAM-29A can be repurposed and improved to target other cell deaths forms LAM-21D selectively inhibited the viability and proliferation of CaSki cells via a reduction of Ki67 expression and induced ROS production which altogether halted the CaSki cell's cycle progression at the S-phase. The *In-silico* studies have also revealed interaction of the compound with anti- apoptotic protein Bcl-2. The compound also showed drug-likeness properties with plausible biological and pharmacokinetic properties. This is the first report describing the anticancer potential of the novel synthesised quinoxaline derivative LAM-21D (6-nitro-2-(oct-1-ynyl) quinoxaline). Of the two quinoxaline derivatives studied, LAM-21D (6-nitro-2-(oct-1-ynyl) quinoxaline) has been demonstrated to be a potential candidate to be explored in the treatment of cervical cancer cells, especially the HPV 16 and 18 positive cells characterising CaSki cervical cancer cells.

REFERENCES

American Cancer Society, (2022). About breast cancer. Available at: https://www.cancer.org/cancer/breast-cancer/about.html. (Accessed: 07 May 2022).

Anisman, H., & Kusnecov, A. W. (2022). Traditional therapies and their moderation. In *Cancer*. Anisman, H., & Kusnecov, A. W. (Eds), Academic Press, pp. 431–459. https://doi.org/10.1016/B978-0-323-91904-3.00015-X

Bakchi, B., Krishna, A. D., Sreecharan, E., Ganesh, V. B. J., Niharika, M., Maharshi, S., Puttagunta, S. B., Sigalapalli, D. K., Bhandare, R. R., & Shaik, A. B. (2022). An overview on applications of SwissADME web tool in the design and development of anticancer, antitubercular and antimicrobial agents: A medicinal chemist's perspective. *Journal of Molecular Structure,* 1259(1): 132712. https://doi.org/10.1016/j.molstruc.2022.132712

Barzaman, K., Moradi-Kalbolandi, S., Hosseinzadeh, A., Kazemi, M. H., Khorramdelazad, H., Safari, E., & Farahmand, L. (2021). Breast cancer immunotherapy: Current and novel approaches. *International Immunopharmacology*, 98(1): 107886. https://doi.org/10.1016/j.intimp.2021. 107886

Besser, A., & Slingerland, J. (2016). CDK Inhibitors in Normal and Malignant Cells. In *Encyclopedia of Cell Biology*, 3(1): 437–446. Elsevier Inc. https://doi.org/10.1016/ B978-0-12-394447-4.30059-1

Borri, F., & Granaglia, A. (2021). Pathology of triple negative breast cancer. *Seminars in Cancer Biology*, 72(1): 136–145. https://doi.org/10.1016/j.semcancer.2020 .06.005

Burmeister, C. A., Khan, S. F., Schäfer, G., Mbatani, N., Adams, T., Moodley, J., & Prince, S. (2022). Cervical cancer therapies: Current challenges and future perspectives. *Tumour Virus Research*, 13(1): 200238. https://doi.org/10.1016/j. tvr.2022.200238

Cao, K., & Tait, S. W. G. (2018). Apoptosis and Cancer: Force Awakens, Phantom Menace, or Both? *International Review of Cell and Molecular*

Biology, 337(1): 135–152. Elsevier Inc. https://doi.org/10.1016/bs.ircmb.2017.12.003

Choi, Y. M., Kim, H. K., Shim, W., Anwar, M. A., Kwon, J. W., Kwon, H. K., Kim, H. J., Jeong, H., Kim, H. M., Hwang, D., Kim, H. S., & Choi, S. (2015). Mechanism of cisplatin-induced cytotoxicity is correlated to impaired metabolism due to mitochondrial ROS generation. *PLoS ONE*, 10(8): e0135083-e0135094 https://doi.org/10.1371/journal.pone.0135083

Conklin, K. A. (2004a). Chemotherapy-associated oxidative stress: Impact on chemotherapeutic effectiveness. *Integrative Cancer Therapies*, 3 (4): 294–300. https://doi.org/10.1177/1534735404270335

Conklin, K. A. (2004b). Chemotherapy-associated oxidative stress: Impact on chemotherapeutic effectiveness. *Integrative Cancer Therapies*, 3(4): 294–300). https://doi.org/10.1177/1534735404270335

Costa, B., Amorim, I., Gärtner, F., & Vale, N. (2020). Understanding Breast cancer: from conventional therapies to repurposed drugs. *European Journal of Pharmaceutical Sciences*, 151(1): 105401. https://doi.org/10.1016/j.ejps.2020. 105401

Dasgupta, A., & Klein, K. (2014). Oxidative Stress and Cancer. In *Antioxidants in Food, Vitamins and Supplements*, Dasgupta, A., & Klein, K. (Eds), Elsevier, pp. 129–150. https://doi.org/10.1016/b978-0-12-405872-9.00008-2

De Rose, F., Meduri, B., De Santis, M. C., Ferro, A., Marino, L., Colciago, R. R., Gregucci, F., Vanoni, V., Apolone, G., Di Cosimo, S., Delaloge, S., Cortes, J., & Curigliano, G. (2022). Rethinking breast cancer follow-up based on individual risk and recurrence management. *Cancer Treatment Reviews*, 109(1): 102434. https://doi.org/10.1016/j.ctrv.2022.102434

Desai, V., Thakkar, J., Wanchoo, R., & Jhaveri, K. D. (2019). Targeted cancer therapies (biologics). In *Onco-Nephrology*, Finkel, K.W., Perazella, M.A., and Cohen E.P. (Eds) Elsevier. (pp. 154-165.e4). https://doi.org/10.1016/B978-0-323-54945-5.00026-6

Dey, S., Singh, A. K., & Kumar, S. (2023). Discovery of Natural Anti-Apoptotic Protein Inhibitor Using Molecular Docking and MM-GBSA Approach: An Anticancer Intervention. *Biointerface Research in Applied Chemistry*, *13*(5): 473-485. https://doi.org/10.33263/BRIAC135.473

Eastman, A., & Barry, M. A. (1992). The Origins of DNA Breaks: A Consequence of DNA Damage, DNA Repair, or Apoptosis? *Cancer Investigation* 10(3): 229-240. https://doi.org/10.3109/07357909209032765

el Newahie, A. M. S., Ismail, N. S. M., Abou El Ella, D. A., & Abouzid, K. A. M. (2016). Quinoxaline-Based Scaffolds Targeting Tyrosine Kinases and Their Potential Anticancer Activity. *Archiv der Pharmazie*, 349(5): 309–326. https://doi.org/10.1002/ardp.201500468

el Newahie, A. M. S., Nissan, Y. M., Ismail, N. S. M., Abou El Ella, D. A., Khojah, S. M., & Abouzid, K. A. M. (2019). Design and synthesis of new quinoxaline derivatives as anticancer agents and apoptotic inducers. *Molecules*, 24(6): 1175. https://doi.org/10.3390/molecules24061175

El-Adl, K., El-Helby, A. G. A., Sakr, H., & Elwan, A. (2020). Design, synthesis, molecular docking and anti-proliferative evaluations of [1,2,4] triazolo[4,3-a] quinoxaline derivatives as DNA intercalators and Topoisomerase II inhibitors. *Bioorganic Chemistry*, 105(1): 104399. https://doi.org/10.1016/j. bioorg.2020. 104399

Elgemeie, G. H., Azzam, R. A., Zaghary, W. A., Aly, A. A., Metwally, N. H., Sarhan, M. O., Abdelhafez, E. M., & Elsayed, R. E. (2022). N-Sulfonated N-benzoazines: Synthesis and medicinal chemistry. In *N-Sulfonated-N-Heterocycles* Elgemeie, G. H., Azzam, R. A., Zaghary, W. A., Aly, A. A., Metwally, N. H., Sarhan, M. O., Abdelhafez, E. M., & Elsayed, R. E. (Eds), Elsevier, pp. 417–446. https://doi.org/10.1016/B978-0-12-822179-2.00012-4

Elkon, K. B., & Oberst, A. (2018). Apoptosis and inflammatory forms of cell death. In *Dubois' Lupus Erythematosus and Related Syndromes*, Wallace, D.J. & Hahn, B.H. (Eds), Elsevier, pp. 237–247. https://doi.org/10.1016/B978-0-323-47927-1.00017-7

Ezz Eldin, R. R., Al-Karmalawy, A. A., Alotaibi, M. H., & Saleh, M. A. (2022). Quinoxaline derivatives as a promising scaffold for breast cancer treatment. *New Journal of Chemistry*, *46*(21): 9975–9984. https://doi.org/10.1039/d2nj00050d

Fagour, S., Thirion, D., Vacher, A., Sallenave, X., Sini, G., Aubert, P. H., Vidal, F., & Chevrot, C. (2017). Understanding the colorimetric properties of quinoxaline-based pi-conjugated copolymers by tuning their acceptor strength: A joint theoretical and experimental approach. *RSC Advances*, *7*(36): 22311–22319. https://doi.org/10.1039/c7ra02535a

Fan, D., Liu, P., Jiang, Y., He, X., Zhang, L., Wang, L., & Yang, T. (2022). Discovery and SAR Study of Quinoxaline–Arylfuran Derivatives as a New Class of Antitumor Agents. *Pharmaceutics*, *14*(11): 2420. https://doi.org/10.3390/pharmaceutics 14112420

Fatemi, S. A., Seifi, N., Rasekh, S., Amiri, S., Moezzi, S. M. I., Bagheri, A., Fathi, S., & Negahdaripour, M. (2022). Immunotherapeutic approaches for HPV-caused cervical cancer. *Advances in Protein Chemistry and Structural Biology*, 129(1) 51–90. Academic Press Inc. https://doi.org/10.1016/bs.apcsb.2021.11.002

Fayed, E. A., Ammar, Y. A., Saleh, M. A., Bayoumi, A. H., Belal, A., Mehany, A. B. M., & Ragab, A. (2021). Design, synthesis, antiproliferative evaluation, and molecular docking study of new quinoxaline derivatives as apoptotic inducers and EGFR inhibitors. *Journal of Molecular Structure*, 1236(1): 130317. https://doi.org/10.1016/j.molstruc.2021.130317

Fleischer, A., Ghadiri, A., Dessauge, F., Duhamel, M., Rebollo, M. P., Alvarez-Franco, F., & Rebollo, A. (2006). Modulating apoptosis as a target for effective therapy. *Molecular Immunology*, 43(8): 1065–1079. https://doi.org/10.1016/j.molimm. 2005. 07.013

Flores-Holguín, N., Frau, J., & Glossman-Mitnik, D. (2021). In Silico Pharmacokinetics, ADMET Study and Conceptual DFT Analysis of Two Plant Cyclopeptides Isolated from Rosaceae as a Computational Peptidology

Approach. *Frontiers in Chemistry*, 9(1): 708364 https://doi.org/10.3389/fchem.2021.708364

Fulda, S. (2015). Targeting apoptosis for anticancer therapy. In *Seminars in Cancer Biology*, 31(1): 84–88. https://doi.org/10.1016/j. semcancer.2014.05.002

Gaglia, M. M., & Munger, K. (2018). More than just oncogenes: mechanisms of tumorigenesis by human viruses. In *Current Opinion in Virology*, 32(1): 48–59. https://doi.org/10.1016/j.coviro.2018.09.003

Ghasemi, M., Turnbull, T., Sebastian, S., & Kempson, I. (2021). The mtt assay: Utility, limitations, pitfalls, and interpretation in bulk and single-cell analysis. *International Journal of Molecular Sciences*, 22(23): 12827. https://doi.org/10.3390/ijms 222312827

Ghattass, K., El-Sitt, S., Zibara, K., Rayes, S., Haddadin, M. J., El-Sabban, M., & Gali-Muhtasib, H. (2014). The quinoxaline di-N-oxide DCQ blocks breast cancer metastasis *in vitro* and *in vivo* by targeting the hypoxia inducible factor-1 pathway. *Molecular Cancer*, 13(1): 12. https://doi.org/10.1186/1476-4598-13-12

Gulcin, İ. (2020). Antioxidants and antioxidant methods: an updated overview. In *Archives of Toxicology*, 94(3): 651–715. https://doi.org/10.1007/s00204-020-02689-3

Guo, M., Lu, B., Gan, J., Wang, S., Jiang, X., & Li, H. (2021). Apoptosis detection: a purpose-dependent approach selection. *Cell Cycle*, 20(11): 1033–1040. https://doi.org/10.1080/15384101.2021.1919830

Harbeck, N., Penault-Llorca, F., Cortes, J., Gnant, M., Houssami, N., Poortmans, P., Ruddy, K., Tsang, J., & Cardoso, F. (2019). Breast cancer. *Nature Reviews Disease Primers*, 5(1): 66. https://doi.org/10.1038/s41572-019-0111-2

Harichand-Herdt, S., Zelnak, A., & O'regan, R. (2009). Endocrine Therapy for Breast Cancer. In *The Breast,* Bland, K.I. & Copeland, E.M. (Eds). W.A.

Sawnders Publidhers, pp.1263–1285. https://doi.org/10.1016/B978-1-4160-5221-0.00077-2

Harnden, K., Mauro, L., & Pennisi, A. (2022). Breast cancer, In *Genomic and Precision* Medicine, Ginsburg, G.S., Willard, H.F., Strickler, J.H. & McKinney, M.S. (Eds), Academic Press, pp 163-172. https://doi.org/10.1016/B978-0-12-800684-9.00013-7

Hausman, D. M. (2019). What is cancer? *Perspectives in Biology and Medicine*, 62(4): 778–784. https://doi.org/10.1353/pbm.2019.0046

Hayes, J. D., Dinkova-Kostova, A. T., & Tew, K. D. (2020). Oxidative Stress in Cancer. *Cancer Cell*, 38(2): 167–197. Cell Press. https://doi.org/10.1016/j.ccell.2020.06. 001

Hopkins, M. P., & Smith, H. O. (2004). Adenocarcinoma of the Cervix. In *Gynecologic Cancer: Controversies in Management,* In *Genomic and Precision* Medicine, Ginsburg, G.S., Willard, H.F., Strickler, J.H. & McKinney, M.S. (Eds), Academic Press, pp. 149–160. Elsevier Ltd. https://doi.org/10.1016/B978-0-443-07142-3.50015-4

Horvath, E. (2021). Molecular subtypes of breast cancer-What breast imaging radiologists need to know. *Journal of Breast Imaging*, 3(1): 12–24, https://doi.org/10.1093/jbi/wbaa110

Huillet, F. D. (1953). Ultraviolet absorption spectra of quinoxaline and some of its Ultraviolet absorption spectra of quinoxaline and some of its derivative's derivatives. Brigham Young University Press, These and Dissertations, 8237: 52-96. https://scholarsarchive.byu.edu/etd/8237

Ismail, M. A., Abusaif, M. S., El-Gaby, M. S. A., Ammar, Y. A., & Ragab, A. (2023). A new class of anti-proliferative activity and apoptotic inducer with molecular docking studies for a novel of 1,3-dithiolo[4,5-b] quinoxaline derivatives hybrid with a sulfonamide moiety. *RSC Advances*, 13(18), 12589-12608. https://doi.org/10.1039/d3ra01635h

Jain, S., Raza, K., Agrawal, A. K., & Vaidya, A. (2021). Immunotherapy of cancer. In *Nanotechnology Applications for Cancer Chemotherapy,* Jain, S.,

Raza, K., Agrawal, A. K., & Vaidya, A. (Eds), Elsevier, pp. 141–174. https://doi.org/10.1016/B978-0-12-817846-1.00008-4

Jalil, A., Wert, J., Farooq, A., & Ahmad, S. (2021). Overcoming drug resistance in cervical cancer: Chemosensitizing agents and targeted therapies. In *Overcoming Drug Resistance in Gynecologic Cancers,* Basha, R.M. & Ahmad, S. (Eds), Elsevier, pp. 195–205. https://doi.org/10.1016/b978-0-12-824299-5.00010-1

Jhingran, A., & Meyer, L. A. (2021). Malignant diseases of the cervix: Microinvasive and Invasive Carcinoma: Diagnosis and Management. In *Comprehensive Gynecology*, Gershenson, D.M., Lentz, G.M., Valea, F.A., & Lobo, R.A. (Eds), Elsevier, pp. 674-690. https://doi.org/10.1016/B978-0-323-65399-2.00040-1

Juríková, M., Danihel, Ľ., Polák, Š., & Varga, I. (2016). Ki67, PCNA, and MCM proteins: Markers of proliferation in the diagnosis of breast cancer. *Acta Histochemica*, 118(5): 544–552. https://doi.org/10.1016/j.acthis.2016.05.002

Kashyap, D., Garg, V. K., & Goel, N. (2021). Intrinsic and extrinsic pathways of apoptosis: Role in cancer development and prognosis. *Advances in Protein Chemistry and Structural Biology*, 125(1): 73–120. https://doi.org/10.1016/bs. apcsb.2021.01.003

Kaushik, P., Kaushik, M., & Parvez, S. (2022). Novel therapeutic approaches targeting oxidative stress in breast and lung cancer. In *Novel Therapeutic Approaches Targeting Oxidative Stress*, Maurya, P.K. & Qamar, I. (Eds), Elsevier. pp. 199–250. https://doi.org/10.1016/b978-0-323-90905-1.00010-9

Khatoon, H., & Abdulmalek, E. (2021). Novel synthetic routes to prepare biologically active quinoxalines and their derivatives: A synthetic review for the last two decades. *Molecules*, *26*(4): 1055. https://doi.org/10.3390/molecules26041055

Khodavirdipour, A., Piri, M., Jabbari, S., Keshavarzi, S., Safaralizadeh, R., & Alikhani, M. Y. (2021). Apoptosis Detection Methods in Diagnosis of Cancer and Their Potential Role in Treatment: Advantages and Disadvantages: a

Review. *Journal of Gastrointestinal Cancer,* 52(2): 422–430. https://doi.org/10.1007/s12029-020-00576-9/

Kim-Campbell, N., Gomez, H., & Bayir, H. (2019). Cell Death Pathways: Apoptosis and Regulated Necrosis. In *Critical Care Nephrology: Third Edition,* Ronco, R., Bellomo, R., Kellum, J.A. & Ricci, R. (Eds), Elsevier, pp. 113-121. https://doi.org/10.1016/B978-0-323-44942-7.00020-0

Knottenbelt, D. C., Patterson-Kane, J. C., & Snalune, K. L. (2015). Squamous cell carcinoma. In *Clinical Equine Oncology,* Knottenbelt, D. C., Patterson-Kane, J. C., & Snalune, K. L. (Eds), Elsevier, pp. 220–236. https://doi.org/10.1016/B978-0-7020-4266-9.00012-X

Krump, N. A., & You, J. (2018). Molecular mechanisms of viral oncogenesis in humans. In *Nature Reviews Microbiology*, 16(11): 684–698. https://doi.org/10.1038/s41579-018-0064-6

Lagoa, R., Marques-da-Silva, D., Diniz, M., Daglia, M., & Bishayee, A. (2020). Molecular mechanisms linking environmental toxicants to cancer development: Significance for protective interventions with polyphenols. *Seminars in Cancer Biology*, 80(1): 118-144 Academic Press. https://doi.org/10.1016/j.semcancer. 2020.02.002

Lekgau, K., Raphoko, L. A., Lebepe, C. M., Mongokoana, D. F., Leboho, T. C., Matsebatlela, T. M., Gumede, N. J., & Nxumalo, W. (2022). Design and synthesis of 6-amino-quinoxaline-alkynyl as potential aromatase (CYP19A1) inhibitors. *Journal of Molecular Structure*, 1255(1): 132473. https://doi.org/10.1016/j.molstruc.2022.132473

Lewandowska, A. M., Rudzki, M., Rudzki, S., Lewandowski, T., & Laskowska, B. (2019). Environmental risk factors for cancer - review paper. *Annals of Agricultural and Environmental Medicine*, 26(1): 1–7. https://doi.org/10.26444/aaem/94299

Li, L. T., Jiang, G., Chen, Q., & Zheng, J. N. (2015). Predic Ki67 is a promising molecular target in the diagnosis of cancer (Review). *Molecular Medicine Reports*, 11(3): 1566–1572. https://doi.org/10.3892/mmr.2014.2914

Liao, D. (2022). Apoptosis, necroptosis, and pyroptosis in health and disease: An overview of molecular mechanisms, targets for therapeutic development, and known small molecule and biologic modulators. In *Mechanisms of Cell Death and Opportunities for Therapeutic Development,* Liao, D. (Ed), Elsevier, pp. 1–46. https://doi.org/10.1016/B978-0-12-814208-0.00008-7

Lim, C. S. H., & Lim, S. L. (2013). Ferric Reducing Capacity Versus Ferric Reducing Antioxidant Power for Measuring Total Antioxidant Capacity. *Laboratory Medicine*, 44(1): 51–55. https://doi.org/10.1309/lm93w7ktfnpzixrr

Loibl, S., Poortmans, P., Morrow, M., Denkert, C., & Curigliano, G. (2021). Breast cancer. *The Lancet*, 397(10286): 1750–1769). https://doi.org/10.1016/S0140-6736(20)32381-3

Luo, J. L., Kamata, H., & Karin, M. (2005). IKK/NF-κB signaling: Balancing life and death - A new approach to cancer therapy. *Journal of Clinical Investigation*, 115(10): 2625–2632. https://doi.org/10.1172/JCI26322

Madkour, L. H. (2020). Cell death mechanisms—Apoptosis pathways and their implications in toxicology. In *Reactive Oxygen Species (ROS), Nanoparticles, and Endoplasmic Reticulum (ER) Stress-Induced Cell Death Mechanisms*, Madkour, L. H. (Ed), Elsevier, pp. 199–228. https://doi.org/10.1016/b978-0-12-822481-6.00009-8

Madkour, L. H. (2020). Programmed cell death mechanisms and nanoparticle toxicity. In *Reactive Oxygen Species (ROS), Nanoparticles, and Endoplasmic Reticulum (ER) Stress-Induced Cell Death Mechanisms*, Madkour, L. H. (Ed), Elsevier, pp. 229–264. https://doi.org/10.1016/b978-0-12-822481-6.00010-4

Makhoul, I. (2018). Therapeutic strategies for breast cancer. In *The Breast: Comprehensive Management of Benign and Malignant Diseases, Bland, K.I., Copeland, E.M., Klimberg, S.V. and Gradishar,* W.J. (Eds), Elsevier, pp. 315-330. https://doi.org/10.1016/B978-0-323-35955-9.00024-6

Mathan, S. v., Rajput, M., & Singh, R. P. (2022). Chemotherapy and radiation therapy for cancer. In *Understanding Cancer,* Jain, B. & Pandey, S. (Eds), Elsevier. pp. 217–236. https://doi.org/10.1016/b978-0-323-99883-3.00003-2

Matsuura, K., Canfield, K., Feng, W., & Kurokawa, M. (2016). Metabolic Regulation of Apoptosis in Cancer. In *International Review of Cell and Molecular Biology*, 327(1): 43–87. https://doi.org/10.1016/bs.ircmb.2016.06.006

Mirabelli, P., Coppola, L., & Salvatore, M. (2019). Cancer cell lines are useful model systems for medical research. *Cancers*, 11(8): 1098. https://doi.org/10.3390/ cancers11081098

Mohiuddin, M. D., & Kasahara, K. (2021). The mechanisms of the growth inhibitory effects of paclitaxel on gefitinib-resistant non-small cell lung cancer cells. *Cancer Genomics and Proteomics*, *18*(5): 661–673. https://doi.org/10.21873/CGP.20288

Montero, V., Montana, M., Khoumeri, O., Correard, F., Estève, M. A., & Vanelle, P. (2022). Synthesis, In Vitro Antiproliferative Activity, and In Silico Evaluation of Novel Oxiranyl-Quinoxaline Derivatives. *Pharmaceuticals*, *15*(7): 781. https://doi.org/10.3390/ph15070781

Nair, R. R., & Yadav, S. S. (2022). Cancer and cell cycle. In *Understanding Cancer: From Basics to Therapeutics,* Chapter 6, Jain, B. & Pandey, S. (Eds), pp. 91–102. Elsevier. https://doi.org/10.1016/B978-0-323-99883-3.00013-5

Natesh, J., Penta, D., & Meeran, S. M. (2022). Epigenetics in precision medicine of breast cancer. In *Epigenetics in Precision Medicine,* Chapter 3, García-Giménez, J.L. (Ed), Elsevier, pp. 43–67. https://doi.org/10.1016/b978-0-12-823008-4.00004-4

Nieuwenhuijs-Moeke, G. J., Pischke, S. E., Berger, S. P., Sanders, J. S. F., Pol, R. A., Struys, M. M. R. F., Ploeg, R. J., & Leuvenink, H. G. D. (2020). Ischemia and reperfusion injury in kidney transplantation: Relevant mechanisms in injury and repair. In *Journal of Clinical Medicine*, 9(1): 253. https://doi.org/10.3390/ jcm9010253

Pfeffer, C. M., & Singh, A. T. K. (2018). Apoptosis: A target for anticancer therapy. In *International Journal of Molecular Sciences*, 19(2):448. https://doi.org/10.3390/ijms19020448

Picollo, M., Aceto, M., & Vitorino, T. (2019). UV-Vis spectroscopy. *Physical Sciences Reviews*, 4(4): 008. https://doi.org/10.1515/psr-2018-0008

Prasad, S. B. (2022). Cancer and apoptosis. In *Understanding Cancer: From Basics to Therapeutics,* Chapter 7, Jain, B. & Pandey, S. (Eds), Elsevier, (pp. 103–116). https://doi.org/10.1016/B978-0-323-99883-3.00015-9

Ramalingam, V., & Rajaram, R. (2021). A paradoxical role of reactive oxygen species in cancer signaling pathway: Physiology and pathology. *Process Biochemistry* 100(1): 69–81. Elsevier Ltd. https://doi.org/10.1016/j.procbio.2020.09.032

Rasha, F., Sharma, M., & Pruitt, K. (2021). Mechanisms of endocrine therapy resistance in breast cancer. *Molecular and Cellular Endocrinology*, 532(1): 322. https://doi.org/10.1016/j.mce.2021.111322

Reeves, D. (2016). Cytostatic Agents—Tyrosine Kinase Inhibitors Utilized in the Treatment of Solid Malignancies. In *Side Effects of Drugs Annual*, 38(1): 479–491). https://doi.org/10.1016/bs.seda.2016.08.006

Ren, X., Zhao, B., Chang, H., Xiao, M., Wu, Y., & Liu, Y. (2018). Paclitaxel suppresses proliferation and induces apoptosis through regulation of ROS and the AKT/MAPK signaling pathway in canine mammary gland tumor cells. *Molecular Medicine Reports*, 17(6): 8289–8299. https://doi.org/10.3892/mmr.2018.8868

Rivas, H. G., & DeCaprio, J. A. (2022). Cell Division/Death: Cell Cycle – The Restriction Point. In *Reference Module in Life Sciences*, 2(1): 235-242. https://doi.org/10.1016/B978-0-12-821618-7.00194-2

Rodrigues, M.-A. (2021). Principles of Radiation Therapy in Breast Cancer. In *Breast Cancer and Gynecologic Cancer Rehabilitation,* Chapter 9, Christian, A. (Ed), pp. 89–97. Elsevier. https://doi.org/10.1016/b978-0-323-72166-0.00009-8

Ryzhov, A., Corbex, M., Piñeros, M., Barchuk, A., Andreasyan, D., Djanklich, S., Ghervas, V., Gretsova, O., Kaidarova, D., Kazanjan, K., Mardanli, F., Michailovich, Y., Ten, E., Yaumenenka, A., Bray, F., & Znaor, A. (2021).

Comparison of breast cancer and cervical cancer stage distributions in ten newly independent states of the former Soviet Union: a population-based study. *The Lancet Oncology*, *22*(3):361–369. https://doi.org/10.1016/S1470-2045(20)30674-4

Samir, B., Kalalian, C., Roth, E., Salghi, R., & Chakir, A. (2020). Gas-phase UV absorption spectra of pyrazine, pyrimidine and pyridazine, *Chemical Physics Letters*, 751(1): 13751. https://doi.org/10.1016/j.cplett.2020.137469

Shahidian, A., Ghassemi, M., Mohammadi, J., & Hashemi, M. (2020). Immunotherapy. *Bio-Engineering Approaches to Cancer Diagnosis and Treatment*, 4(2) 69–114. Elsevier. https://doi.org/10.1016/B978-0-12-817809-6.00004-2

Sheaffer, A. K., Lee, M. S., Qi, H., Chaniewski, S., Zheng, X., Farr, G. A., Esposito, K., Harden, D., Lei, M., Schweizer, L., Friborg, J., Agler, M., McPhee, F., Gentles, R., Beno, B. R., Chupak, L., & Mason, S. (2016). A small molecule inhibitor selectively induces apoptosis in cells transformed by high-risk human papilloma viruses. *PLoS ONE*, 11(6): 371. https://doi.org/10.1371/journal.pone.0155909

Shiovitz, S., & Korde, L. A. (2015). Genetics of breast cancer: A topic in evolution. *Annals of Oncology*, 26(7): 1291–1299. https://doi.org/10.1093/annonc/mdv022

Sibiya, M. A., Raphoko, L., Mangokoana, D., Makola, R., Nxumalo, W., & Matsebatlela, T. M. (2019). Induction of Cell Death in Human A549 Cells Using 3-(Quinoxaline-3-yl) Prop-2-ynyl Methanosulphonate and 3-(Quinoxaline-3-yl) Prop-2-yn-1-ol. *Molecules*, 24(3): 407. https://doi.org/10.3390/molecules 24030407

Siddik, Z. H. (2013). Apoptosis in Cancer. Mechanisms, Deregulation, and Therapeutic Targeting. In *Cancer Drug Design and Discovery: Second Edition,* Chapter 12, Niadle, S. (Ed), Elsevier, pp. 357–390. https://doi.org/10.1016/B978-0-12-396521-9.00012-7

Singh, A. K., Rana, H. K., & Pandey, A. K. (2022). The oxidative stress: Causes, free radicals, targets, mechanisms, affected organs, effects,

indicators. In *Antioxidants Effects in Health,* Chapter 1.2, Nabavi, S.M. & Silva, A.S. (Eds), (pp. 33–42). Elsevier. https://doi.org/10.1016/B978-0-12-819096-8.00012-4

Skala, M. C., Ayuso, J. M., Burkard, M. E., & Deming, D. A. (2022). Breast cancer immunotherapy: Current biomarkers and the potential of in vitro assays. *Current Opinion in Biomedical Engineering* 21(1): 100348, https://doi.org/10. 1016/j.cobme. 2021.100348

Sung, H., Ferlay, J., Siegel, R. L., Laversanne, M., Soerjomataram, I., Jemal, A., & Bray, F. (2021). Global Cancer Statistics 2020: GLOBOCAN Estimates of Incidence and Mortality Worldwide for 36 Cancers in 185 Countries. *CA: A Cancer Journal for Clinicians*, 71(3): 209–249. https://doi.org/10.3322/caac.21660

Suthar, S. K., Chundawat, N. S., Singh, G. P., Padrón, J. M., & Jhala, Y. K. (2022). Quinoxaline: A comprehension of current pharmacological advancement in medicinal chemistry. *European Journal of Medicinal Chemistry* Reports, 5(1): 100040. https://doi.org/10.1016/j.ejmcr.2022.100040

Takatsuka, M., Goto, S., Kobayashi, K., Otsuka, Y., & Shimada, Y. (2022). Evaluation of pure antioxidative capacity of antioxidants: ESR spectroscopy of stable radicals by DPPH and ABTS assays with singular value decomposition. *Food Bioscience*, 48(1): 101714. https://doi.org/10.1016/j.fbio.2022.101714

Taylor, W. R., & Grabovich, A. (2009). Targeting the Cell Cycle to Kill Cancer Cells. In *Pharmacology,* Chapter 8, Hacker, M., Messer, W. & Bachmann K. Elsevier (pp. 429–453). Inc. https://doi.org/10.1016/B978-0-12-369521-5.00017-8

Teruel, E., Gruffat, H., Tommasino, M., & Journo, C. (2019). Viral oncogenesis and genomic instability: The centr(osom)al connection. *Virologie*, 23(5): E16–E31. https://doi.org/10.1684/vir.2019.0793

Thind, T. S., & Arora, S. (2012). Role of isothiocyanates as anticancer agents and their contributing molecular and cellular mechanisms. *Medicinal*

Chemistry & Drug Discovery, 3(2): 79-93. https://www.researchgate.net/publication/266508172

Urruticoechea, A., Smith, I. E., & Dowsett, M. (2005). Proliferation marker Ki-67 in early breast cancer. *Journal of Clinical Oncology*, 23(28): 7212–7220. https://doi.org/10.1200/JCO.2005.07.501

Vijaya Rachel, K., & Sivaraj, N. (2021). Cervical cancer metabolism: Major reprogramming of metabolic pathways and cellular energy production. In *A Theranostic and Precision Medicine Approach for Female-Specific Cancers*, Chapter 12, Malla, R.R.& Nagarajupp, G.P. (Eds), Elsevier, pp. 223–233. https://doi.org/10.1016/ b978-0-12-822009-2. 00012-1

Vishlaghi, N., & Lisse, T. S. (2020). Exploring vitamin D signalling within skin cancer. In *Clinical Endocrinology*, 92(4): 273–281. https://doi.org/10.1111/cen.14150

Walia, R., Madaan, R., Chaudhary, K., Mehta, B., & Bala, R. (2021). Molecular pathways of apoptotic cell death. In *Clinical Perspectives and Targeted Therapies in Apoptosis*, Chapter 3, Rupinder K. & Madan, S.J. (Eds), Elsevier. pp. 79–109. https://doi.org/10.1016/b978-0-12-815762-6.00003-2

Wang, Y., Zhang, W., Sun, P., Cai, Y., Xu, W., Fan, Q., Hu, Q., & Han, W. (2019). A novel multimodal NIR-II nanoprobe for the detection of metastatic lymph nodes and targeting chemo-photothermal therapy in oral squamous cell carcinoma. *Theranostics*, 9(2): 391–404. https://doi.org/10.7150/thno.30268

Yamaguchi, R., & Perkins, G. (2020). An Emerging Model for Cancer Development from a Tumor Microenvironment Perspective in Mice and Humans. *Advances in Experimental Medicine and Biology,* 1225(1): 19–29. Springer. https://doi.org/10.1007/978-3-030-35727-6_2

Yazbeck, V., Alesi, E., Myers, J., Hackney, M. H., Cuttino, L., & Gewirtz, D. A. (2022). An overview of chemotoxicity and radiation toxicity in cancer therapy. *Advances in Cancer Research*, 155: 1-27. https://doi.org/10.1016/bs.acr.2022.03.007

Yerushalmi, R., Woods, R., Ravdin, P. M., Hayes, M. M., & Gelmon, K. A. (2010). Ki67 in breast cancer: prognostic and predictive potential. *The Lancet Oncology*, 11(2): 174–183. https://doi.org/10.1016/S1470-2045(09)70262-1

Yılmaz Sarıaltın, S., Üstündağ, A., Mhlanga Chinheya, R., İpek, S., & Duydu, Y. (2022). Cytotoxicity, genotoxicity, oxidative stress, apoptosis, and cell cycle arrest in human Sertoli cells exposed to boric acid. *Journal of Trace Elements in Medicine and Biology*, 70(1): 126913. https://doi.org/10.1016/j.jtemb.2021. 126913

Zeb, A. (2020). Concept, mechanism, and applications of phenolic antioxidants in foods. In *Journal of Food Biochemistry*, 44(9): 13394. Blackwell Publishing Ltd. https://doi.org/10.1111/jfbc.13394